PENNSTATE

Radiation Science and Engineering Center
College of Engineering
The Pennsylvania State University
Breazeale Nuclear Reactor Building
University Park, PA 16802-2301

(814) 865-6351
Fax: (814) 863-4840

Annual Operating Report, FY 05-06
PSBR Technical Specifications 6.6.1
License R-2, Docket No. 50-5

December 20, 2007

U. S. Nuclear Regulatory Commission
Attention: Document Control Desk
Washington, D. C. 20555

Dear Sir:

Enclosed please find the Annual Operating Report for the Penn State Breazeale Reactor (PSBR). This report covers the period from July 1, 2006 through June 30, 2007, as required by technical specifications requirement 6.6.1. Also included are any changes applicable to 10 CFR 50.59.

A copy of the Fifty-Second Annual Progress Report of the Penn State Radiation Science and Engineering Center is included as supplementary information.

Sincerely yours,

C. Frederick Sears

C. Frederick Sears
Director, Radiation Science
and Engineering Center

Enclosures:
Annual Operating Report, FY 06-07 – 5 pages
Radiation Science & Engineering Center 52nd Annual Progress Report

mat

cc. E. J. Pell
D. N. Wormley
L. C. Burton
E. J. Boeldt
S. Pierce
K. Witt

A020
NRR

PENN STATE BREAZEALE REACTOR

Annual Operating Report, FY 06-07
PSBR Technical Specifications 6.6.1
License R-2, Docket No. 50-5

Reactor Utilization

The Penn State Breazeale Reactor (PSBR) is a TRIGA Mark III facility capable of 1 MW steady state operation, and 2000 MW peak power pulsing operation. Utilization of the reactor and its associated facilities falls into two major categories:

EDUCATION utilization is primarily in the form of laboratory classes conducted for graduate and undergraduate students and numerous high school science groups. These classes vary from neutron activation analysis of an unknown sample to the calibration of a reactor control rod. In addition, an average of 2500 visitors tour the PSBR facility each year.

RESEARCH/SERVICE accounts for a large portion of reactor time which involves Radionuclear Applications, Neutron Radiography, multiple research programs by faculty and graduate students throughout the University, and various applications by the industrial sector.

The PSBR facility operates on an 8 AM - 5 PM shift, five days a week, with occasional early morning, evening, and weekend shifts to accommodate laboratory courses, public education and research or service projects.

Summary of Reactor Operating Experience - Tech Specs requirement 6.6.1.a.

Between July 1, 2006 and June 30, 2007, the PSBR was

critical for	882 hours	or 3.2 hrs/shift
subcritical for	459 hours	or 1.7 hrs/shift
used while shutdown for	776 hours	or 2.8 hrs/shift
not available	0 hours	or 0 hrs/shift
Total usage	2117 hours	or 7.7 hrs/shift

The reactor was pulsed a total of 192 times with the following reactivities:

< \$2.00	19
\$2.00 to \$2.50	141
> \$2.50	32

The square wave mode of operation was used 30 times to power levels between 100 and 500 KW.

Total energy produced during this report period was 582 MWH with a consumption of 30 grams of U-235.

Unscheduled Shutdowns - Tech Specs requirement 6.6.1.b.

One unscheduled reactor shutdown occurred on July 26, 2006 when a reactor "watchdog" scram initiated. If the control computer (DCC-X) software fails to reset the watchdog relay due to failure or computer overload, the reactor protection system will initiate a scram. An operator's rapid repeated manipulation of the "bar charts" function keys loaded the DCC-X computer sufficiently to prevent watchdog reset and resulted in the scram. Procedural expectations and training were used to prevent recurrence.

Major Maintenance With Safety Significance - Tech Specs requirement 6.6.1.c.

In September of 2006, the safety rod magnet and wiring was replaced to correct observed dropping of the safety rod into the core during reactor pulse evolutions. Weak electromagnetic coupling of the rod combined with the mechanical shock of the transient rod ejection resulted in the safety rod dropping before the pulse timeout scram signal. While this had no direct safety consequence, further degradation could affect reliable operations.

In October of 2006, the shim rod drive mechanism was disassembled and realigned after the rod failed to respond to a manual in-command. The rod scrammed properly when demanded and the failure has no direct safety consequence. Following realignment the rod operated as designed.

In January of 2007, the evacuation horn failed to sound correctly during daily checkout. The amplifier volume control was removed and cleaned to correct the problem. Daily testing assures prompt identification of similar problems.

Major Changes Reportable Under 10 CFR 50.59 - Tech Specs requirement 6.6.1.d.

Facility Changes -

In March of 2007, radiation safety in the Neutron Beamhole Laboratory was improved by installation of a reactor operation interlock with the beam tube shield cave door. The new interlock initiates a reactor "operation inhibit" if the shield door is not fully closed when the reactor is located at the beam lab operating position. If the reactor is moved to the beam lab operating position with the shield door not fully closed or the door is opened when the reactor is positioned at the laboratory, 3 of 4 control rods will be fully inserted into the core and audible annunciators will sound in the reactor control area.

Procedures -

One new procedure (SOP-11 *Reactor Operation at the Beam Ports*) was issued in March of 2007. This procedure standardizes operating practices and safety checks associated with reactor operations in support of the Neutron Beamhole Laboratory.

Procedures are normally reviewed biennially, and on an as needed basis. Numerous minor changes and updates were made to maintain procedures during the year and they will not be listed.

New Tests and Experiments -

None

Radioactive Effluents Released - Tech Specs requirement 6.6.1.e.

Liquid – Less than 25% of the allowed or recommended concentrations

There were no planned or unplanned liquid effluent releases under the reactor license for the report period.

Liquid radioactive waste from the radioisotope laboratories at the PSBR is under the University byproduct materials license and is transferred to the Radiation Protection Office for disposal with the waste from other campus laboratories. Liquid waste disposal techniques include storage for decay, release to the sanitary sewer as per 10 CFR 20, and solidification for shipment to licensed disposal sites.

Gaseous – Less than 25% of the allowed or recommended concentrations

Gaseous effluent Ar-41 is released from dissolved air in the reactor pool water, air in dry irradiation tubes, air in neutron beam ports, and air leakage to and from the carbon-dioxide purged pneumatic sample transfer system.

The amount of Ar-41 released from the reactor pool is very dependent upon the operating power level and the length of time at power. The release per MWH is highest for extended high power runs and lowest for intermittent low power runs. The concentration of Ar-41 in the reactor bay and the bay exhaust was measured by the Radiation Protection staff during the summer of 1986. Measurements were made for conditions of low and high power runs simulating typical operating cycles. Based on these measurements, an annual release of between 520 mCi and 1339 mCi of Ar-41 is calculated for July 1, 2006 to June 30, 2007, resulting in an average concentration at ground level outside the reactor building that is 0.7 % to 2.1 % of the effluent concentration limit in Appendix B to 10 CFR 20.1001 -

20.2402. The concentration at ground level is estimated using only dilution by a 1 m/s wind into the lee of the 200 m^2 cross section of the reactor bay.

During the report period, several irradiation tubes were used at high enough power levels and for long enough runs to produce significant amounts of Ar-41. The calculated annual production was 520 mCi. Since this production occurred in a stagnant volume of air confined by close fitting shield plugs, much of the Ar-41 decayed in place before being released to the reactor bay. The reported releases from dissolved air in the reactor pool are based on measurements made, in part, when a dry irradiation tube was in use at high power levels; some of the Ar-41 releases from the tubes are part of rather than in addition to the release figures quoted in the previous paragraph. Even if all of the 520 mCi were treated as a separate release, the percent of the Appendix B limit given in the previous paragraph would still be no more than 3 %.

Production and release of Ar-41 from reactor neutron beam ports was minimal. Beam port #7 has only three small collimation tubes (each 1 cm^2 area) exiting the port and any Ar-41 production in these small tubes is negligible. Beam port #4 has an aluminum cap installed inside the outer end of the beam tube to prevent air movement into or out of the tube as the beam port door is opened or closed. The estimated Ar-41 production in beam port #4 for all beam port operations is 23 mCi. With the aforementioned aluminum cap in place, it is assumed that this Ar-41 decayed in place. Radiation Protection Office air measurements have found no presence of Ar-41 during beam port #4 reactor operations with the beam port cap in place.

The use of the pneumatic transfer system (rabbit) was minimal during this period and any Ar-41 release would be insignificant since the system operates with CO-2 as the fill gas. A small amount of Ar-41 is released from each rabbit capsules. A 2 minute irradiation @900kW will produce .0026 mCi. In the 2006-07 reporting period 438 rabbit capsules were irradiated at a variety of power/time combinations (typically less than 900kW). The resulting 11 mCi of Ar-41 are not a significant contributor.

Ar-41 is also produced by the facility for use in commercial applications. On several occasions during the reporting period, small amounts of Ar escaped the production system into the reactor bay and were exhausted to the environment. These releases were estimated to be between 340 mCi (from sample results) and 1920 mCi (worst case calculated value) and represent an additional 3% of the annual limits for Ar-41 release.

Tritium release from the reactor pool is another gaseous release. The evaporation rate of the reactor pool was checked previously by measuring the loss of water from a flat plastic dish floating in the pool. The dish had a surface area of 0.38 ft^2 and showed a loss of 139.7 grams of water over a 71.9 hour period giving a loss rate of 5.11 g ft^{-2} hr^{-1}. Based on a pool area of about 395 ft^2 the annual evaporation rate would be 4680 gallons. This is of course dependent upon relative humidity, temperature of air and water, air movement, etc. For a pool ^3H concentration of 29695 pCi/l (the average for July 1, 2006 to June 30, 2007) the tritium activity released from the ventilation system would be 526 μCi. A dilution factor of 2 x 10^8 ml s^{-1} was used to calculate the unrestricted area concentration. This is from 200 m^2 (cross-section of the building) times 1 m s^{-1} (wind velocity). These are the values used in the safety analysis in the reactor license. A sample of air conditioner condensate a previous year showed no detectable ^3H. Thus, there is probably very little ^3H recycled into the pool by way of the air conditioner condensate and all evaporation can be assumed to be released.

^3H released	526 μC
Average concentration, unrestricted area	8.34 x 10^{-14} μCi/ml
Permissible concentration, unrestricted area	1 x 10^{-7} μCi/ml
Percentage of permissible concentration	8.34 x 10^{-5} %
Calculated effective dose, unrestricted area	4.2 x 10^{-5} mRem

Environmental Surveys - Tech Specs requirement 6.6.1.f.

The only environmental surveys performed were the routine TLD gamma-ray dose measurements at the facility fence line and at control points in two residential areas several miles away. This reporting year's net measurements (in millirems) are tabulated below represent the July 1, 2006 to June 30, 2007 period.

	3rd Qtr '06	4th Qtr '06	1st Qtr '07	2nd Qtr '07	Total
Fence North	7.9	8.4	9.8	14.5	40.6
Fence South	6.9	9.7	14.0	10.8	41.4
Fence East	9.6	7.7	10.4	11.2	38.9
Fence West	7.9	8.1	5.1	16.9	38.0
Control	7.5	7.6	6.6	10.2	31.9
Control	-.4	.1	4.6	2.1	6.4

There is no meaningful increase in exposure at the facility fenceline due to licensed operations for the '06-'07 fiscal year.

PENNSTATE

1855

Radiation Science & Engineering Center

52nd Annual Progress Report

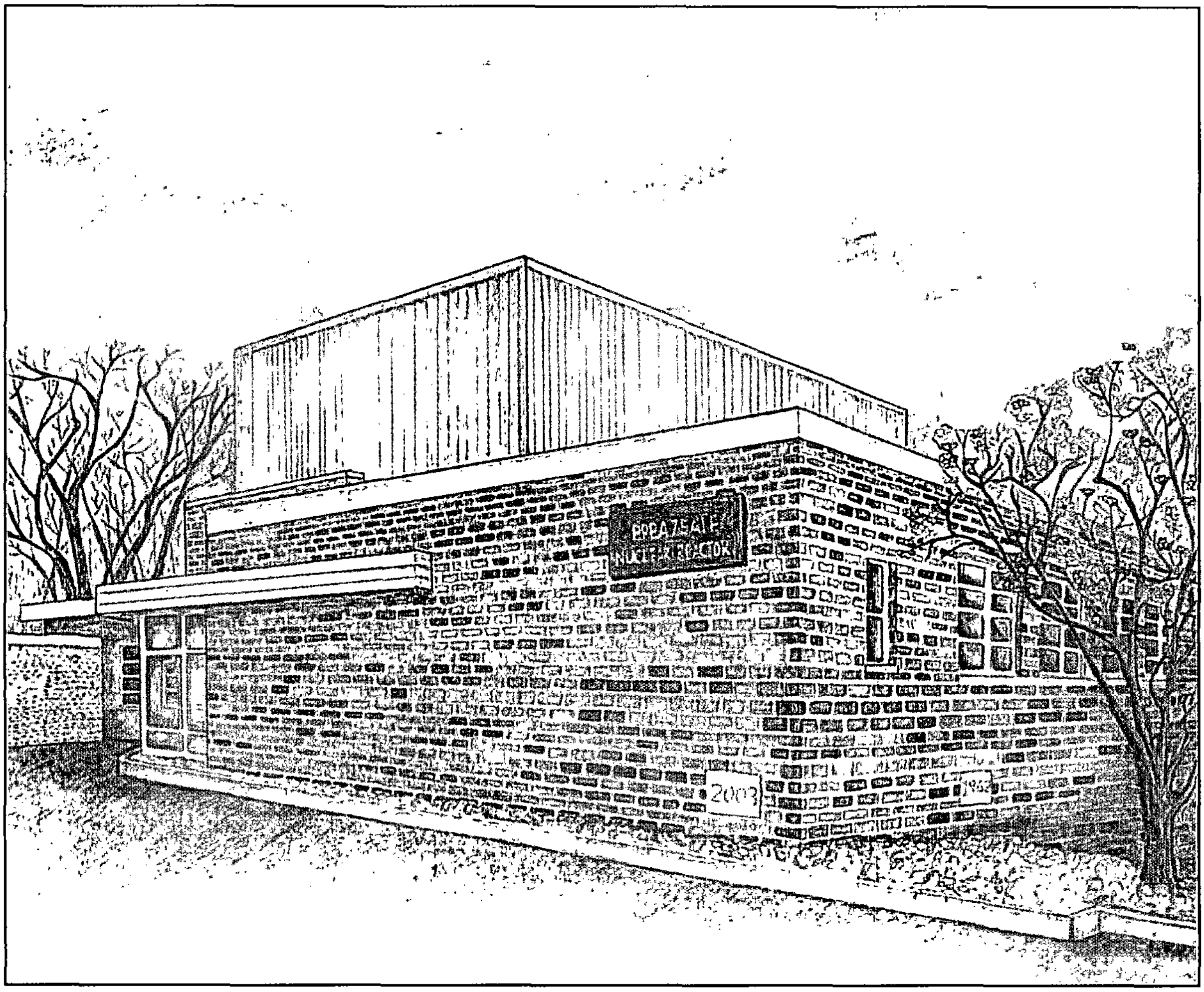

Breazeale Nuclear Reactor
College of Engineering
University Park, PA 16802

December 2007

52^{st} ANNUAL PROGRESS REPORT

PENN STATE RADIATION SCIENCE & ENGINEERING CENTER

July 1, 2006 to June 30, 2007

Submitted to:

United States Department of Energy

By:

C. Frederick Sears (Director)
Kenan Ünlü (Associate Director for Research)
Mark A. Trump (Associate Director for Operations)
Candace Davison (Research & Education Specialist, Editor)
Wendy Belinc (Staff Assistant, Editor)
Radiation Science and Engineering Center
University Park, PA 16802

December 2007
Contract DE-AC07-99ID13727
Contract 0036822
U.Ed. ENG 08-39

TABLE OF CONTENTS

TABLES

FIGURES

PREFACE

Administrative responsibility for the Radiation Science and Engineering Center (RSEC) resides in the College of Engineering. Overall responsibility for the reactor license resides with the Senior Vice President for Research and the Dean of the Graduate School. The reactor and associated laboratories are available to all Penn State colleges for education and research programs. In addition, the facility is made available to assist other educational institutions, government agencies and industries having common and compatible needs and objectives, providing services that are essential in meeting research, development, education, and training needs.

The Penn State Radiation Science and Engineering Center's 52st Annual Progress Report (July 2006 through June 2007) is submitted in accordance with the requirements of Contract DE-AC07-99ID13727 between the United States Department of Energy and Bechtel (BWXT Idaho), and their Contract 00036822 with The Pennsylvania State University. This report also provides the University administration with a summary of the utilization of the facility for the past year.

Numerous individuals are to be recognized and thanked for their dedication and commitment in this report. Special thanks are extended to those responsible for the individual sections as listed in the table of contents and to the individual facility users whose research summaries are compiled in Section X.

INTRODUCTION

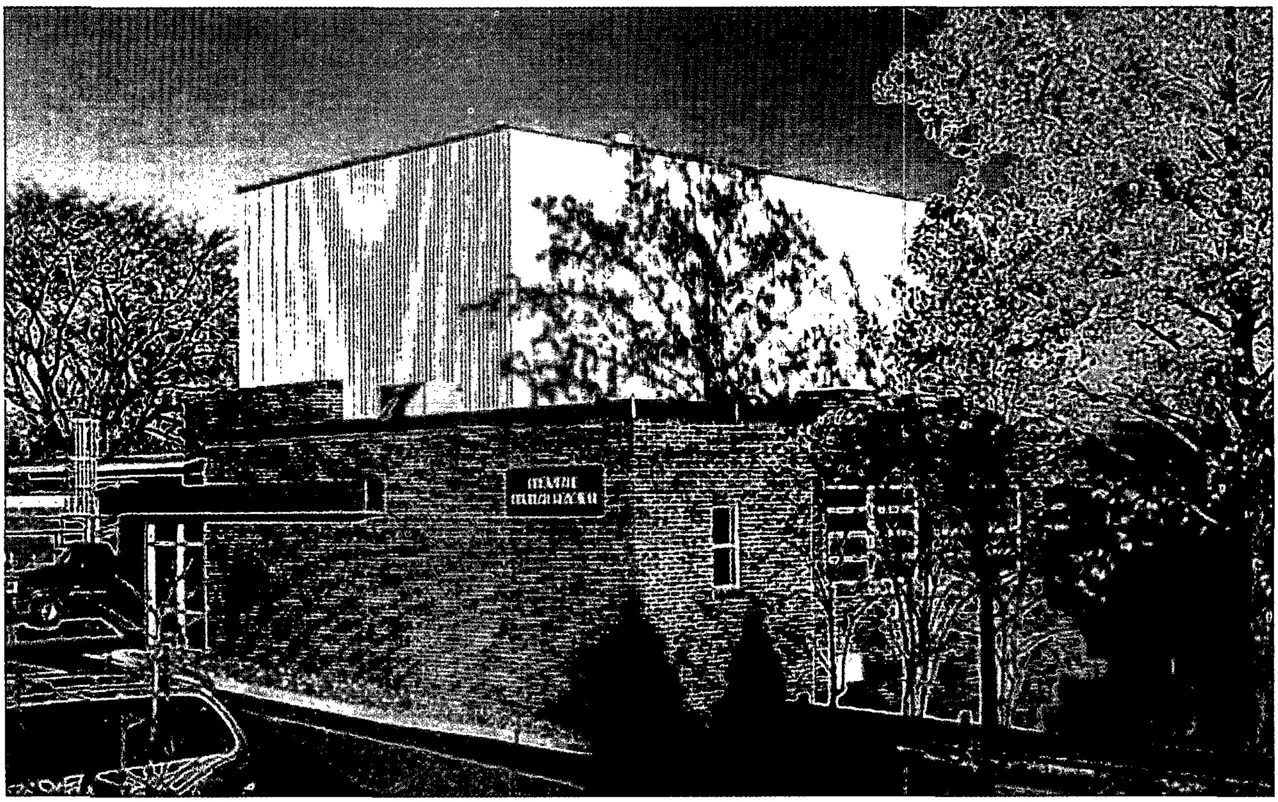

MISSION

The mission of the Penn State Radiation Science and Engineering Center (RSEC), in partnership with faculty, staff, students, alumni, government, and corporate leaders, is to safely utilize nuclear technology to benefit society through education, research, and service.

The RSEC facilities have a diverse and dedicated staff with a commitment to safety, excellence, quality, user satisfaction, and education by example and teaching.

VISION

It is the vision of the faculty and staff of the Radiation Science and Engineering Center to become a leading national resource and make significant contributions in the following areas:

Safety Actively promote nuclear and personal safety in everything we do.

Education Develop and deliver innovative educational programs to advance societal knowledge of nuclear science and engineering through resident instruction and continuing education for students of all ages and their educators.

Research Expand leading edge research that increases fundamental knowledge of nuclear science and engineering particularly in the area of materials research applications of nuclear techniques.

Service Expand and build a diverse array of services and users by maintaining excellence, quality, user satisfaction, and efficient service to supplement university funding and enhance education and research.

In conducting this mission in pursuit of the stated vision, the following activities are highlighted among the numerous accomplishments reported in the pages that follow:

Considerable faculty and staff effort was rewarded when DOE issued the Innovations in Nuclear Infrastructure and Education (INIE) grants. The initial INIE Big-Ten Consortium, led by Penn State and along with Purdue University, the University of Illinois and the University of Wisconsin received approximately $1.97 million per year in FY02 and FY03, $2.1 million in FY 04, and $1.9 million in FY 05. The Ohio State University and the University of Michigan joined the Big-Ten Consortium during the FY 04. The consortium funding is about $1.9 million per year currently and DOE plans to continue the grant program until 2010. The objective of the INIE program is to strengthen the nation's university nuclear engineering programs through innovative use of the university research and training reactors. During the five-year period of the INIE grant the following was accomplished at Penn State –

A state-of-the-art Compton Suppression System was purchased, installed and operated at the RAL Laboratory to increase our capabilities in NAA.

The Room 2 laboratory/classroom and Room 111 classroom was totally refurbished and equipped with state of the art computer work stations and audio-visual equipment with partial funding from the INIE.

A refurbished GammaCell was purchased and installed during the '02-'03 fiscal year. The upgraded Cobalt-60 loading decreased irradiation times by a factor of ten, providing much better service for campus users.

A slow neutron chopper system was developed with a chopper brought from the Cornell University, Ward Center for Nuclear Sciences to characterize the neutron beam used for radiography and radioscopy. As part of the INIE grant, this system is available for loan to other research reactors. As part of neutron beam characterization efforts, a He-3 neutron spectrometer system was purchased and tested to determine the spectrum of high-energy neutrons.

Mini-grants were awarded on a competitive basis to Penn State and non-Penn State individuals submitting proposals to use the Penn State Radiation Science and Engineering Center facilities.

Efforts continue to lay the groundwork for the development of a cold neutron beam and new neutron beam port facilities. Both thermal and thermo-hydraulic behavior of two university based cold neutron sources are being evaluated in order to build a third generation mesitylene based cold neutron source at Penn State. Code development also continues to model the existing beam ports and various future designs.

Improvements in the neutron beam quality and the neutron imaging hardware and software are continuing.

The neutron irradiation of semi-conductors for commercial, military, and space applications continued at a very healthy pace.

The use of neutron radioscopy and neutron transmission as a research and service tool for industry continued for companies who fabricate boron containing metals used in the nuclear industry. Efforts are under way to upgrade the software and hardware associated with this work.

Income from service work done for industrial users was used to continue the support of two Ph.D. graduate students in the nuclear engineering department. The students worked in the area of modeling the Penn State TRIGA reactor core and developed better computer code tools for fuel depletion tracking and core loading designs.

Numerous high school, Penn State, and non-Penn State college/university groups participated in educational programs at the RSEC under the direction of Candace Davison during the year. In many cases, experiments teaching nuclear concepts were performed. The RSEC also supported educational events such as Boy Scout and Girl Scout merit badge programs. The facility hosted over 2700 visitors during the fiscal year. A complete list of groups hosted is presented in Appendix B.

Increased reactor usage for university courses continued this year as multiple sessions were needed in the NE 451 and NE 450 laboratory courses. An increased emphasis on graduate students taking NE 497F, Nuclear Reactor Operations and Testing, resulted in more reactor usage during the year.

In light of concern for terrorist activities that could be directed against university research reactors, continuing efforts were made in expanding the total scope of facility security. Additional attention to security issues is expected to continue, both self-directed and in response to NRC guidance. The staff is meeting the challenge of providing security without compromising the education and research mission of the reactor facility.

Dr. Kenan Ünlü, and Drs. Vijaykrisnan Narayanan, Mary Jane Irwin and Yuan Xie of the Department of Computer Science and Engineering continue testing of neutron induced soft errors in semiconductor memories and started to develop a soft error analysis toolset program. This research project has received wide recognitions within the academic and industrial circles. A major grant from NSF was awarded to this research project for the next three years.

Drs. Matthew Mench, Jack Brenizer, Kenan Ünlü, and graduate students of the Department of Mechanical and Nuclear Engineering continue major research projects using neutron radioscopy and neutron radiography for investigation of fuel cells for several major automotive companies. DOE-NEER grant was awarded last year for the extension of this project for the development of neutron tomography at RSEC is continued.

Dr. Kenan Ünlü, and Dr. Peter I. Kuniholm from Cornell University continued neutron activation analysis of absolutely dated tree rings to identify climatically significant marker events in history and prehistory. A DOE-NEER grant was awarded last year for this project for the next three years. Also this project received wide national and international recognition in 2005. The project is featured in numerous web pages worldwide including NSF web page: (http://www.nsf.gov/news/news_summ.jsp?cntn_id=104245&org=NSF&from=news). The NSF has also prepared an audio clip for the "Imagine That" program for this project. This clip was broadcasted over 500 radio stations nationwide during the August/September months. The audio clip can be downloaded from the link below:http://www.flpradio.com/features, click on the Imagine That! link, click on the 8.22.05-9.16.05 dated link, and then select the 23_IT_9.5.05.mp3 link.

Dr. Kenan Ünlü obtained a grant from DOE, Radiochemistry Education Award Program (REAP) to build a radiochemistry education program at Penn State. Penn State Radiochemistry Laboratory is going to placed in RSEC. Room 112 at RSEC is being converted to a radiochemistry teaching laboratory. All the equipment needed for this laboratory was purchased from REAP, State Matching Funds, and Tuition Recovery funds. Renovation of Room 112 is taking place with RSEC funds. The Penn State Radiochemistry Education Program is a collaborative initiative and the main collaborator is the Los Alamos National Laboratory. A graduate student spent last summer at LANL as a result of this collaboration. A close collaboration with Oak Ridge National Laboratory is being initiated.

Dr. Warren Frank Witzig
March 26, 1921—June 14, 2007

This annual report is dedicated to Dr. Warren F. Witzig, affectionately known as the "The Great White Father." He shared his passion for learning with those he met. He strongly believed in the value of education, especially on nuclear topics, and developed innovative outreach programs in these areas. He served as Nuclear Engineering Department head from 1967-1986 and as Interim Director of the Radiation Science and Engineering Center 1996-1997.

Dr. Witzig received a B.S. in electrical engineering in 1942, from Rensselaer Polytechnic Institute, in Troy, NY, an M.S. in electrical engineering in 1944, from the University of Pittsburgh, and a Ph.D. in physics from the University of Pittsburgh. From 1942 to 1960, Dr. Witzig was employed at the Westinghouse Research Laboratories and Bettis Plant in Pittsburgh, PA. During World War II, he worked on the Manhattan District program on high vacuum systems, heat transfer, mass spectroscopy, and ionic centrifuge. He served as the first experimenter in the Materials Testing Reactor and later as engineering manager of in-pile tests for the naval reactor program in Hanford, Chalk River, and the MTR-ETR complex. Dr. Witzig served as Senior Engineer and took the USS Nautilus, the world's first nuclear-powered ship, reactor critical in 1954. This engineering was used in the Skipjack and George Washington series of nuclear submarines, which have been the backbone of the U.S. nuclear navy. Dr. Witzig was the co-author of the first FSAR for the Nautilus and numerous classified reports.

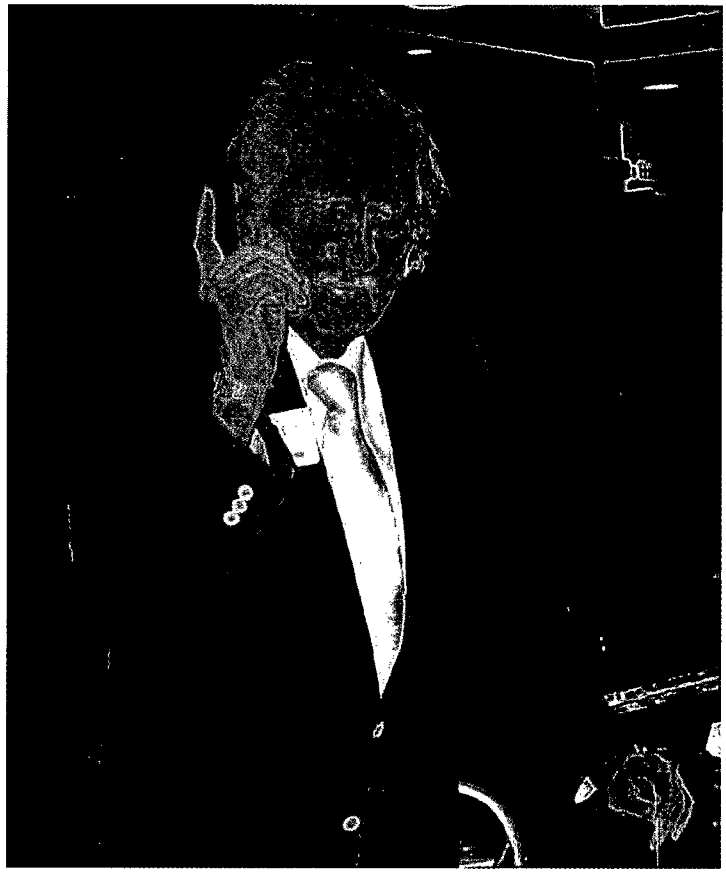

Dr. Witzig at the Reactor 50th anniversary celebration.

Ken Rudy and Dr. Witzig during April 97, pool drain.

In 1960 he co-founded Nuclear Utilities Services (NUS) Corporation in Washington D.C., where he served as senior vice president and member of the board of directors. The corporation grew from a two-man organization to the largest independent group of nuclear consultants in the nation. Dr. Witzig held overall responsibility for technical direction of work related to the application of nuclear energy for the production of electricity, small military reactors, test reactors, the use of nuclear reactors and isotopes in aerospace. He traveled worldwide in his consulting practice.

Dr. Witzig became Professor and Department Head of Nuclear Engineering at Penn State in 1967. He was responsible for one of the earliest student programs in nuclear engineering in the United States. He established the undergraduate and associate degree programs and initiated the continuing education Program on Radiation, Nuclear Safety and Environmental Effects for Public Education. He supervised the Triga Mark III Reactor, Cobalt-60 Facility, and Low-level Radiation Monitoring Laboratory. Dr. Witzig conducted research in areas of reactor design and safety, fuel cycle, nuclear safeguards, rad-waste disposal, emergency planning and radiation monitoring.

Retiring from the University in 1986, he served on several oversite committees and safety review boards. Dr. Witzig chaired the Westinghouse GOCO Sites Nuclear Safety and Environmental Institute Board of Directors from 1988 to 1993. In 1979 Gov. Richard Thornburgh called him into the service of the Commonwealth of Pennsylvania during the emergency shutdown of Three Mile Island II. In June 1992, Witzig presented the paper, "The Value of a Nuclear Safety and Environmental Committee," at the Ukraine Academy of Science at Chelyabinski State University. He toured the site of the explosion at the Chernobyl nuclear power plant. Dr. Witzig had been a life-long advocate of nuclear energy as a clean, safe, and efficient source of energy and also for the training, accreditation, and oversite of nuclear operators. Among Dr. Witzig's honors are Fellow, American Nuclear Society; Fellow, American Association for the Advancement of Science; Sigma Xi, Sigma Pi Sigma, and Eta Kappa Nu honor societies; Special Citation for an Engineering educator in Excellence in Engineering Education, EEI Power Engineering; Who's Who in Engineering and America; and Penn State's Outstanding Service Award for retirees.

Dr. Witzig receives a plaque of appreciation from the Penn State Nuclear Engineering Society, April 21, 2007.

PERSONNEL

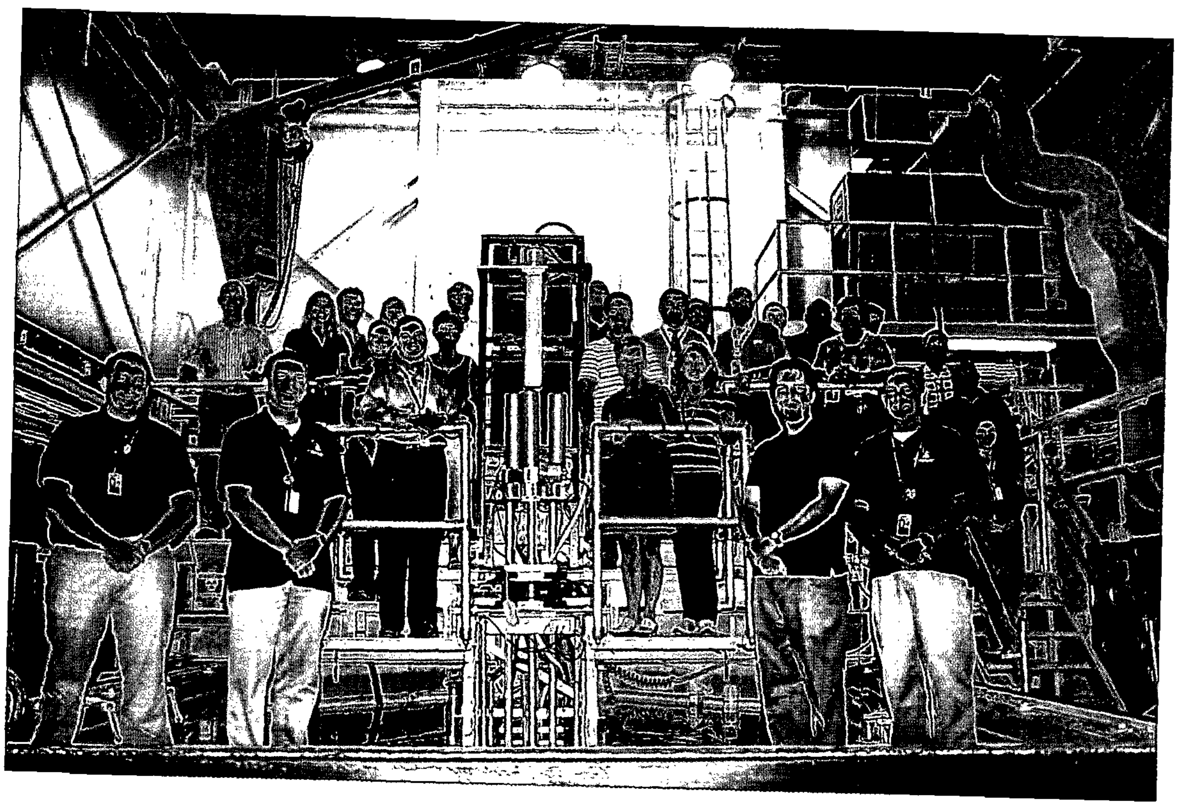

Several undergraduate students worked in work-study or wage payroll positions during the year. Mark Dorn, Amy Miller, Dennis Spielman, Korrie Yetzer, and Doug Yocum assisted Candace Davison in facility educational programs for high school students

Undergraduates Todd Beaver, Adina LaFrance, Joshua LaFrance, Brian Schmoke, Eric Schwarz, and Dennis Spielman served as licensed senior reactor operators in reactor intern positions.

Todd Beaver, Brian Schmoke, Dennis Spielman, and Mark Trump received their Senior Reactor Operators license on June 29, 2007.

Adina LaFrance, Joshua LaFrance, and Seth May graduated in May 2007.

Terry Flinchbaugh retired Jan. 1, 2007.

Mark A. Trump was hired as the new Associate Director for Operations starting on Feb. 12, 2007.

Ron Eaken, Machinist A

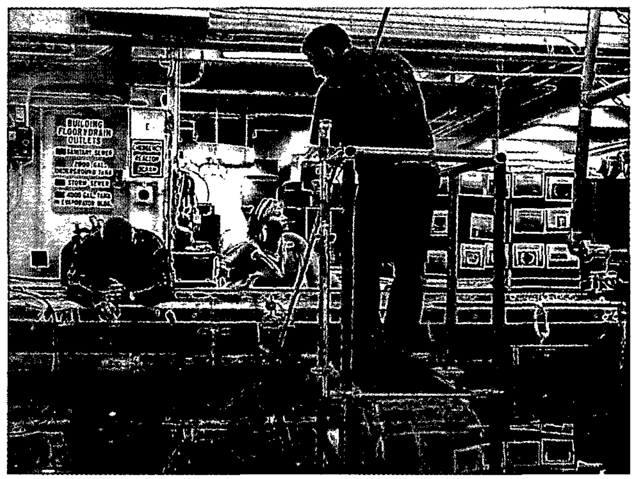

Mike Morlang, Alison Portanova, and Thierry Daubenspeck, Senior Reactor Operators

Terry Flinchbaugh retired as Associate Director for Operations (ADO) of the Radiation Science and Engineering Center at the end of 2006. Terry served Penn State for 39 years. Even after retirement he continued to work on a temporary basis until June 2007 while helping to assure a smooth turnover of his position to Mark Trump, our new ADO. Over the span of four decades Terry was a continual contributor and leader to activities including the Low Level Radiation Measurement Laboratory and overall reactor operations and training. Terry provided an example for all with his devotion to the reactor as well as for his meticulous record keeping and scheduling. It was a real pleasure for all of us to be blessed with knowing Terry and working with him. Terry, HAPPY RETIREMENT!

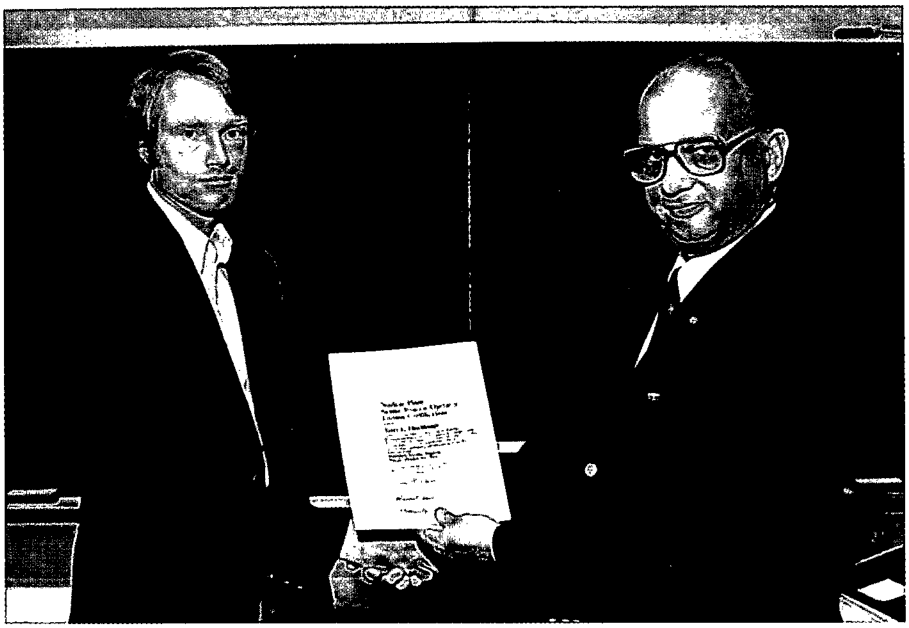

Terry Flinchbaugh being present his Senior Reactor Operator license renewal by an NRC official on April 30, 1983.

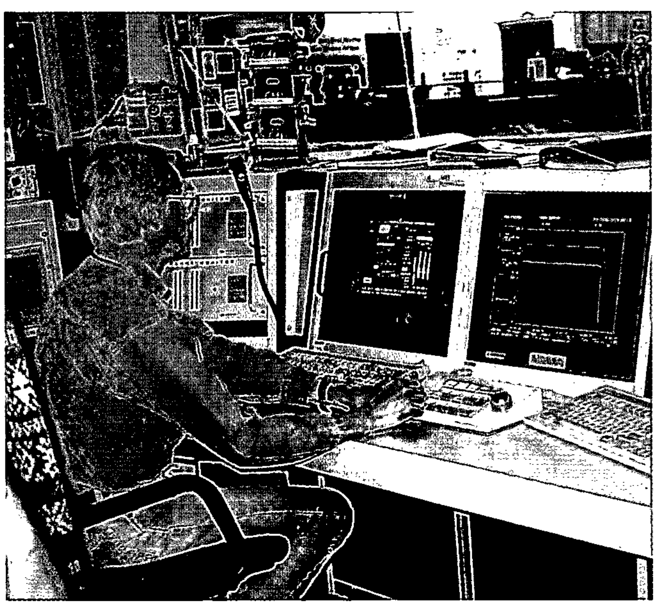

Terry operating the reactor.

Mark Trump joined the facility staff this year as Associate Director for Operations. He fills the position recently vacated by the retirement of Terry Flinchbaugh following 39 years of service. Mark received his B.S. in Nuclear Engineering from Penn State in 1979. He returns having spent the majority of the intervening 27 years working in operations, operations engineering, and training at multiple commercial nuclear sites. His experience includes certification as Engineering Officer of the Watch at the now de-commissioned S1C Naval Reactor prototype and Senior Reactor Operator license at Three Mile Island Unit 1. Mark also served as a senior evaluator with the Institute of Nuclear Power Operations. Mark joined the facility in February 2007 and received his facility SRO license in July. Mark brings new utility ties to the facility as well as recent commercial nuclear experience.

TABLE 1

	Faculty and Staff	Title
**	Todd Beaver	Reactor Operator Intern
	Wendy R. Belinc	Staff Assistant VII
	Jack S. Brenizer	Professor & Program Chair, Nuclear Engineering
**	Mac E. Bryan	Research Engineer/Supervisor, Reactor Operations
	Gary L. Catchen	Professor, Nuclear Engineering
**	Thierry H. Daubenspeck	Activation & Irradiation Specialist/Supervisor, Reactor Operations
**	Candace C. Davison	Research & Education Specialist/Supervisor, Reactor Operations
	Ronald L. Eaken	Reactor Machinist
**	Terry L. Flinchbaugh	Associate Director for Operations
**	Brenden J. Heidrich	Senior Research Assistant
**	Adina K. LaFrance	Reactor Operator Intern
**	Joshua A. LaFrance	Reactor Operator Intern
	Jana Lebiedzik	Research Support Technician III
**	Gary M. Morlang	Senior Supervisor/Reactor Engineering Operations
**	Alison R. Portanova	Research & Service Support Specialist/Supervisor, Reactor Operations
	Paul R. Rankin	Radiation Measurement Technician
	Susan K. Ripka	Administrative Aide III
**	Eric A. Schwarz	Reactor Operator Intern
**	Brian Schmoke	Reactor Operator Intern
**	C. Frederick Sears	Senior Scientist/Director, RSEC, Associate Professor, Nuclear Engineering
	Michael G. Smith	Information Technology Specialist I
**	Dennis Spielman	Reactor Operator Intern
	Sally Thomas	Staff Support
**	Mark A. Trump	Associate Director for Operations
	Kenan Ünlü	Senior Scientist/Associate Director for Research, Professor, Nuclear Engineering

* *Licensed Operator*
** *Licensed Senior Operator*

Wage Payroll/Work Study

Mark Dorn	Zach VanHorn
Amy Miller	Korrie Yetzer
Daniel Skilone	Doug Yocum

Graduate Students

Sacit M. Cetiner	Jung Rim
Nesrin O. Cetiner	Danielle Schwarz
Cihangir Celik	Liang Shi
Kyu Cho	Corey Trivelpiece
A. Kevin Heller	Ahmet Turhan
Seth May	

TABLE 2

	<u>Penn State Reactor Safeguards Committee</u>	
***	Y. Azmy	Professor of Nuclear Engineering, Penn State
	D. Sathianathan	Head of SEDTAPP, Penn State
	E. Boeldt	Manager, Radiation Protection, Penn State Environmental Health & Safety
	F. Eisenhuth	Sr. Engineer, Pennsylvania Power & Light Susquehanna Steam Electric Station
	L. Hochreiter	Professor of Mechanical and Nuclear Engineering, Penn State
**	K. Hunt	Exelon Nuclear Corporation
	K. Ivanov	Associate Professor in Charge of Fuel Management, Penn State
	T. Litzinger, Chairman	Professor & Director of Leonhard Center, Penn State
	M. Mench	Assistant Professor of Mechanical Engineering, Penn State
	C.F. Sears	Ex-Officio, Director RSEC
*	R. Tropasso	Manager of Nuclear Design, Exelon

* *Served through January 1, 2007*

** *Initial Appointment January 1, 2007*

*** *Reappointed effective January 1, 2007*

FIGURE 1
RSEC Organization Chart

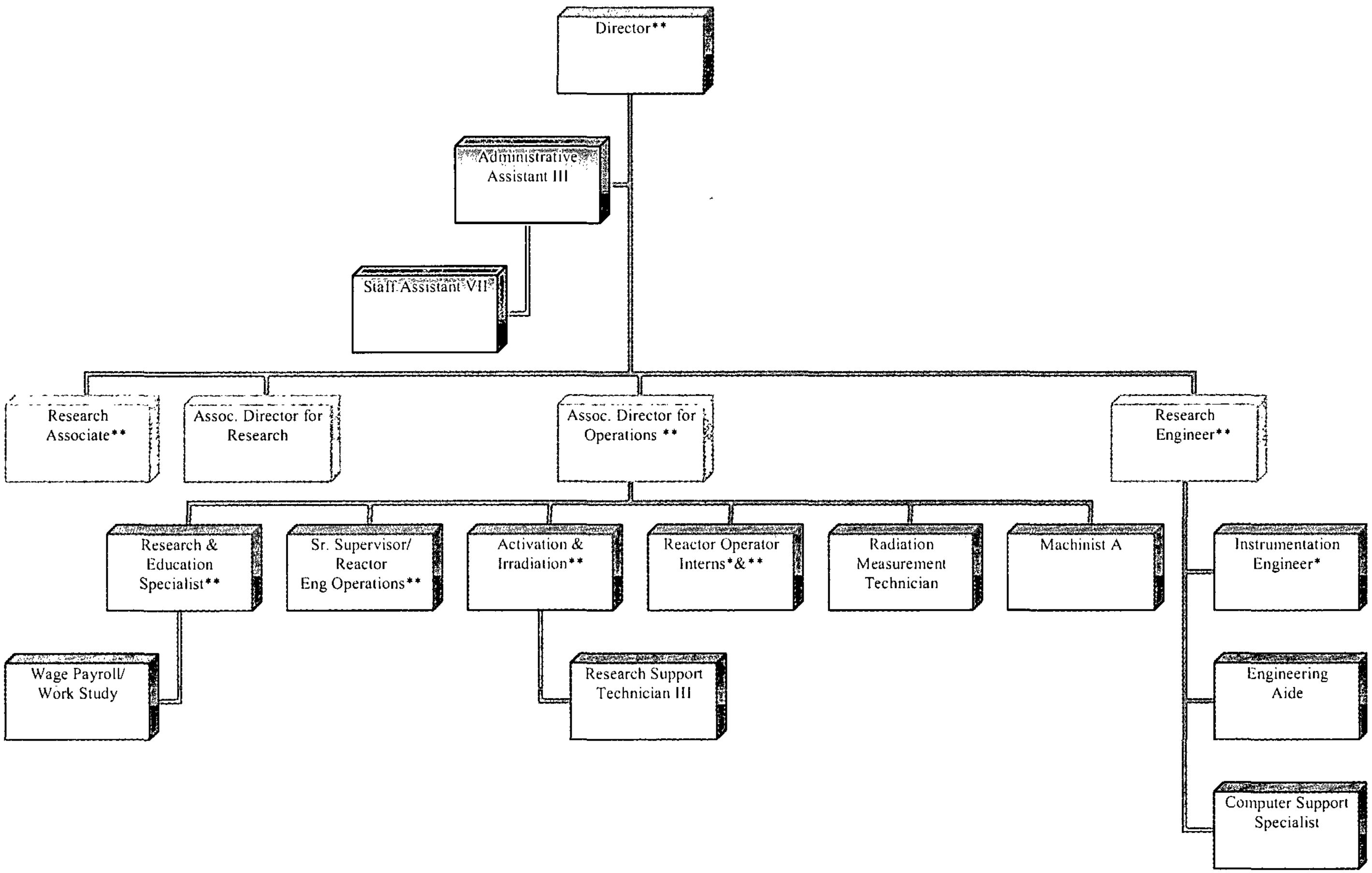

* *Licensed Operator*
** *Licensed Senior Operator*

REACTOR OPERATIONS

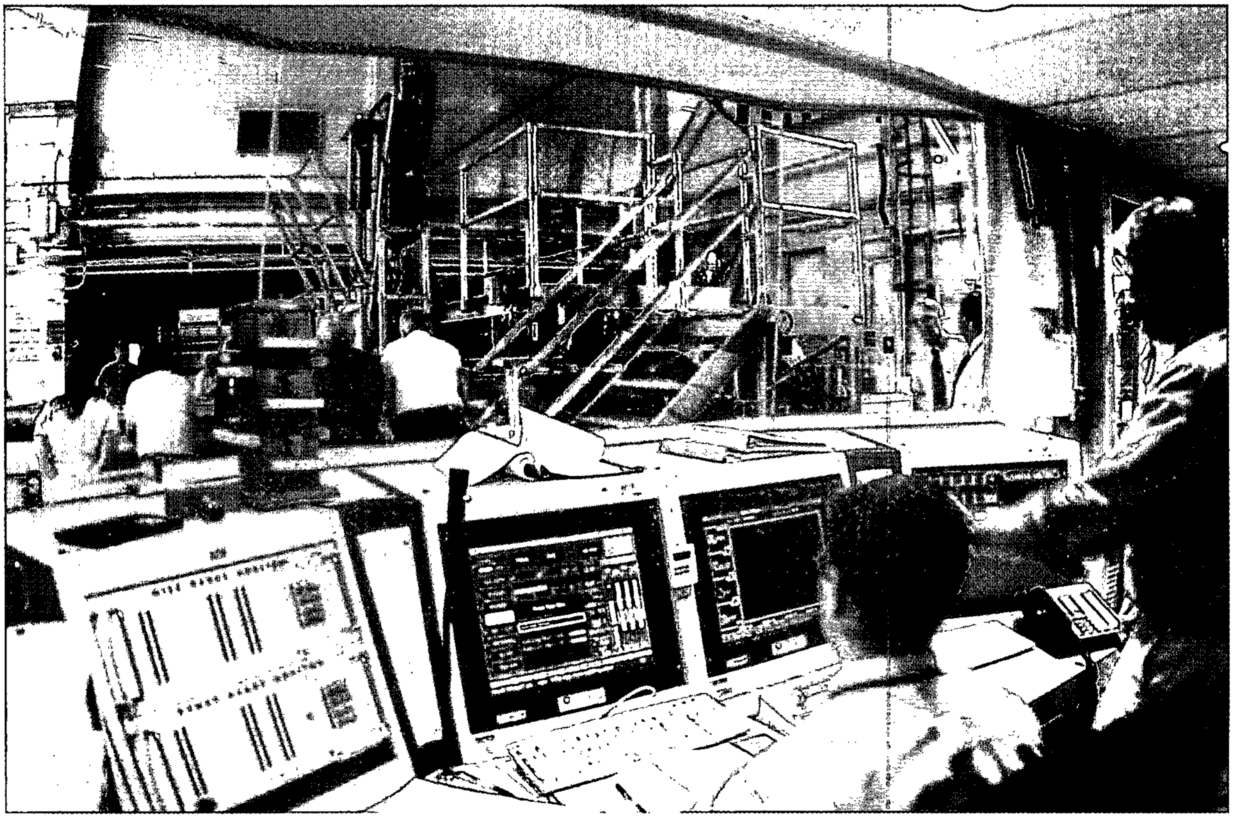

Research reactor operation began at Penn State in 1955. In December 1965, the original 200 kW reactor core and control system was replaced by a more advanced General Atomics TRIGA core and analog control system. TRIGA stands for Training, Research, Isotope Production, built by General Atomic Company. The new core is capable of operation at a steady state power level of 1000 kW with pulsing capabilities to 2000 MW for short (milliseconds) periods of time.

In 1991, the reactor console system was upgraded to an AECL/Gamma-Metrics dual digital/analog control system. Further enhancements were made in 2004. This system provides for improved teaching and research capabilities and features a local area network whereby console information can be sent to laboratories and emergency support areas.

Utilization of the Penn State Breazeale Reactor (PSBR) falls into four major categories:

Education
Utilization is primarily in the form of laboratory classes conducted for graduate and undergraduate degree candidates and numerous high school science groups. These classes will vary from the irradiation and analysis of a sample, non-destructive examinations of materials using neutrons or x-rays, or transient behavior of the reactor to the calibration of a reactor control rod.

Research
Involves radionuclear applications, neutron depth profiling, neutron radiography, gamma irradiation, several research programs by faculty and graduate students throughout the University, and various applications by the industrial sector.

Training
Programs for PSBR Reactor Operations Staff.

Service
Involves radionuclear applications, neutron transmission measurements, radioscopy, semiconductor irradiations, isotope production and other applications by the industrial sector.

OPERATIONS

The PSBR core, containing about 7.5 pounds of Uranium-235 in a non-weapons form, operates at a depth of approximately 18 feet in a pool of demineralized water. The water provides the shielding and cooling necessary for the operation of the reactor. It is relatively simple to expose a sample by positioning it in the vicinity of the reactor at a point where it will receive the desired radiation dose. A variety of fixtures and jigs are available for such positioning. Various containers and irradiation tubes can be used to keep samples dry. A pneumatic transfer system offers additional possibilities. A heavy water tank and neutron beam laboratory provide for neutron transmission, neutron radiography, and neutron beam activities. Core rotational, east-west and north-south movements, provide flexibility in positioning the core against experimental apparatus.

In normal steady state operation at 1000 kW, the thermal neutron flux available varies from approximately 1×10^{13} $n/cm^2/second$ at the edge of the core to approximately 3×10^{13} $n/cm^2/second$ in the central region of the core.

When using the pulse mode of operation, the peak flux for a maximum pulse is approximately 6×10^{16} n/cm2/second with a pulse width of 15 milliseconds at half maximum.

Support facilities include hot cells, a machine shop, electronic shop, darkroom, laboratory space, and fume hoods.

STATISTICAL ANALYSIS

Tables 3 and 4 list Reactor Operation Data and Reactor Utilization Data-Shift Averages, respectively, for the past three years. In Table 3, the Critical Hours of Reactor Operations is a summation of the hours the reactor was operating at some power level. The Subcritical Hours of Reactor Operations is the total hours that the reactor key and console instrumentation were on and under observation, less the Critical time.

Subcritical Hours of Reactor Operations reflects experiment set-up time and time spent approaching reactor criticality.

The Number of Pulses reflects demands of undergraduate labs, researchers, and reactor operator training programs. Square Waves are used primarily for demonstration purposes for public groups touring the facility, as well as researchers and reactor operator training programs.

The Number of Scrams Planned as Part of Experiments reflects experimenter needs. Unplanned Scrams from Personnel Action are due to human error. Unplanned Scrams Resulting from Abnormal System Operation are related to failure of experimental, electronic, electrical or mechanical systems.

Table 4, Part A, Reactor Usage per shift, describes total reactor utilization on a shift basis. The summation of Hours Critical and Hours Subcritical gives the total time the reactor console key is on. Hours Shutdown includes time for instruction at the reactor console, experimental setup, calibrations or very minor maintenance that occupies the reactor console but is done with the key off. Significant maintenance or repair time spent on any reactor component or system that prohibits reactor operation is included in Reactor Usage as Reactor Not Available.

Table 4, Part B gives a breakdown of the Type of Usage in Hours. The reactor facility receives compensation for Industrial Research and Service. University Research and Service includes both funded and non-funded research, for Penn State and other universities. The Instruction and Training category includes all formal university classes involving the reactor, experiments for other University and high school groups, demonstrations for tour groups and in-house reactor operator training.

Table 4, Part C statistics, Users/Experimenters, reflects the number of users, samples and sample hours per shift.

Table 4, Part D gives a summation of 8 Hour Shifts for each year.

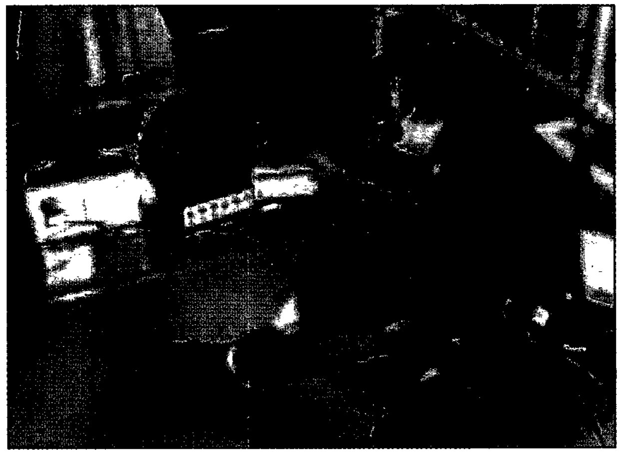

Thierry Daubenspeck, senior reactor operator, assists in performing a calibration proecedure.

INSPECTIONS AND AUDITS

During November 27-29 2006, Kevin Witt and Jessie Quichocho of the NRC conducted a routine inspection of reactor operations as conducted under the R-2 license. No issues of non-compliance were identified.

During September 5-21, 2006, an audit of the PSBR was conducted to fulfill a requirement of the Penn State Reactor Safeguards Committee charter as described in the PSBR Technical Specifications. The audit was conducted by Dr. Gordon Robinson, a Penn State Nuclear Engineering professor emeritus and former member of the PSBR Reactor Safeguards Committee. The reactor staff implemented changes suggested by that report, all of which exceed NRC requirements.

During June 4-7 2007, Kevin Witt, Johnny Eads and Patrick Issac of the NRC conducted a routine inspection of reactor operations as conducted under the R-2 license. A parallel security inspection was also performed. No issues of non-compliance were identified

TABLE 3

Reactor Operation Data
July 1, 2003 – June 30, 2007

		03-04	04-05	05-06	06-07
A.	Hours of Reactor Operation				
	1. Critical	1070	1034	851	882
	2. Subcritical	417	450	357	459
	3. Fuel Movement	6	16	38	1
B.	Number of Pulses	116	152	184	192
C.	Number of Square Waves	62	39	38	29
D.	Energy Releases (MWH)	736	657	539	582
E.	Grams U-235 Consumed	38	34	28	30
F.	Scrams				
	1. Planned as Part of Experiments	1	4	14	26
	2. Unplanned – Resulting From:				
	a) Personnel Action	1	3	0	0
	b) Abnormal System Operation	2	0	0	1

TABLE 4

Reactor Operation Data
July 1, 2003 – June 30, 2007

		03-04	04-05	05-06	06-07
A.	Reactor Usage Per Shift				
	1. Hours Critical	3.9	3.7	3.1	3.2
	2. Hours Subcritical	1.5	1.6	1.3	1.7
	3. Hours Shutdown	2.4	2.2	2.0	2.8
	4. Reactor Not Available	0.1	0.2	0.5	0
	TOTAL HOURS PER SHIFT	7.9	7.7	7.0	7.7
B.	Type of Usage – Hours Per Shift				
	1. Industrial Research and Service	3.5	3.0	2.3	3.0
	2. University Research and Service	1.4	2.0	1.6	1.7
	3. Instruction and Training	1.9	1.1	1.4	1.8
	4. Calibration and Maintenance	1.1	1.6	1.6	1.3
	5. Fuel Handling	0	0.1	0.1	0
C.	Users/Experiments Per Shift				
	1. Number of Users	3.2	2.9	2.6	3.5
	2. Pneumatic Transfer Samples	0.1	1.3	1.6	1.6
	3. Total Number of Samples	3.5	4.8	4.5	5.2
	4. Sample Hours	3.5	3.8	2.9	3
D.	Number of 8 Hour Shifts	273	282	269	274

Gamma Irradiation Facility

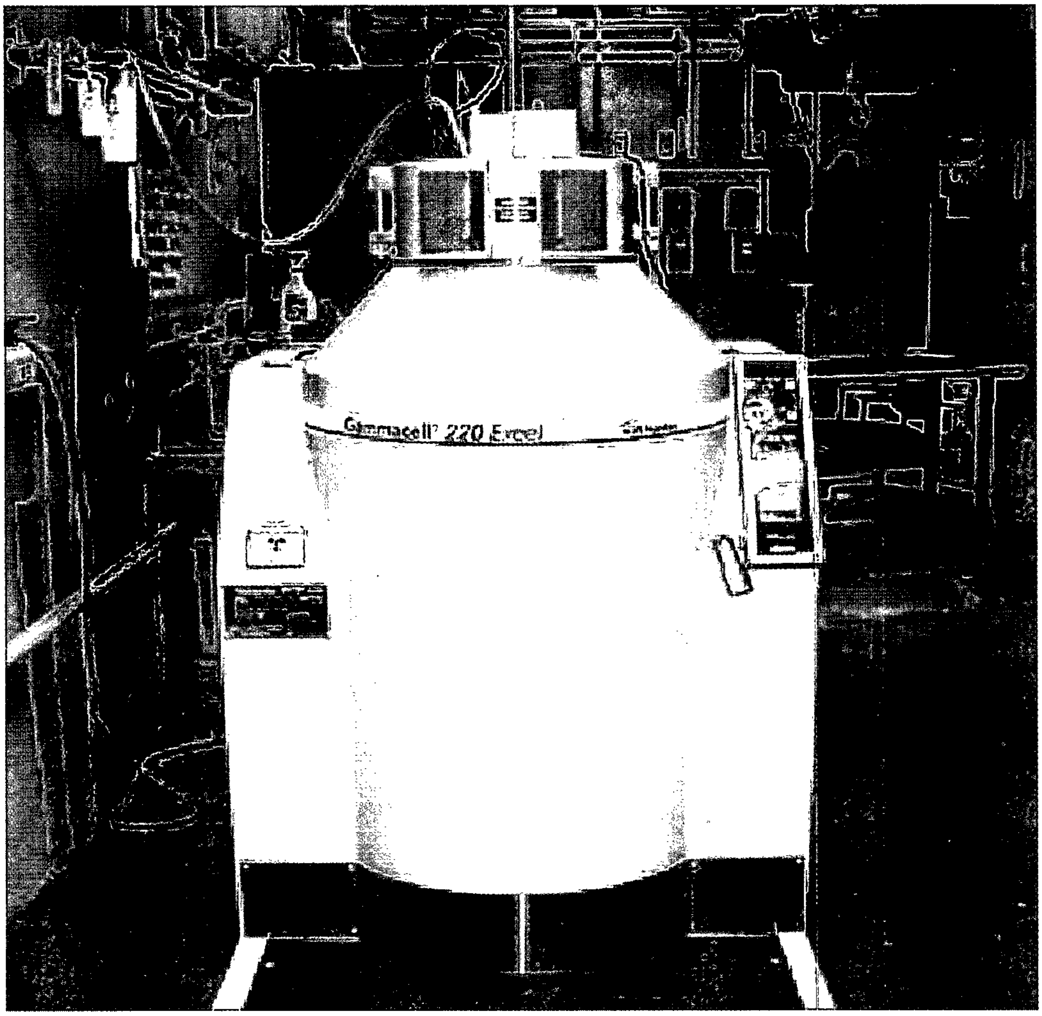

The Gamma Irradiation Facility includes in-pool dry tube irradiators and a separate lead-shielded stand-alone irradiator. This provides a great deal of flexibility for dose rates and irradiation configurations.

IN-POOL IRRADIATORS

For the in-pool irradiators, the source rods are stored and used in a pool that is 16 feet by 10 feet, filled with 16 feet of demineralized water. The water provides a shield that is readily worked through and allows great flexibility in using the sources. Due to the number of sources and the size of the pool, it is possible to set up several irradiators at a time to vary the size of the sample that can be irradiated, or to vary the dose rate. Experiments in a dry environment are possible by use of either a vertical tube or by a diving bell type apparatus. Four different irradiation configurations have been used depending on the size of the sample and the dose rate required. The advantage of the in-pool irradiators is that the dose rate can be varied in a manner which is optimal for agricultural and life science research. The variable dose rate has also allowed for several different set-ups for electronic testing of materials.

LEAD-SHIELDED IRRADIATOR

A new lead-shielded irradiator was acquired in July 2003 through funding from the U.S. Department of Energy INIE grant, replacing an older irradiator. This irradiator has the highest dose rate of all the irradiation chambers in the facility. Other advantages of the irradiator include a large irradiation chamber (approximately 6 inches in diameter and 7.5 inches high), an automatic timer to move the sample chamber away from the source and the ability to conduct in-situ testing of components during irradiation. The disadvantages are the inability to change the dose-rate significantly and the decay heat from the higher dose rate, which increases the temperature of the irradiation chamber.

USE OF GAMMA IRRADIATION SERVICES

There are many different applications utilizing gamma radiation from sanitization and sterilization, crosslinking and polymerization, F-center formation in crystals and cryogenic reduction of proteins. Several new projects involving other universities and industry were started over the past year. These projects required calibration of one of the dry irradiation tubes with radiochromic dosimeters. This calibration allowed for a lower dose-rate for electronic testing of components. Figure 2 shows some of the variety of samples and purposes for irradiations in the past. The total number of irradiations has been increasing steadily over the last few years while the irradiation hours have varied depending on the total dose requested. Other university and pre-college educational institutions utilized the gamma irradiation facility for research projects, INIE minigrant projects or the Reactor Sharing program. Several departments on campus utilized the services of the Gamma Irradiation Facility. This information is outlined in the Research and Service utilization section and in Appendix A. The past few years' utilization of the Cobalt-60 Irradiation Facility is compared in Table 5 and also in Figure 3.

TABLE 5

Cobalt-60 Utilization Data July 1, 2004-June 30, 2007							
		<u>04-05</u>	<u>04-05</u>	<u>05-06</u>	<u>05-06</u>	<u>06-07</u>	<u>06-07</u>
		Pool Irradiator	**Lead- Shield Irradiator**	**Pool Irradiator**	**Lead- Shield Irradiator**	**Pool Irradiator**	**Lead- Shield Irradiator**
A.	Time Involved (Hours)						
	1. Set-Up/Admin. Time	5	73	16	99	2	29
	2. Total Sample Hours	121	1267	441	4639	7	1653
B.	Numbers Involved						
	1. Total Irradiations	64	290	50	283	25	312
	2. Samples Containers Run[1]	638	1178	171	5212	37	1075
	3. Different Experimenters	14	32	17	46	11	43

[1] Sample containers can contain multiple samples, but are only counted as one sample.

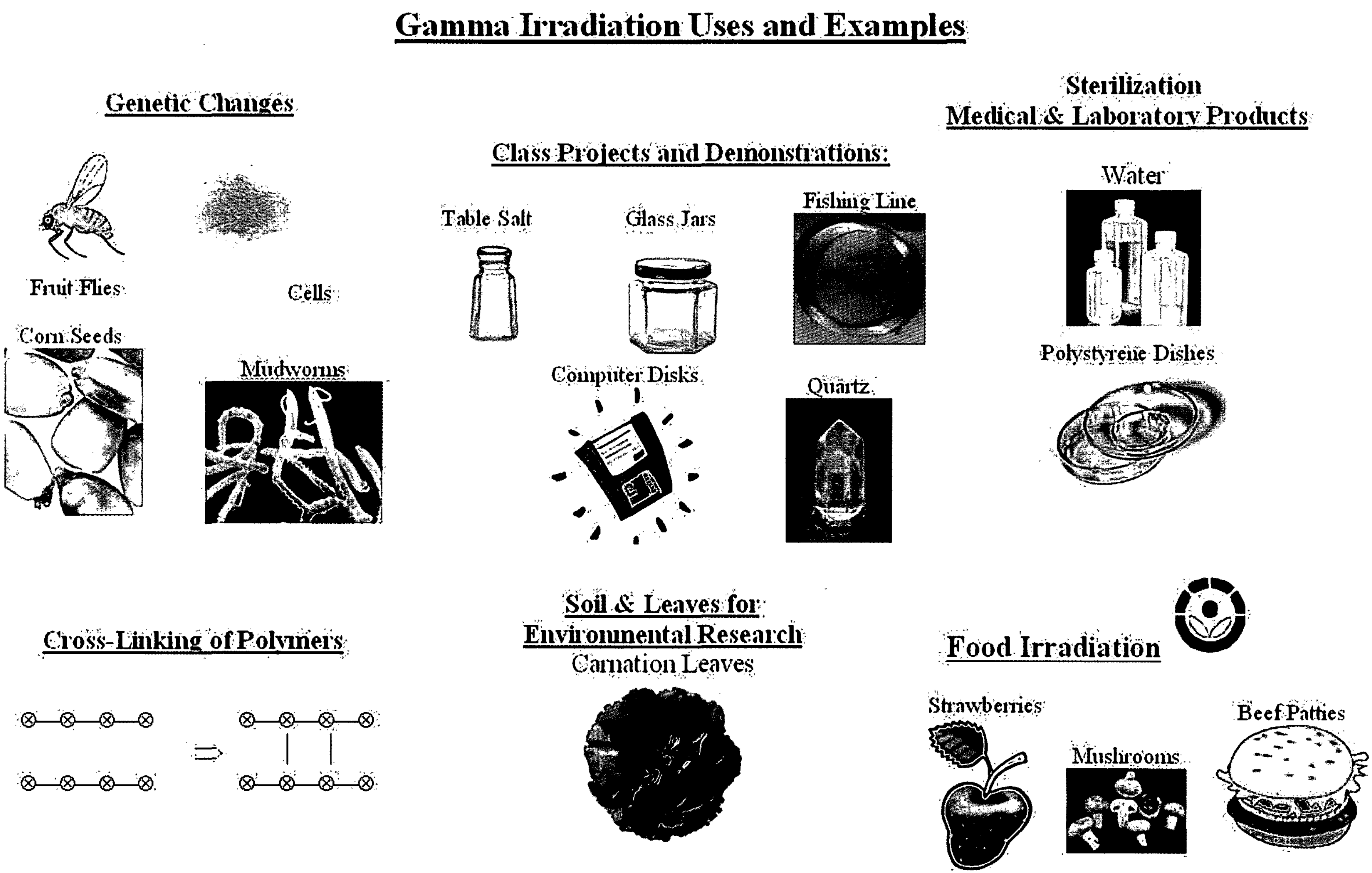
Gamma Irradiation Uses and Examples
Genetic Changes
Fruit Flies
Cells
Corn Seeds
Mudworms
Class Projects and Demonstrations:
Table Salt
Glass Jars
Fishing Line
Computer Disks
Quartz
Sterilization
Medical & Laboratory Products
Water
Polystyrene Dishes
Cross-Linking of Polymers
Soil & Leaves for
Environmental Research
Carnation Leaves
Food Irradiation
Strawberries
Mushrooms
Beef Patties

Figure 2

Figure 3

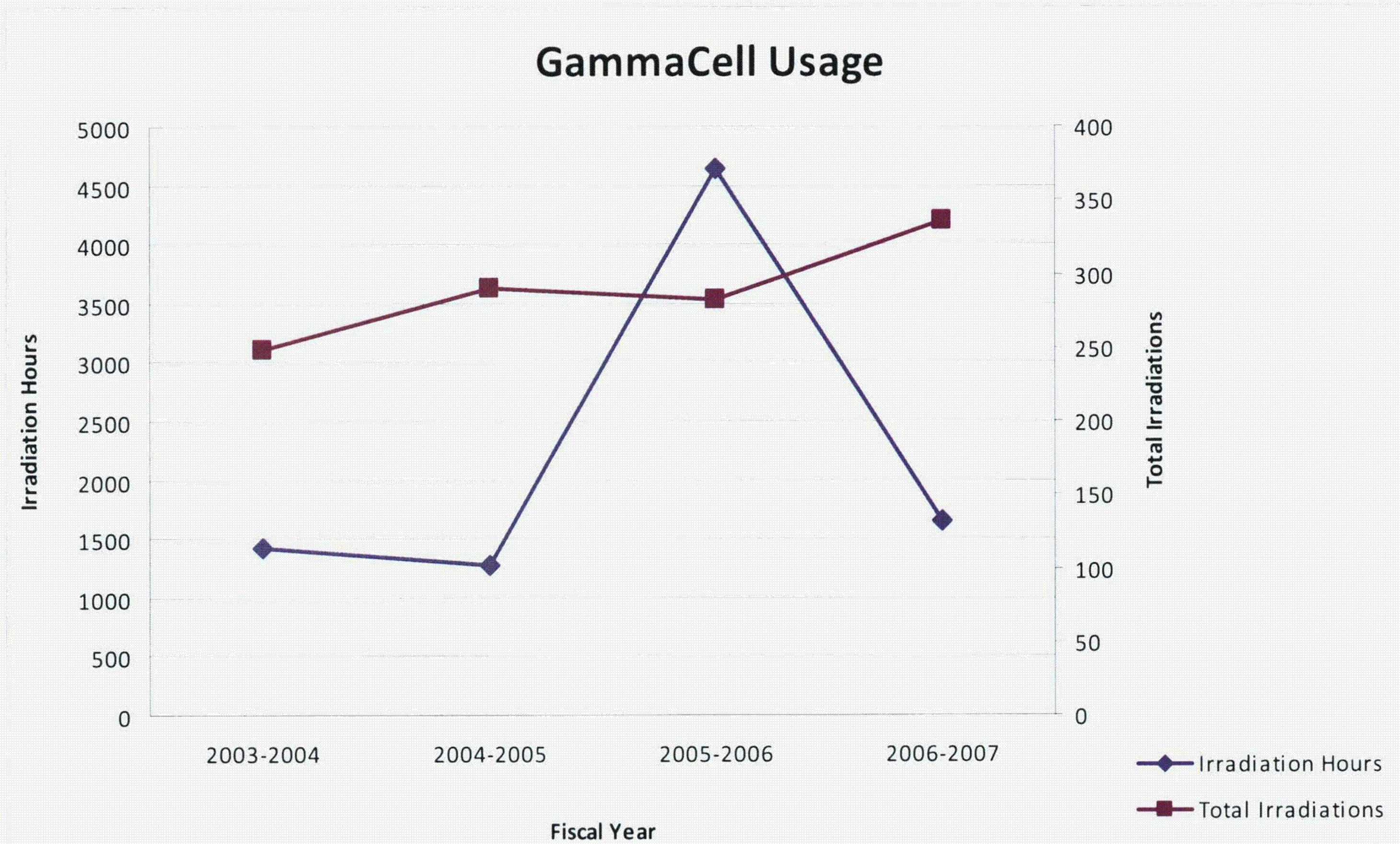
GammaCell Usage
Irradiation Hours
Total Irradiations
Fiscal Year
5000
4500
4000
3500
3000
2500
2000
1500
1000
500
0
400
350
300
250
200
150
100
50
0
2003-2004
2004-2005
2005-2006
2006-2007
Irradiation Hours
Total Irradiations

EDUCATION AND TRAINING

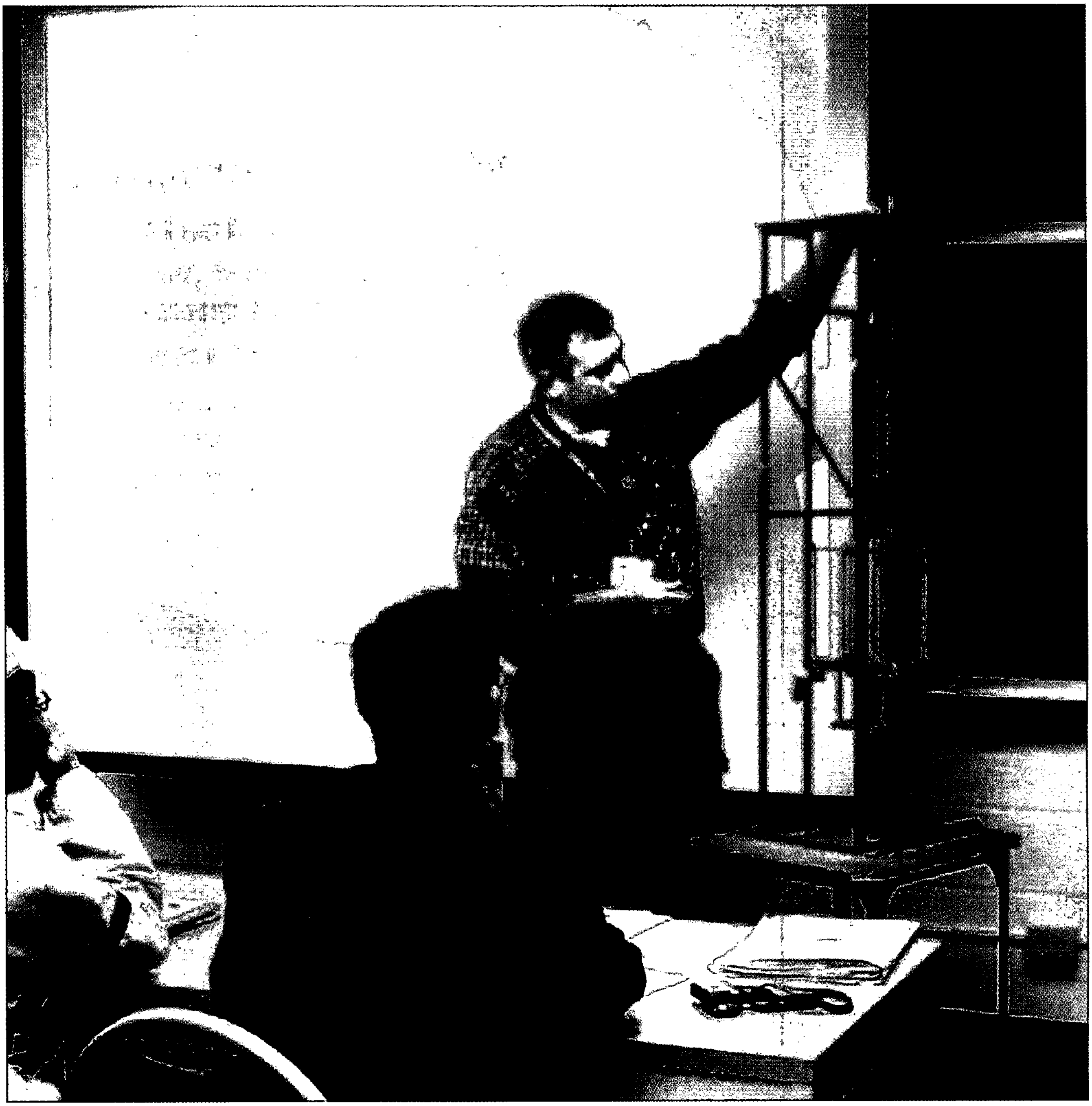

During the past year, Penn State's RSEC was used for a variety of educational services, in-house training, formal laboratory courses, and many continuing education programs and tours. The continuing education programs and tours accommodated over 2,700 visitors. The RSEC staff utilized the facilities and equipment to provide educational opportunities and tours for student and teacher workshops, many of which were conducted as part of other programs on campus. These programs are typically conducted through the Penn State College of Engineering, the Women in Science and Engineering (WISE) Institute, the Continuing and Distance Education Program, Campus Admissions and the University Relations Offices. The student programs included: the Upward Bound program, Pennsylvania Junior Academy of Sciences, PSU GREATT (Graduate Research and Education in Advanced Transportation Technologies) and other programs associated with campus activities.

RSEC STAFF and ANS STUDENTS ASSIST WITH BOY SCOUT MERIT BADGE

The Radiation Science and Engineering Center provided the setting for many of the photographs utilized in the new Boy Scout Nuclear Science Merit Badge Booklet, which was published in early 2005. Candace Davison was one of several ANS members who provided input into the new requirements. The Penn State ANS student chapter conducted several one-day workshops where scouts earned their Nuclear Science Merit badge. Three one-day workshops were conducted on Saturdays in December, March and April for a total of 252 scouts and leaders. The feedback from both the scouts and leaders was very positive concerning the experience. Students and staff also provided suggestions for the requirements of a nuclear science interest patch for Girl Scouts.

U.S. DEPARTMENT OF ENERGY – INIE MINI-GRANT

Several educational institutions participated in minigrant projects at the RSEC facility through the INIE minigrant process. The following is a synopsis of the institutions that participated in educational outreach and educational research projects utilizing the Penn State Reactor Facility. All of the participants traveled to the reactor facility to learn about nuclear applications and understand some of the procedures and equipment utilized in the projects. Some of the activities that were not funded by the mini-grant were covered by the Reactor Sharing program. The Central Virginia Governor's School conducted radiation laboratory experiments including half-life, cloud chambers, gamma spectroscopy instruction, and reactor demonstrations. Neutron activation analysis, neutron irradiation and neutron radiography were demonstrated, but this presented a problem in conducting projects due to the production of radioactive materials. Therefore, most of the projects involved gamma irradiation so the students could test the samples afterward. The Westinghouse Science Honors Institute (WSHI) conducted three Saturday programs during the fall of 2006 at Penn State. These programs included three main sessions conducted at the RSEC or the Academic Project building and a fourth session at Mount Nittany Medical Center. The sessions included: 1) radiation laboratory activity with cloud chambers and instruction on Instrumental Neutron Activation Analysis 2) reactor basics, tour of the gamma irradiation facility, and demonstration of a reactor pulse 3) research applications at the RSEC with a demonstration of neutron radiography and thermoluminescence concepts along with discussion of careers. Hollidaysburg High School and Elizabeth Forward High School students traveled to the reactor to participate in educational activities that could not be conducted at their schools. Students from Elizabeth Forward HS sent samples for Neutron Activation Analysis. Bloomsburg University faculty and students conducted gamma irradiation of electrical components and conducted NAA on these items.

An educational advisory committee was formed to provide input into the development of educational materials for the RSEC Educational Outreach Minigrant coordinated by Candace Davison. A group of teachers met at the facility and worked together using the PSU course management system, ANGEL, to interact and review materials. Progress was made toward the completion of many of the activities that educators can use which will be posted on the facility web-page.

REACTOR SHARING PROGRAM

The University Reactor Sharing Program is sponsored by the U.S. Department of Energy. The purpose of this program is to increase the availability of the university nuclear reactor facilities to non-reactor-owning colleges and universities. The main objectives of the University Reactor Sharing program are to strengthen nuclear science and engineering instruction, and to provide research opportunities for other educational institutions including universities, colleges, and pre-college schools.

Over 900 students and teachers from thirty-four different educational institutions and three colleges/universities came to the RSEC for experiments and instruction. This nearly doubled the participation compared to last year. Student Operator Interns - Adina LaFrance, Josh LaFrance, and Dennis Spielman assisted with tours and instruction on reactor operations. Nuclear Engineering students Daniel J. Skilone, Amy Miller, Doug Yocum, Mark Dorn, Zach VanHorn, and Korrie Yetzer assisted with instruction and provided information about their major during student visits. Danielle Hauck Schwarz provided instruction on INAA. Thierry Daubenspeck, Jana Lebiedzik and Brenden Heidrich provided instruction and technical assistance for experiments.

Several small research projects with faculty and students from the University of Pittsburgh at Greensburg were conducted during the academic year. Dr. Katrina Brown's students used neutron activation of wax and other samples looking for heavy metals and other elements. Reactor Sharing funding was also used to assist in the support of a University of Iowa project on selenium in toenail samples.

PENNSYLVANIA GOVERNOR'S SCHOOL FOR AGRICULTURAL SCIENCES

The twenty-first session of the Pennsylvania Governor's School for Agricultural Sciences (PGSAS) was held at Penn State's University Park campus during the summer of 2006. Sixty-four high school scholars participated in the five-week program at Penn State. The Governor's School for Agricultural Sciences includes introduction and experience in many different agricultural disciplines. The participants of the Governor's School received a tour of the Reactor facility with some time for hands-on instruction. Candace Davison, Doug Yocum and Dennis Spielman along with other licensed personnel assisted with the tours.

TOURS

Over 2,700 people toured the reactor facility during this reporting period. In addition to the full or half-day programs with experiments, educational tours were conducted for students, teachers and the general public. All groups, including those detailed in the above sections, that toured the facility are listed in Appendix B. The RSEC operating staff along with the Mechanical and Nuclear Engineering Department conducted several open house events for the Parent and Family Weekend, the general public and potential undergraduate or graduate students. Over 450 people participated in Open House and "Spend a Summer Day" experiences.

TRAINING PROGRAMS

The RSEC operating staff has maintained reactor operator competence and safe facility operation through training and requalification. During a two-year training cycle, theory, principles, regulations and actions needed for the safe operation of the reactor facility are covered. Training sessions during the year include lectures, exercises and tabletop drills. In-house reactor operator requalification consisted of an oral examination on abnormal events and emergency procedures, an operating test and a written examination. The exam set was administered in late 2006 and early 2007. During the months of December 2006, January, May and June 2007, Penn State University police officers were given training by Candace Davison and Dr. Sears at the RSEC to ensure familiarity with the facilities and to meet Nuclear Regulatory Commission requirements.

ACADEMIC INSTRUCTION

The RSEC supports academic instruction by providing information and expertise on nuclear technology topics, tours and experiments conducted at the facility and through the availability of specialized equipment and classroom/laboratory space.

The reactor classroom was utilized as the base of instruction for several courses including Freshman Seminar (Fall 2006 and Spring 2007) and NucE 497F. The TRIGA reactor and Cobalt-60 irradiation facilities were used by several Nuclear Engineering courses and courses in other departments of the university as outlined in the Table 6. NucE 450, 451, and 497F laboratories make extensive use of the reactor and associated facilities. NUCE 497F is a unique opportunity for students to have hands-on experience operating the reactor. Many times this course helps students to better understand and appreciate the classroom theory that they learn.

Fred Sears teaches the Reactor Operations Course, NucE 497F

Table 6

Semester	Course	Instructor	Students	Hours	Facility Hours
Fall 2006	Food Science 413	R. Beelman	22	0.5*	1.25
Fall 2006	STS (2 classes)		34/4	1	2.5
Fall 2006	Nuc E 001S- Freshman Seminar	J. S. Brenizer	16/18	2	37.5
Fall 2006	Nuc E 301- Fundamentals of Reactor Physics	R. M. Edwards	40	0.5	0.5
Fall 2006	Nuc E 401- Introduction to Nuclear Engineering	L. Hochreiter	13	0.5	0.5
Fall 2006	Nuc E 451-Experimental Reactor Physics	R. M. Edwards	16/12/16	24	18
Fall 2006	Nuc E 497F-Reactor Operations and Testing	C. F. Sears	3	60	23
Spring 2007	Bio Sci 415	Denise Woodward	30	0.5	0.75
Spring 2007	Nuc E 001S- Freshman Seminar	J. S. Brenizer	16	1	18.75
Spring 2007	Nuc E 450- Radiation Detection and Measurement	K. Unlu	28/19	4	12
Spring 2007	Nuc E 497F- Reactor Operations and Testing	C. F. Sears	5	67	23
Spring 2007	PSU – Altoona Chemistry	C.S. Reed	13	0.5	1

Note – Facility hours estimate the use of laboratory/classroom time for instruction and do not include the reactor time

NEUTRON BEAM LABORATORY

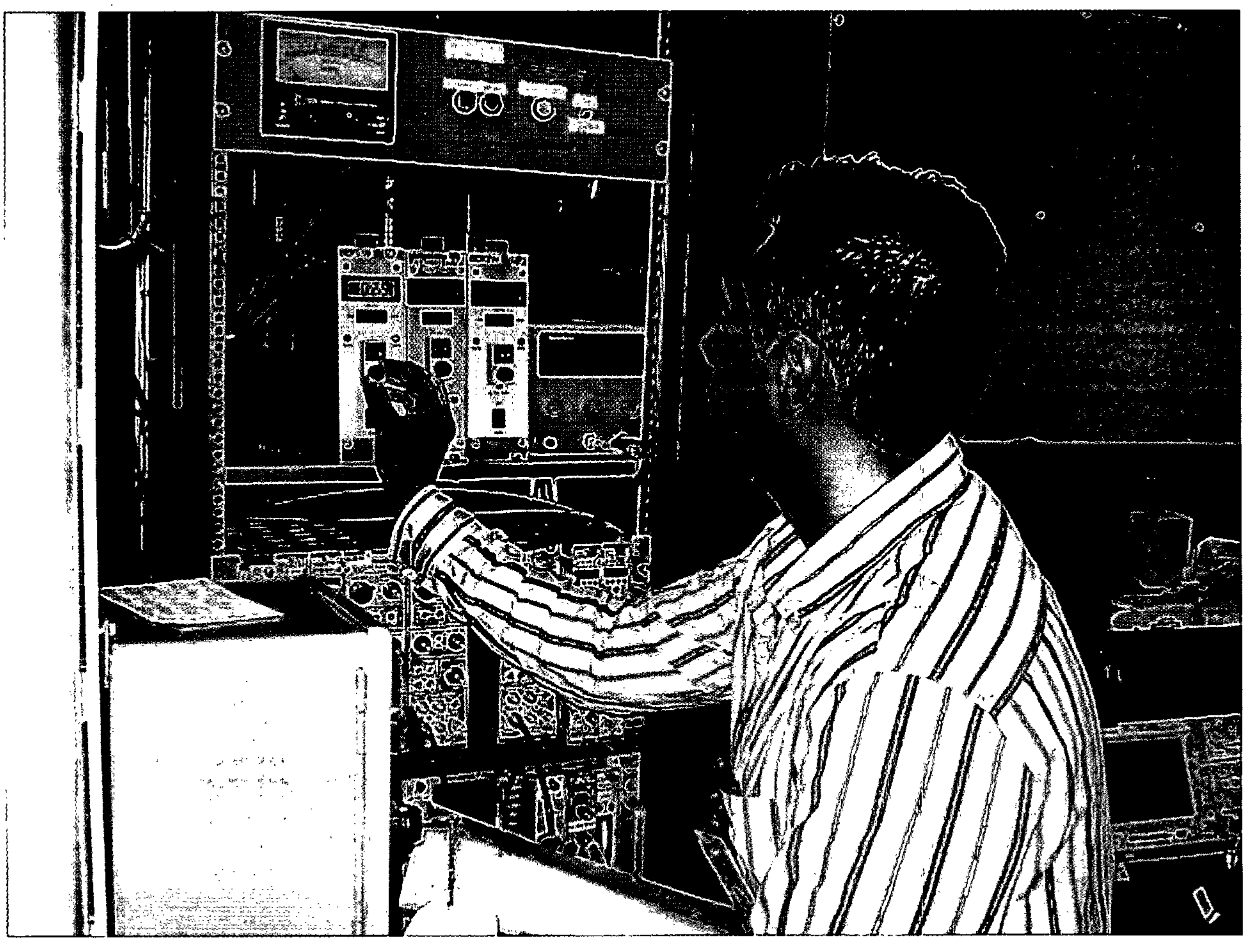

NEUTRON BEAM LABORATORY

The Neutron Beam Laboratory (NBL) is one of the experimental facilities at the RSEC. Well-collimated beams of neutrons, thermalized by D_2O, are passed into the NBL for use in various neutron beam techniques. When the reactor core is placed next to a D_2O tank and graphite reflector assembly near the beam port locations, thermal neutron beams become available for neutron transmission and neutron radiography measurement from two of the seven existing beam ports. In steady state operation at 1 MW, the thermal neutron flux is 1×10^{13} n/cm^{2}sec at the edge of the core and 3×10^{13} n/cm^{2}sec at the central thimble. The Penn State Breazeale Reactor (PSBR) can also pulse with the peak flux for maximum pulse ~ 6×10^{16} n/cm^{2}sec with a pulse width of 15 msec at half maximum.

Current Status of PSBR Beam Ports:

The PSBR has seven beam ports. The internal diameter of the beam ports are four inches for BP #3 and BP #5; five inches for BP #1 and BP #7; and six inches for BP #2, BP #4 and BP #6. The center of BP #4 is sixty five inches from the pool floor while BP #1, BP #3, BP #5 and BP #7 are sixty inches and BP #2 and BP #6 are fifty four inches from the pool floor. With the current setup of reactor-core-moderator assembly only BP #4 is at the centerline of the TRIGA core. (Active length of TRIGA fuel is 15"). BP #1, 3, 5 and 7 are five inches below the centerline of the core and BP #2 and 6 are eleven inches below the centerline of the core. The core grid assembly does not permit lowering the core more than the current arrangement. When the PSBR reactor was built, MTR type fuel elements with an active length of 24" were used. With the MTR fuel the beam port arrangement did not limit the maximum neutron output. In 1965, the PSBR was converted from MTR type to TRIGA type fuel. Because of these inherited limitations only two beam ports are currently being used. BP #4 with 3×10^7 n/cm^{2}sec flux at the aperture is used for research, primarily neutron radiography and radioscopy, and BP #7 with ~ 10^5 n/cm^{2}sec neutron flux is used for service activities involving neutron transmission measurements. Since the BP #4 collimators are primarily designed and optimized for neutron radiography and radioscopy measurements, it is not possible to obtain desired results for other measurements. We are currently trying to use BP #4 for all of our research projects. Due to space limitations, we must shuffle delicate research equipment around. More importantly, each project or experimental techniques require a special or dedicated neutron beam with different collimations and neutron flux.

New Beam Ports and Beam Hall Expansion:

Due to inherited design issues with the current arrangement of beam ports and reactor core-moderator assembly, the development of innovative experimental facilities utilizing neutron beams is extremely limited. Therefore, a new core-moderator location in the PSBR pool and beam port geometry needs to be determined in order to build useful neutron beam facilities. A study is continuing with the support of DOE-INIE funds to examine the existing beam ports for neutron output and to investigate new core and moderator designs that would be accessible by new additional beam ports. We envision a location in the pool where the reactor core would be "parked" and surrounded by a moderator (D_2O or graphite). New beam ports would be geometrically aligned with the core-moderator assembly for optimum neutron output.

The new core-moderator and beam port arrangement requires expansion of the existing beam laboratory in order to place instrumentation, neutron guides, beam catcher, etc. The new beam hall will have a total of 3,700 sq ft of experimental area (the existing area of ~1,000 sq ft plus a new additional area of ~2,700 sq ft). Also, about 3,100 sq ft of new office and meeting/classroom space will be added in the second floor of the expanded beam hall to support students and faculty working in this area.

Architectural plans for the RSEC expansion for a new Neutron Beam Hall and Neutron Beam Ports facilities are completed. Working with a professional architectural firm, a contractor, and related personnel from various university functions, we obtained a firm estimate for the expansion cost. Internal benefactors of the new neutron beam facilities are identified. We obtained support letters or expression of interests from about 30 faculty members from four different colleges within the university. More than half of the total budget for expansion is currently available, and efforts to raise the remaining portion of budget continue. The Penn State University has responded to US Department Energy's request for an Expression of Interest (EOI) April 2005 for the RSEC expansion for a new Neutron Beam Hall and Neutron Beam Ports. The response for the EOI submitted with active support and participation of the Dean of the College of Engineering and the Senior Vice President for Research. DOE did not act on this initiative up to this date. We are waiting for new DOE initiatives to proceed with this project.

Research areas envisioned for RSEC's new beam port/beam hall design are as follows. Neutron Depth Profiling facility for depth vs. concentration measurements, impurity determination of He-3 and B-10 in semiconductors, metal and alloys; Cold Neutron Source and Cold Neutron Prompt Gamma Activation Analysis for neutron focusing research, materials characterization and determination of impurities in historically or technologically important material; Neutron Powder Diffraction for structural determination of materials, and a Triple Axis Diffractometer to train students on neutron diffraction and perform preliminary structural determinations of materials.

Projects utilizing the NBL during the year included the following:

- Time-of-Flight Neutron Depth Profiling at the Penn State University Breazeale Nuclear Reactor, (see Research and Service Utilization Section)

- Testing Neutron-Induced Soft Errors in Semiconductor Memories (see Research and Service Utilization Section)

- Soft Error Analysis Toolset (SEAT) Development (see Research and Service Utilization Section)

- Study of Water Distribution and Transport in a Polymer Electrolyte Fuel Cell Using Neutron Imaging (see Research and Service Utilization Section)

- Neutron Imaging System Improvements (see Research and Service Utilization Section)

- Neutron transmission measurements and neutron radioscopy were conducted for borated metals and other borated materials for numerous companies.

- Radiographic and radioscopic techniques were demonstrated as part of several student projects; including demonstration of neutron and x-ray imaging for the Governor's School students and students enrolled in the freshman seminar (NucE 001S). The students assembled plaques containing a variety of objects and predicted their neutron & x-ray attenuation characteristics. Experiments with neutron & x-ray radiography confirmed their predictions.

RADIONUCLEAR APPLICATIONS LABORATORY

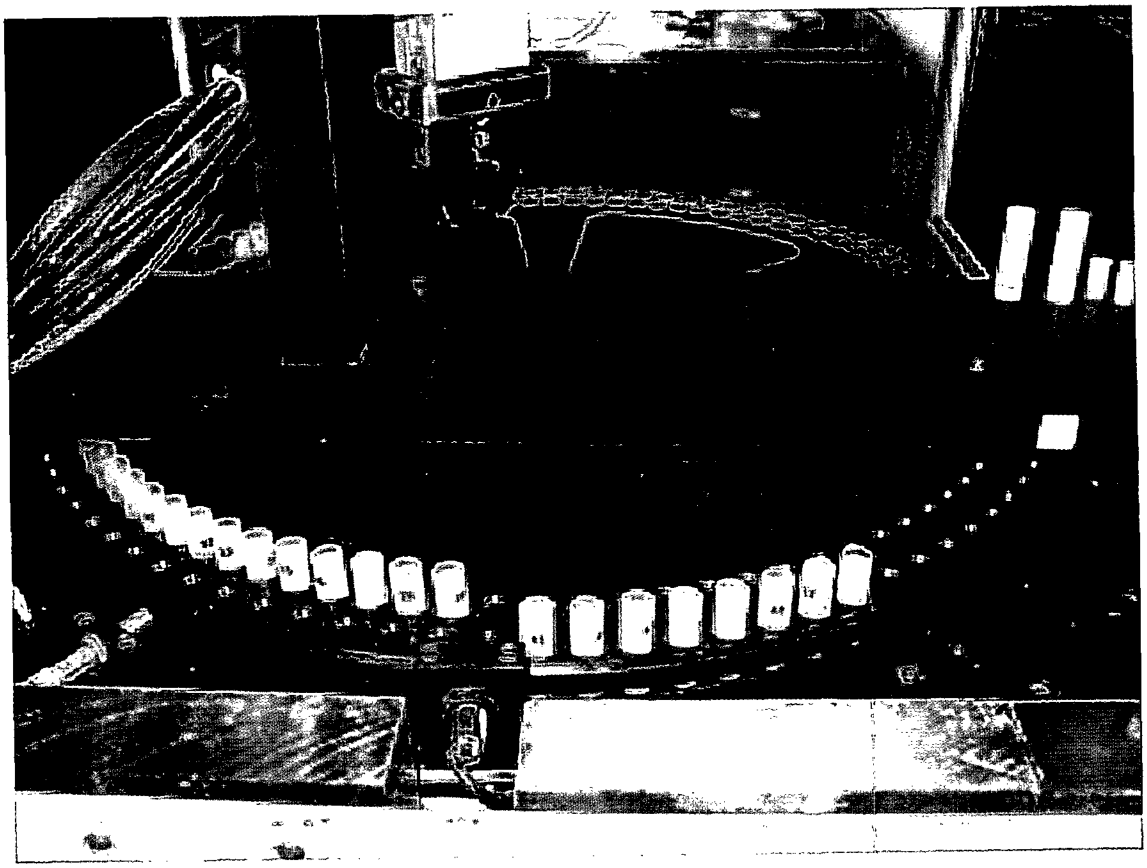

A. Service
B. Research

A. Service

The Radionuclear Applications Laboratory (RAL) provides consulting and technical assistance to University personnel who wish to use radionuclear techniques in their research. The majority of these research projects involve neutron activation, but the staff is also able to provide services in radioactive tracer techniques, radiation gauging, radiation processing, and isotope production for laboratory, radionuclear medicine or industrial use. Laboratory personnel support RSEC operations by performing analyses of water, air monitor filters, and other samples as needed.

439 semiconductor irradiations were performed at the RSEC for various companies during the past year. Devices were prepared for irradiation, irradiated and shipped back in accordance with NRC and DOT regulation. After the irradiation and prior to shipment, the 1-MeV Silicon Equivalent fluence received by the devices was calculated and determined. The radioisotopes produced in the devices were also determined by gamma analysis prior to shipment.

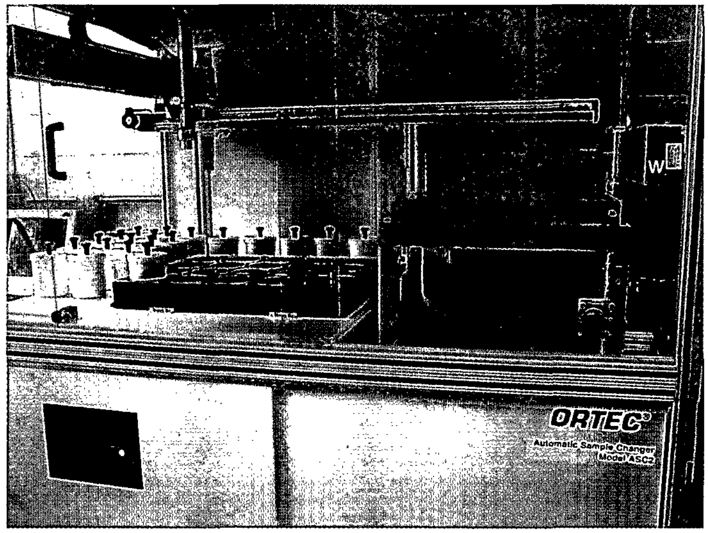

Ortec Automatic Sample Chamger used for long-lived isotopes.

A new chemical was analyzed, tested and approved for radioisotope production. Test runs were made on a Manganese- Doped Fluid Cracking Catalyst (FCC) to be used for industrial tests. The facility performed 29 isotope production runs of Sodium-24, Bromine-82, Argon-41 and Manganese-56.

The RAL assisted 3 different persons from the Materials Research Institute requiring our Neutron Activation Analysis (NAA) services. These samples included various soil, rock and CVD diamond samples. The samples were irradiated and concentrations of various elements were determined.

NAA was also performed for various high schools and colleges. One high school's project involved NAA on environmental samples to investigate pollution. A University of Pittsburgh at Greensburg project had students providing wax, wick, and filter paper for NAA. The University of Iowa continued its NIH project involving NAA of toenail samples.

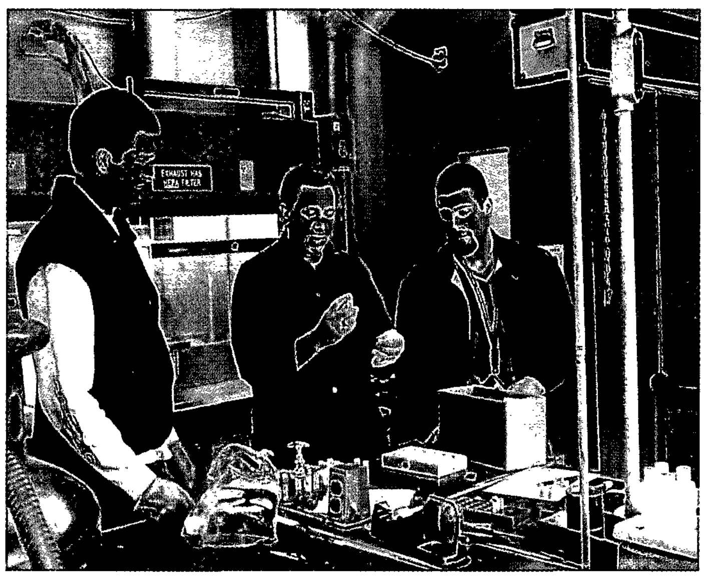

Thierry Daubenspeck, activation analysis and utilization specialist/ senior reactor operator explains Pneumatic Transfer system to students from the University of Pittsburgh

B. Research

The main research oriented activity taking place at the RAL is a continued study in dendrochemistry using Neutron Activation Analysis (NAA). Dendrochemistry refers to the compositional analysis of tree rings for environmental or pollution studies. The objective of the dendrochemistry project at RSEC is to determine the correlation between environmental stress and trace element uptake by trees. NAA provides parts-per-million to parts-per-trillion sensitivity on all isotopes that have been identified in tree-rings so far.

The dendrochemistry study began at RSEC in 2003 when it was transferred from the Ward Center for Nuclear Sciences at Cornell University. Since then four long tree chronologies (each over 350 years in length) and five short chronologies (each 30 to 60 years in length) have been analyzed for several environmentally significant isotopes. For more information on the dendrochemistry project in the past year see Page 81 of this report.

The Compton Suppression System (CSS), was purchased in 2005 to compliment the other NAA facilities already available in the RAL. The main use of the CSS will be for the dendrochemistry project. However, it is available for other research projects which require gamma spectroscopy with the added benefit of Compton suppression. In the past year this system has been validated through comparison with NIST standards and other NAA systems already active at the facility. A 60 year tree chronology which dates to the eruption of Thera, c. 1630 BC, has been analyzed for its gold content. For more information on the CSS see page 54 of this report.

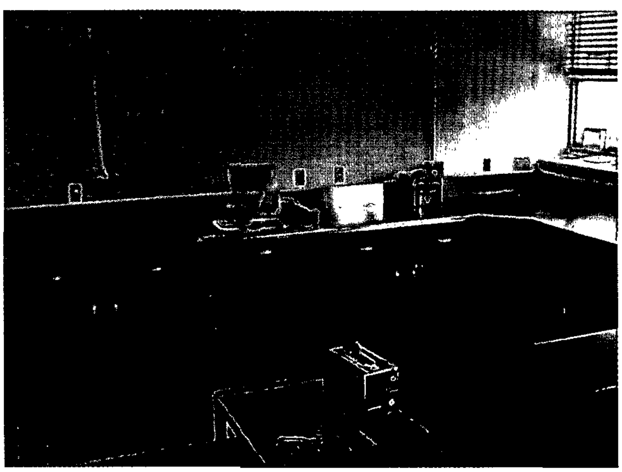

Figure 1: Room 4 - Sample Prep Laboratory

A new addition to the RAL (shown in Figure 1) is a sample preparation area located in Room 4. This area can be used for the temporary storage of radioactive samples and preparation for counting. A semi-permanent work area has been set up with shielding (lead bricks and leaded Plexiglas) and beta containers.

To summarize, the NAA facility now includes two in core dry irradiation tubes, a high-purity germanium detector with an associated Automatic Sample Handling System, the Compton Suppression System and the associated hardware and software for these systems. The RAL also contains a fume hood with a pneumatic transfer system and a sample preparation area.

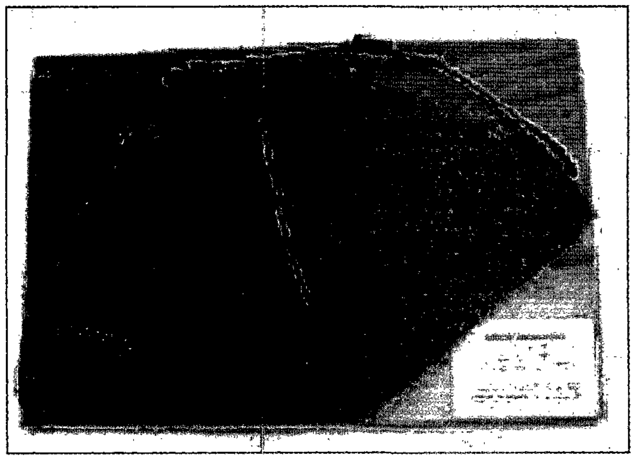

A tree sample from Istanbul, Belgrade Forest. The innermost pin is placed at 1800 A.D., other pins follow at 5o-year intervals.

Environmental Health and Safety

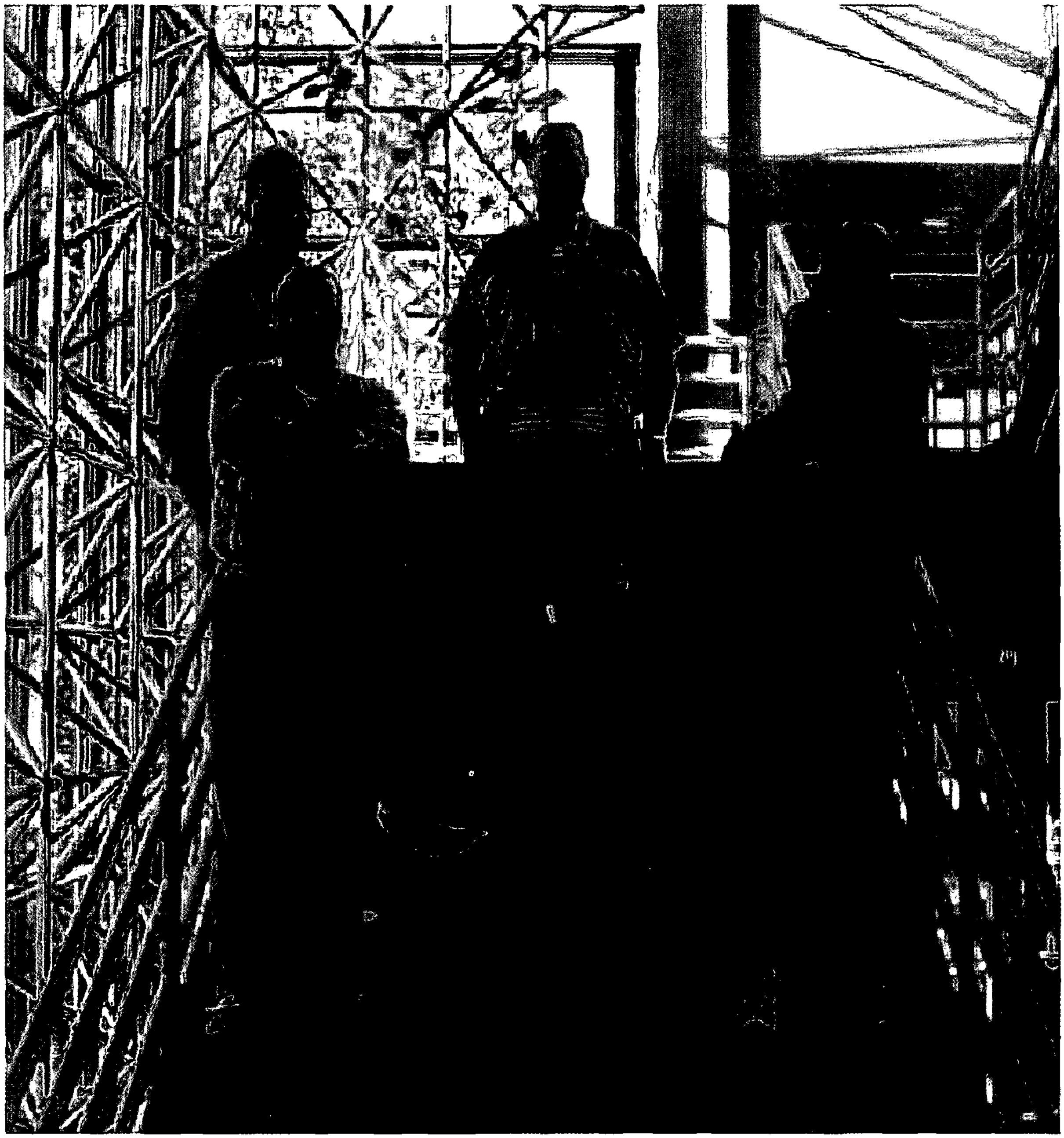

Environmental Health and Safety (EHS) is an active participant in ensuring the overall safety of the Radiation Science and Engineering Center (RSEC) operations. The RSEC and EHS are committed to the health and safety of the environment, public, students and employees. EHS is responsible for the overall administration of the radiation safety program for The Pennsylvania State University. The University is licensed by the U.S. Nuclear Regulatory Commission (NRC) to receive, acquire, possess, and transfer byproduct material (radioactive material produced by a nuclear reactor), source material (naturally occurring radioactive material, uranium compounds), and special nuclear material (radioactive material that has the potential to undergo nuclear fission) and to operate the Breazeale Nuclear Reactor at the Radiation Science and Engineering Center. The College of Engineering has administration responsibility for the reactor operations license (R-2 license).

The ALARA radiation protection philosophy, keeping the radiation exposure As Low As Reasonably Achievable, is the basis for the RSEC and EHS radiation protection and safety programs. Both groups collaborate to maintain the highest level of health and safety programs necessary for the administration of nuclear programs and compliance with federal and state regulations

Services provided to the RSEC fall into the following categories: ALARA programs, customer service, licensing and regulatory requirements, and training.

ALARA Programs

This year EHS performed over 118 radiation surveys at the RSEC. Survey results showed that all radioactive material was being handled in a safe and controlled manner. The surveys were conducted to detect possible transferable contamination from radioactive materials work or to survey radiation sources such as activation products, sealed sources, equipment, and reactor operations. The radioactive contamination surveys are performed in laboratories where radioactive materials are used and in the balance of the RSEC's public areas to ensure that no radioactive material has been transferred to these areas. Both the contamination surveys and the radiation surveys are redundant to the surveys performed routinely by the RSEC staff. The redundancy of the contamination and radiation surveys is fundamental to the University's ALARA program.

EHS also performs radiation surveys prior to approving any new procedures, changes to existing procedures, or modifications to radiation shielding that may affect the normally expected radiation levels.

EHS staff regularly attend scheduled RSEC operation meetings. The meetings provide a forum for participants to review the current reactor operations and experiments. This active participation has established an open line of communication between the RSEC and EHS. Input by the radiation protection staff has contributed to the facility's safety and ALARA programs.

Service

EHS is responsible for ensuring the safe packaging and shipping / transfer of radioactive materials (RAM) to customers of the RSEC. The U.S. Nuclear Regulatory Commission and U.S. Department of Transportation mandate complex requirements for the packaging, shipping and transfer of radioactive materials. EHS shipped 24 RAM shipments to RSEC customers. Customer support included packaging and shipping Ar-41, Br-82 and Na-24 for TracerCo. and Na-24 for NWT Inc. All containers were packaged, labeled, surveyed, and documented in accordance with applicable federal regulations. The shipping and transfer of radioactive materials includes the disposal of reactor radioactive waste materials.

Mark Linsley of radiation protection surveys samples in a laboratory

During June 2007 a team of EHS staff, representing various disciplines, worked with the College of Engineering to perform safety audits of all the engineering departments and facilities. Only relatively minor safety items were identified during the audit of the RSEC. The list of items identified was corrected by reactor staff within a few days of the inspection. EHS staff also assisted RSEC staff with improvements made to the Ar-41 production system and improved methods for handling irradiated electronic components.

Licensing and Regulatory Requirements

Dosimetery requirements are administered by EHS and dosimetry is issued to RSEC personnel to measure staff, student, and worker radiation exposures. This year EHS issued a total of 672 dosimeters to RSEC personnel, all were below established limits. Administration of the dosimeter program includes issuing dosimeters, processing dosimeters and maintaining all dosimetery records. EHS has administered a thermal neutron dosimeter program to check exposures more accurately for those working around the neutron radiography laboratory. One neutron dosimeter is a permanent fixture in the laboratory, and individuals wear the others as they work in the lab. A total of hundred and twenty thermal neutron dosimeters were monitored with no indication of any measurable thermal neutron exposures to personnel. Self-reading dosimeters are issued to transient persons and visitors to the RSEC. The information for the temporary dosimetry is documented in logbooks maintained by the administrative staff at the facility.

HazMat Training being conducted by the Penn State HazMat Response Team

The Radiation Safety Officer (RSO) is a member of the Reactor Safeguards Committee. Eric Boeldt, the RSO, has taken an active role in the Safeguards Committee and has provided guidance and input regarding many reactor safety issues brought to the committee's floor this year.

Training

Training programs provided by EHS to the RSEC are license and regulatory driven. Forty seven new reactor personnel and students attended the radiation safety orientation. Required retraining for all radiation workers was provided to the RSEC by means of a newsletter distributed to all laboratory supervisors. All RSEC personnel also completed the annual Chemical & Chemical Waste Refresher Training. In September EHS provided Preparedness, Prevention, and Contingency (PPC) plan training to RSEC personnel. The RSEC has a history of being in compliance with Penn State's Chemical & Chemical Waste Handlng programs.

Dave Bertocchi of radiation protection and Thierry Daubenspeck, senior reactor operator, load a shipment of RAM

RADIATION SCIENCE AND ENGINEERING CENTER

RESEARCH AND SERVICE UTILIZATION

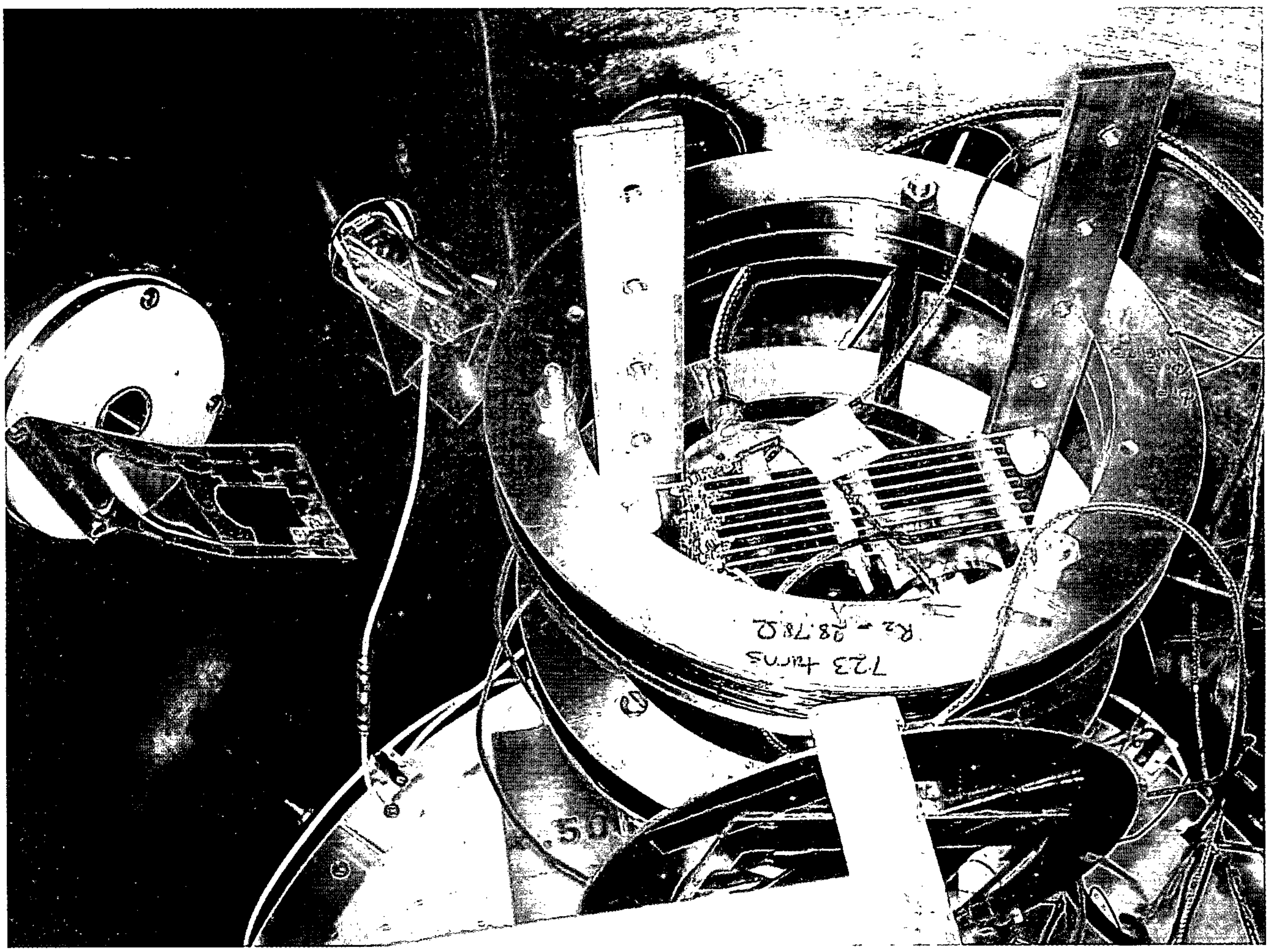

Research and service continues to be a major focus of the RSEC. A variety of research and service projects are currently in progress as indicated on the following pages. The university-oriented projects are arranged by department in Section A. Theses, publications, papers and technical presentations follow the research description to which they pertain. In addition, Section B lists users from industry and other universities.

The reporting of research and service information to the editor of this report is the option of the user and therefore the projects in Section A and B are only representative of the activities at the facility. The examples cited are not to be construed as publications or announcements of research. The publication of research utilizing the RSEC is the prerogative of the researcher.

Appendix A lists all University, industrial, and other users of RSEC facilities, including those listed in Sections A and B. Names of personnel are arranged under their department and college or under their company of other affiliation. During the past year, 39 faculty and staff members, 37 graduate students, and approximately 235 undergraduate students have used the facility for education, research and service activities. This represents a usage by 17 departments or sections in 4 colleges of the University. In addition, 58 individuals from 33 industries, research organizations, other universities, or high schools used the RSEC facilities.

SECTION A. PENN STATE RESEARCH UTILIZING THE FACILITIES OF THE RSEC

COLLEGE OF ENGINEERING

MECHANICAL AND ENGINEERING DEPARTMENT

NE 497F, REACTOR OPERATIONS AND TESTING LABORATORY

Participants: C.F. Sears, Professor and Director, RSEC

NE 497F is a three-credit laboratory course which provides students the opportunity to individually operate the Penn State TRIGA Reactor and perform selected reactor experiments including checkout, approach to critical, numerous startups, power operations in manual and automatic control, power coefficient measurements, rod worth measurements both manually and with a reactivity computer, reflector measurements and pulse operations. This brings a hands on applications to their analytical and theoretical class work.

NE 450, UNDERGRADUATE LABORATORY-RADIATION DETECTION AND MEASUREMENT

Participants: K. Ünlü, Professor and Associate Director for Research, RSEC

Services Provided: Laboratory Space, Machine Shop, Electronics Shop, Reactor Instrumentation and Support Staff

The Nuclear Engineering 450 course is the first of two three-credit laboratory courses required of all Penn State nuclear engineering undergraduates and is typically taken during the Spring of the junior year. Each weekly laboratory exercise consists of two lectures and one laboratory session. NucE 450 introduces the student to many of the types of radiation measurement systems and associated electronics used in the nuclear industry as well as many of the mathematical techniques used to process and interpret the meaning of measured data. The radiation instruments studied in this course include GM detectors, gas flow proportional counters, NaI (Tl) detectors, BF3 counters, ion chambers, wide range GM detectors, high-purity Germanium detector and gamma spectroscopy, and surface barrier detectors. The data collection and analysis techniques studied include radiation counting statistics, gamma ray and charged particle spectroscopy, and the interfacing of computers with nuclear instrumentation.

The wide range GM detector and BF3 detector are studied in the Cobalt Irradiation Facility. Ion chambers are studied with the reactor.

NE 451, UNDERGRADUATE LABORATORY OF REACTOR EXPERIMENTS

Participants: R.M. Edwards, Professor

Services Provided: Laboratory Space, Machine Shop, Electronics Shop, Neutron Irradiation Using Subcritical Pile, Reactor Instrumentation and Support Staff

The Nuclear Engineering 451 course is the second of two three-credit laboratory courses required of all Penn State nuclear engineering undergraduates and is typically taken during the Fall of the senior year. Each weekly laboratory exercise consists of two lectures and one laboratory session. By the beginning of the senior year, the students have already covered the LaMarsh Introduction to Nuclear Engineering text including reactor point kinetics. The 451 couse emphasizes experiments using the instrumentation that was covered in Nuce 450 and is divided into two "tracks". These tracks can be coarsely described as TRIGA and non-TRIGA experiments. The non-TRIGA track includes three graphiite pile experiments.

In 2003, the TRIGA track included:

1. Digital Simulation of TRIGA Reactor Dynamics
2. Large Reactivity Insertion (Pulsing)
3. Control Rod Calibration
4. Reactor Frequency Response
5. Neutron Noise
6. Reactor Control
7. Source Effects and Feedback

The laboratory utilizes Macintosh computers with GW Electronics MacAdios Jr. data acquisition hardware and Superscope II software. The Superscope II software was a major software upgrade for 1993, and with its new point-by-point seamless mode enabled effective reactivity calculations and control experiments. The Mathworks SIMULINK simulation software was used for the digital simulation exercise for the first time in 1992. Reactor control is offered as a graduate course in our department but our undergraduates do not receive a complete introduction to feedback control. The reactor control experiment interfaces a general purpose PC computer to an Experimental Changeable Reactivity Device (ECRD). Control experiments make use of one of two ERCD's implemented as a moveable experiment where an aluminum tube containing an absorber material is positioned within the central thimble of the reactor. The first ERCD with a worth of approximately $0.35 has a maximum insertion rate of about $0.12/s while the second with a worth of about $0.94 may be inserted up to $0.35/s. ERCD #1 is used for experiments of up to 65 percent where temperature changes produce significant reactivity changes. ERCD #2, added in 2000, is for use at low power (less than 0.1 percent) where temperature change and its reactivity effect are negligible. The SIMULINK Real Time Workshop is used to implement an experimental control algorithm. The SIMULINK automatic C code generation process produces and downloads the necessary real-time program for execution in a microprocessor-based controller with an ETHERNET network interface to the host workstation.

The 1994 version of the control experiment thus unified all of the MATLAB/ SIMULINK instruction earlier in the course into a demonstration of state-of-the-art CASE-based control system design and implementation.

MATERIAL SELECTION AND DEVELOPMENT OF ULTRA-HIGH-SPATIAL-RESOLUTION NEUTRON IMAGING SYSTEM

Participants: J. Brenizer, Prof. Mechanical and Nuclear Engineering Dept.
T. Mayer, Prof. of Electrical Engineering

Overview

The spatial resolutions of current neutron imaging techniques are at best on the order of tens of microns. Such techniques are hindered by many different factors. Methods utilizing gaseous amplifiers are constrained by electron cloud interference – scintillators are limited by light cones – digital methods are restricted by pixel size. All these factors limit the application of such techniques to imaging scenarios at a rather macroscopic level, compared to the spatial resolution of techniques such as XRD, TEM or AFM. However, due to the atomic and nuclear properties of materials, XRD, TEM, and AFM cannot adequately provide investigators with all the information they might wish to obtain from a specimen. We are working on a new neutron imaging method that will allow for non-destructive testing while at the same time providing information not available with traditional sub-micron imaging methods.

The proposed solution involves using neutron converting materials deposited in thin films combined with position sensitive cross-delay-line amplifiers (XDLA) mounted on the back of standard multichannel plates (MCP) arranged in a predetermined geometry around the thin film(s). Neutrons penetrate the converter film, interact with a neutron sensitive isotope in the material, and as a result of this interaction, two charged particles are diametrically emitted. The spatial resolution of the XDLA and the precise timing information one can obtain with modern nuclear instrumentation coupled with a good understanding of charged particle physics, allows this method to achieve the desired sub-micron spatial resolution.

Method

As mentioned above, the entire premise for this imaging technique hinges upon a nuclear reaction, an inelastic scattering event, between a neutron and a neutron sensitive isotope, from which two charged particles are diametrically emitted. For example, a ^{6}Li inelastic neutron scatter is described by the equation:

$$^{6}Li + n \xrightarrow{yields} {}^{4}He\,(\alpha) + {}^{3}H + 4.78\ MeV$$

A simpler representation of such an equation takes the form: $^{6}Li(n,\alpha)^{3}H$. The basic geometry for the experimental setup is shown in Figure 1 below.

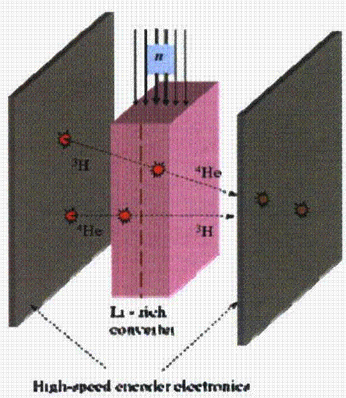

Figure 1: Experimental setup geometry for the high resolution neutron imaging system. Converter film sandwiched between the two XDLAs or encoders. (Not to scale.)

As seen in Figure 1, after the reaction occurs, the two charged particles are incident on the encoder electronics. It should be noted that the entire system will be under vacuum, minimizing the chance for a charged particle to interact after escaping the converter film before reaching an encoder. The lighter ion, regardless of where the neutron interacts within the converter, will always reach its respective encoder before its heavier counterpart. Take note that there is no preferential emission angle for either particle, other than always being emitted diametrically to each other. Because of this and geometry constraints, not every interaction will produce particles that strike encoders.

Three pieces of data are obtained from each interaction that results in both particles striking the encoders. The encoders are position sensitive. Detection of one charged particle will produce one set of (x,y) coordinates, the detection of the other will produce a second set of (x,y) coordinates. These two sets of coordinates will enable us to construct a ray trace through the converter, on which we know the neutron interaction must have taken place. The other piece of information results from our knowing that the lighter particle will always be the first to reach an encoder, regardless of where it is produced in the converter. We will use the detection of this particle as a "start" signal in our timing circuit. The detection of the second within a specific time window will indicate a coincidence event has occurred, and we will use this particle's detection as a "stop" signal. The duration of time between the start and stop signal, combined with our knowledge of the charged-particle-stopping power of the converter material, will allow us to calculate whereupon the predetermined ray trace the neutron interaction occurred. Once this information is established for every detectable coincidence event, we will perform line integration along the direction of neutron travel through the converter (shown in Figure 1 with the black arrows) thereby establishing a 2-D image of whatever object was placed in front of the converter (above Figure 1).

Thin Film Material Selection

A limiting factor for the selection of a material for the thin converter film is that the material must contain some element or isotope for which there is a high probability of a neutron interaction producing a charged particle pair. Other factors such as material strength, durability, reactivity, etc. are also very important properties. Along the lines of material strength and durability, the chosen material must also be able to be "free standing", which means that a significant portion of the surface area of the film must be free from the substrate upon which the film is deposited. This must hold for both sides of the film. This feature is necessary to ensure that both charged particles can travel from the converter to the encoders. Charged particles have a finite range in matter, which is strongly dependent on the atomic number (Z) of the charged particle or ion, and the elemental composition of the material through which the particle is travelling. The higher the electron and physical density, the shorter the particles' ranges. Ergo, the thickness of the film is a function of these two densities.

Several isotopes have high neutron interaction cross sections. In our case, we desire the product of the reaction to be a charged particle pair. Table 1 below shows some of the various isotopes that have been considered to date.

Table 1: Nuclear properties of isotopes considered for the neutron converter film.

Reaction	Cross section (barns)	Light particle Energy (keV)	Heavy particle energy (keV)
$^3He(n,p)^3H$	533	572	191
$^6Li(n,\alpha)^3H$	940	2727	2054
$^{10}B(n,\alpha)^7Li$	3837	1472	840

Of these isotopes, ^3He is the least viable as it is expensive and extremely difficult to contain due to its highly diffusive nature. Many materials containing either ^6Li or ^{10}B have been considered for the neutron converter. To date, the Li containing materials that have been considered are: Lithium Niobate, Lithium Fluoride, and Lithium metal. Also, the materials containing B that have been considered include: borosilicate glass (BSG), borophosphosilicate glass (BPSG), and boron metal.

The best materials from a nuclear physics viewpoint are Li containing materials. The particles produced from the $^6Li(n,\alpha)^3H$ reaction each have sufficient energy to escape LiF/$LiNbO_3$ film of up to 4.5 μm thick and a Li metal film of over 20 μm thick. We aspire to maximize the thickness of the film in order to increase the available viewing area while ensuring that both ions escape. However, due to difficulties with maintaining a free standing structure with the desired film thickness using LiF/$LiNbO_3$, not to mention the very reactive nature of Li metal, a more suitable material is necessary to at least complete the proof-of-principle experiment for this concept. That material is BSG, or as an alternative, BPSG.

Borosilicate glasses have the desired physical properties required for such a film, and with the naturally high ^{10}B isotopic ratio (~20%), no additional B doping of the films is required until later in the project. The drawback to this material is the high Z number of the ^{10}B reaction products, a He and L ion, which drastically reduces the range of the charged particles in the glasses. The maximum range of a Li ion in BSG is approximately 2 μm, thereby limiting the thickness and viewing area of the converter. A possible solution is to arrange multiple films in a step geometry, as is shown in Figure 2.

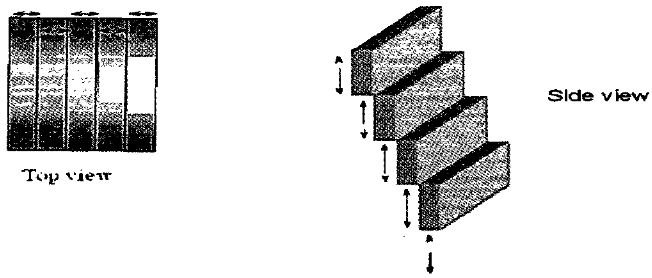

Figure 2: Top and side view of the proposed step geometry using BSG.

The step geometry allows the experimenter to greatly increase the available viewing area while compromising nothing in terms of spatial or timing resolution. Discussions about how such a design might be practically achieved have yielded some interesting and optimistic results. For the time being, BSG/BPSG will continue to be viewed as the primary material, at least for the proof-of-principle experiment; although, if a more feasible method for depositing and maintaining LiF or $LiNbO_3$ films becomes available, we will certainly reconsider the notion of utilizing these materials.

Applications of the technique

Several practical applications for this experimental technique have already been proposed; of which, one of the most exciting being the imaging of biological cells for cancer research. The idea involves placing multitudes of cancer cells, into which cancer treating drugs have been introduced, in front of the converter and imaging the cells to determine what effects are brought about by the drugs. This concept has the possibility of creating a paradigm shift in our understanding and application of medical, as well as non-medical, neutron imaging techniques.

COMPTON SUPPRESSION SYSTEM (CSS) at PSU-RSEC

Participants: K. Ünlü, Prof. of Mechanical and Nuclear Engineering Department, Assoc. Director for Research, RSEC
J. S. Brenizer, Nuclear Engineering Program Chair and Professor
N. O. Cetiner, M.S. student, Mechanical and Nuclear Engineering Dept.
D. K. H. Schwarz, Ph.D. student, Mechanical and Nuclear Eng. Dept.

Services Provided: Radionuclear Application Laboratory

Sponsors: US Department of Energy (INIE and NEER), RSEC

INTRODUCTION

The three major interaction mechanisms of gamma-rays with matter are photo-electric absorption, Compton scattering and pair production. In all these interactions, gamma-ray photon energy is partially or completely transferred to electron energy. In the photoelectric absorption, photon interacts with an atom and the photon completely disappears. In the Compton scattering the gamma ray interacts with an electron, causing an increase in the electron's energy. A new gamma ray with a smaller energy is then emitted. The new gamma ray can escape from the matter or can be absorbed through the photoelectric effect. In the pair production high-energy gamma rays are absorbed and two particles are created (an electron and a positron) and share the energy of the gamma ray. The positron loses its energy through ionization or excitation. If it is stationary, the positron interacts with an electron creating two gamma rays with energies of 511 keV each (annihilation radiation). These two gamma rays can escape or interact with matter through the Compton scattering or Photoelectric effect. Pair production does not occur below 1.022 MeV. The Compton effect is the predominant effect at intermediate gamma energies (200keV to several MeV).

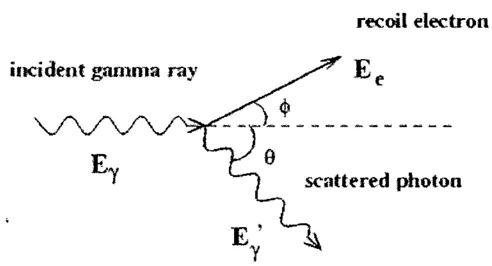

Figure 1. Compton scattering diagram

The vast majority of the scattered photons in Compton Scattering escape the detector by causing background counts in the gamma spectrum. If all of the energy of the incident photon is not absorbed in the detector, then there is a continuous background in the energy spectrum, known as the Compton continuum. This continuum extends up to an energy corresponding to the maximum energy transfer, where there is a sharp cut-off point, known as Compton edge.

In order to reduce the contribution of scattered gamma-rays the detector can be surrounded by a guard detector. The two detectors are operated in anti-coincidence, which means that if an event occurs at the same time in both detectors, then the event is rejected. The guard detector catches the escape photons and the effect of those photons is subtracted from the background. Compton suppressors provide a tool to suppress the unwanted background. The combination of a central NaI(Tl) and a germanium detector is called a Compton suppression spectrometer.

COINCIDENCE/ANTI-COINCIDENCE

Coincidence and anti-coincidence are detection modes used to produce a simplified spectrum from certain types of detector systems. In a system of two detectors, each detector produces separate signals. In coincidence mode those signals are counted. In anti-coincidence the signals produced at the detectors cancel or veto each other, leaving the non coincident signals to be counted. The advantage of coincidence or anti-coincidence techniques is achieving greater accuracy in the determination of full energy peaks in the spectrum.

COMPTON SUPPRESSION SYSTEM AT PSU FACILITY

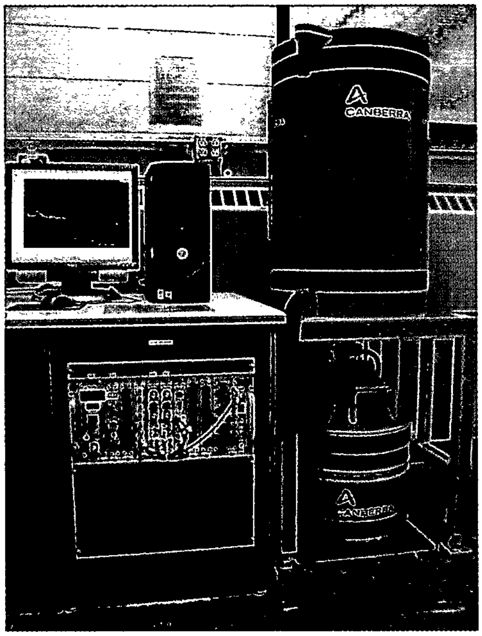

Figure 2. Compton Suppression System at PSU

Compton Suppression System at the facility includes

- HPGe detector
- NaI guard detector in a lead shield.
- NIM Bin /Power supply(Canberra Model 2100)
- PC desktop
- Genie 2000 software

Canberra Model 3106D NIM high voltage power supply is used for operation with HPGe detector.

The HPGe detector properties:

- Reverse electrode closed-end coaxial Ge detector
- Realative efficiency 54%
- Resolution 2.2 keV(FWHM) at 1.33 MeV
- Peak/Compton 58:1
- Diameter 64mm
- Length 71mm
- Cryostat description vertical slimline dipstick cryostat having 2.5'' endcap, 4'' long remotedetector chamber, and ultra low background cryostat hardware.

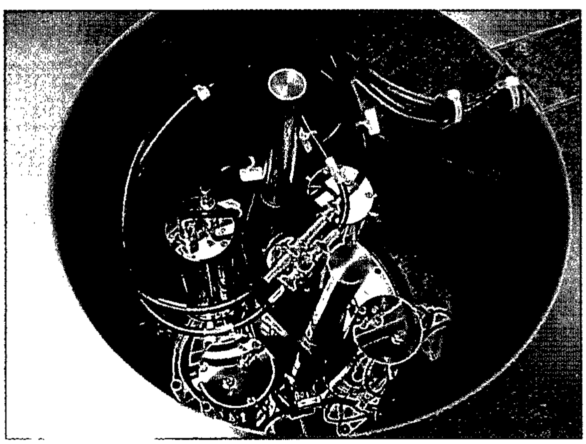

Figure 3.
Inside view of the shield where plug detector and PM tubes can be seen

The suppression of Compton events can only be as good as the ability of the guard detector to detect the scattered photons. Canberra Model 3002D high voltage power supply is used with NaI(TI) guard detector. NaI(TI) detector is consist of annulus and plug detector. Addition of plug above the sample will greatly reduce the Compton edges.

TESTING RESULTS

The ^{137}Cs source is counted in Compton Suppression System. Peak/Compton ratio, which is the ratio of the full energy peak to the Compton continuum, is calculated in order to see the performance of the system. Figure 6 shows the comparison of counting when suppression (SUP) is on with Pile Up Rejection (PUR) and when suppression is off (NOSUP) with Pile Up Rejection (PUR).

$$Peak\,/\,Compton = \frac{Number\ of\ counts\ in\ highest\ channel\ of\ 662.2\ keV\ peak}{Average\ counts\ per\ channel\ (396\ keV\ and\ 422\ keV)}$$

$$Peak\,/\,Compton = 1001.00$$

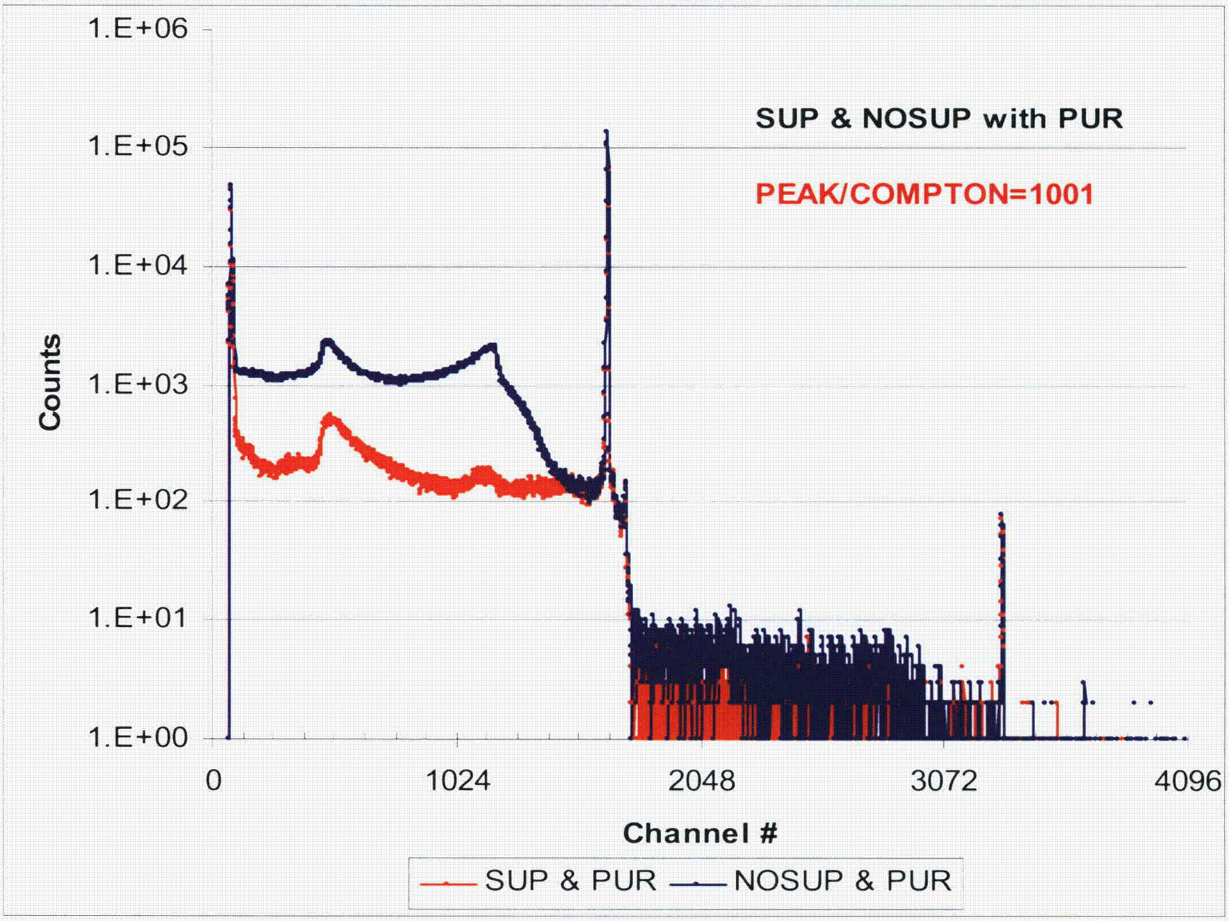

Figure 4.
Spectra of ^{137}Cs counted with the Compton Suppression System with suppression enabled (red) and disabled (blue)

Another test was carried out using samples from the ongoing determination of trace element concentrations (in particular trace amount of gold) in Dendrochronologically-Dated Tree Ring samples using the Neutron Activation Analysis (NAA) technique at Penn State University, Radiation Science and Engineering Center (RSEC). The ultimate objective of this study is to come up with a correlation between annual uptake of gold and major environmental or climatologic changes, e.g. volcanic eruptions. Several thousand wood samples have been analyzed by employing conventional NAA. All samples used in this study have been independently dated by researchers at The Malcolm and Carolyn Wiener Laboratory for Aegean and Near Eastern Dendrochronology at Cornell University, where over 40,000 individually-dated wood samples with 4.5 million rings, spanning the period from 7000 BC to the present, are archived. Samples containing elevated levels of gold are being analyzed again for short and long half-life elements, e.g., silver, copper, etc., to investigate other elemental signatures of environmental changes using the CSS. Elemental analysis of a wood sample from Porsuk, central Anatolian region of Turkey with 819 Relative Gordion Year was performed by using the CSS. The CTUPOR-819 wood sample was activated at 1 MW in the PSU Breazeale Nuclear Reactor and then counted in the CSS. Fig.5 shows the comparison of suppressed and unsuppressed spectra with determined gamma peaks. As demonstrated in the Fig.6, the 411.8 keV gold peak was buried in the Compton continuum without the suppression, whereas with the CSS, it was possible to resolve the gold peak.

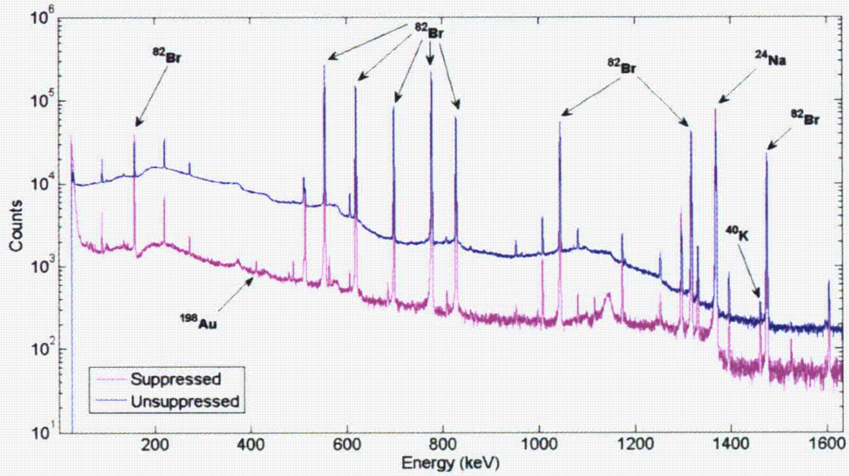

Figure 5.
Comparison of CTUPOR3-819 wood sample gamma-ray spectrum with and without Compton suppression

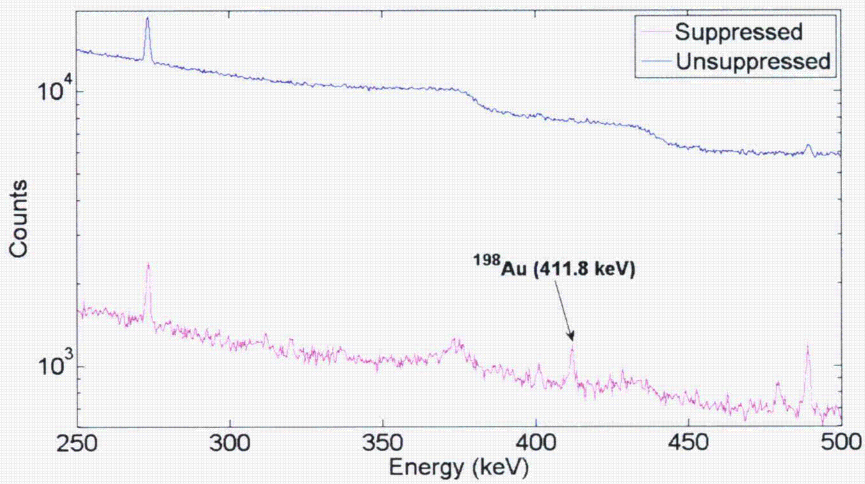

Figure 6.
Expanded region of the CTUPOR3 spectrum showing the gold (Au) peak is visible under suppression

CONCLUSIONS AND FUTURE WORK

A radioactive nucleus in an excited state can reach the ground level through single or cascade gamma emissions. Since the gamma-rays are emitted isotropically, there is a probability due to the geometry of the Compton Suppression System, that successive gamma-rays in a cascade process will be registered in different detectors. If the gamma rays are temporally separated by a tiny fraction of time, the counts will be falsely eliminated by the anti-coincidence circuit resulting in suppression of the full energy peak. Therefore, two separate efficiency calibrations must be used for the suppressed and unsuppressed modes. In the unsuppressed mode, both single and cascade gamma emitters can be used in the calibration with a wide energy range. For the suppressed spectrum, an efficiency calibration based on the single emitters must be applied to any single emitter that is counted. The cascade emitters must be treated separately each with their own efficiency values. Irradiation of V, Mg, Al, Dy, Zn, Zr, Cu, Au, Nb, Mn foils that are single gamma emitters is being planned. The efficiency calibration will be performed in the suppressed mode on the collected spectra and the selected cascade emitters will be individually evaluated. The calibration database will be then used to quantitatively determine the constituents of the tree-ring samples.

DEVELOPMENT OF A TIME-OF-FLIGHT SPECTROMETER FOR APPLICATION TO NEUTRON DEPTH PROFILING

Participants: K. Ünlü, Prof. of Mechanical and Nuclear Engineering Dept.
S. M. Çetiner, Ph.D. Candidate, Mechanical and Nuclear Eng. Dept.
R. Gregory Downing, National Institute of Standards and Technology (NIST)
Michael Gordon, IBM T. J. Watson Research Center

Services Provided: Neutron Beam Laboratory

Sponsor: U.S. Department of Energy under the Nuclear Engineering Education Research (NEER)
U.S. Department of Energy under the Innovations in Nuclear Education and Infrastructure (INIE)
The Pennsylvania State University, Radiation Science and Engineering Center

INTRODUCTION

Neutron depth profiling (NDP) is a near-surface analysis technique to measure the spatial distribution of certain light isotopes of technological importance in substrates with low neutron affinity. Ziegler [0, 2] first reported the use of neutron depth profiling as a nuclear reaction analysis (NRA) technique to obtain boron profiles in semiconductors. Biersack et al [3] later thoroughly investigated and improved the technique to almost present capabilities.

Upon neutron absorption, certain light isotopes emit a charged particle, either a proton or alpha depending on the isotope, and a recoil nucleus. The particle emission is monoenergetic and isotropic. As the charged particle and the recoil move in the substrate they lose kinetic energy through nuclear and coulombic interactions with host atoms. The amount of energy loss can then be correlated to the distance traveled by the particles, which is an indication of the depth at which the particles are created.

Conventionally, neutron depth profiling is based on the direct measurement of particle energies by charged particle detectors, mostly by silicon semiconductor detectors. This technique is called conventional because almost all of the NDP measurements to date have been done through direct measurements of particle energies. Charged particle semiconductor detectors can be one of surface barrier detectors (SBD), passivated implanted planar silicon (PIPS) detectors or PIN photodiodes.

Neutron depth profiling has been used extensively for obtaining the depth profile of light elements in various fields. However, proportional to the advances in scientific and technological applications, depth profiling with higher resolutions has become a necessity. It can be shown that neutron depth profiling has reached the limits of resolution that can be attained by the conventional techniques. Time-of-flight neutron depth profiling (TOF-NDP) is proposed as an alternative approach to overcome the restraints that keep the conventional technique from achieving a higher resolution.

PARALLEL ELECTRIC MAGNETIC (PEM) FIELD SPECTROMETER

In the PEM field spectrometer, the nominal electron velocity is parallel to the direction of both the electric and magnetic fields. The electron accelerates as it approaches the detector because of the electrostatic force exerted on it. However, the net magnetomotive force is zero for an electron moving in the direction of the magnetic field.

A three-dimensional drawing of the spectrometer is shown in Figure 1. The ion beam enters through a 5-*mm* aperture on a tantalum disk at an angle of 15°. The first disk has the carbon foil on a 3-*mm* aperture. The ion beam continues on its path with insignificant distortion in its direction. However, it loses a portion of its kinetic energy as it passes the foil, which must be taken into account in obtaining the energy spectra. The beam is extracted on the exit side of the stages through the apertures, where it is finally detected by the ion microchannel plate. The electrons generated by the ion emerge from the carbon foil and attracted by acceleration stages. At each stage, the electron gains equal kinetic energy. The surface potential of the electron microchannel plate was adjusted so that the electric field between the exit plate and the microchannel plate surface equals the electric field across the stages.

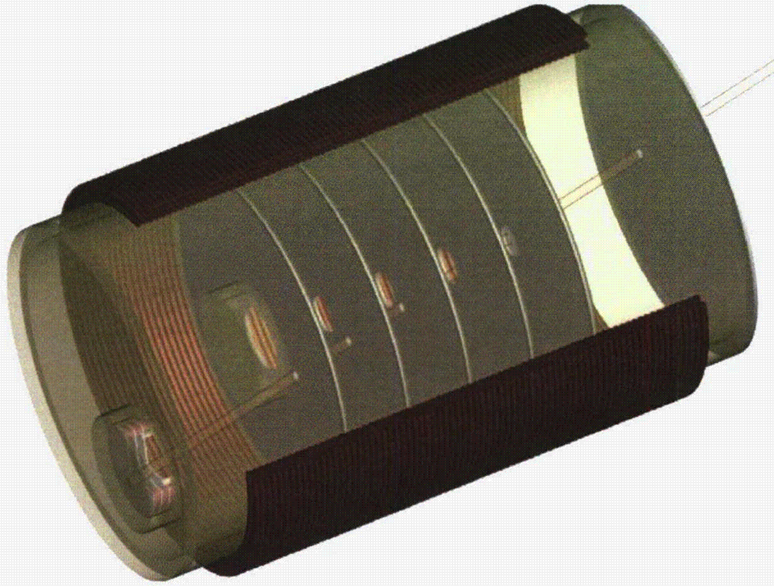

Figure 1. Three-dimensional drawing of the PEM field spectrometer

Response of the Spectrometer to Beam Energy

Time-of-flight spectra were taken with 1.0, 1.5 and 2.0-MeV alpha beams. In these measurements, the electron detector signal was used as the start trigger and the ion detector signal as the stop trigger. The carbon foil used as the secondary electron generator was 202-nm thick. The acceleration potential was set to 1000 V, which produced an electric field of $10^4\ V/m$. The magnetic field value required to map the electron beam with unity magnification was calculated $35 \times 10^{-4}\ T$, which corresponds to a solenoid current of 0.5 A. The time-of-flight spectra are shown in Figure 2. Since the signal from the electron microchannel plate was used as the start trigger, the spectrum shifts left as the ion energy increases.

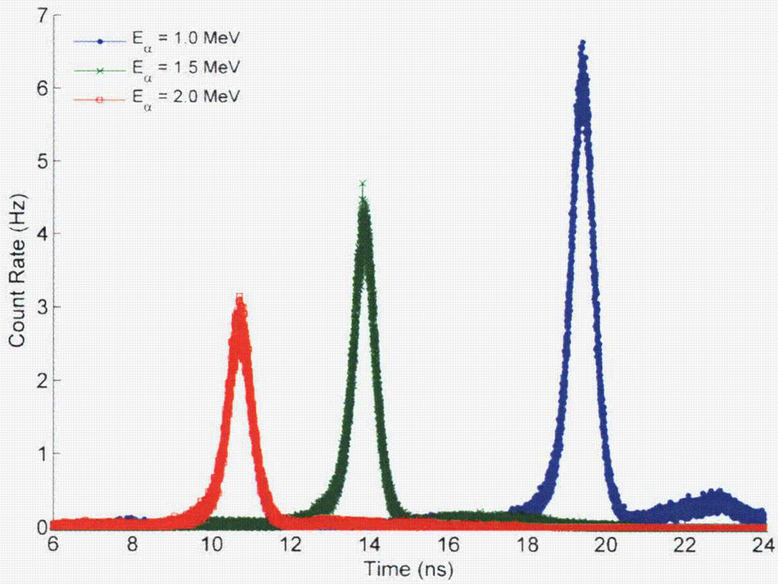

Figure 2. Time spectra obtained with 1.0, 1.5 and 2.0-MeV alpha beams

The standard deviations of the peaks were calculated as $266.6\ ps$, $253.5\ ps$, and $267.1\ ps$, respectively for 1.0, 1.5 and 2.0-MeV alpha beams. The energy spectra can be obtained from the offset and delay corrected time-of-flight spectra. Figure **3** shows the energy spectra of the alpha beams at 1.0, 1.5, and 2.0-MeV energy.

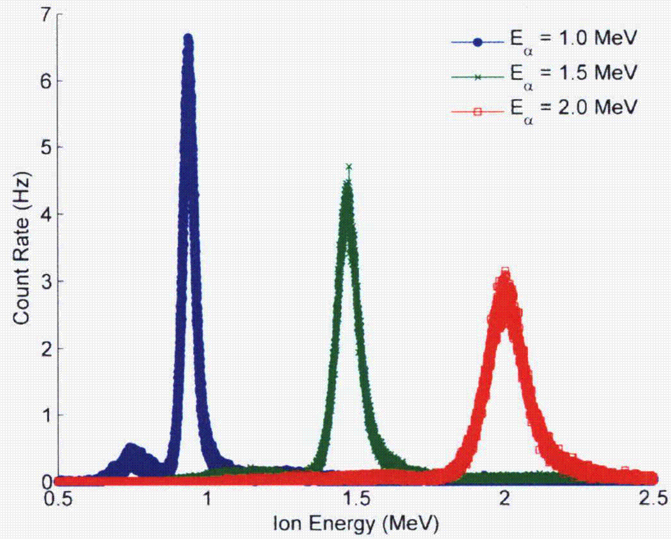

Figure 3. Energy spectra obtained from the offset and delay corrected time spectra

Response of the Spectrometer to Electron Accelerating Potential

A set of measurements was made to observe the effect of electron acceleration on peak resolution. The alpha beam energy was set to 1.5 MeV. A 50-nm thick carbon foil was used. The acquired spectra are plotted in Figure **4**. The accelerating potential was varied from $500\ V$ to $5000\ V$ in $500\ V$ increments.

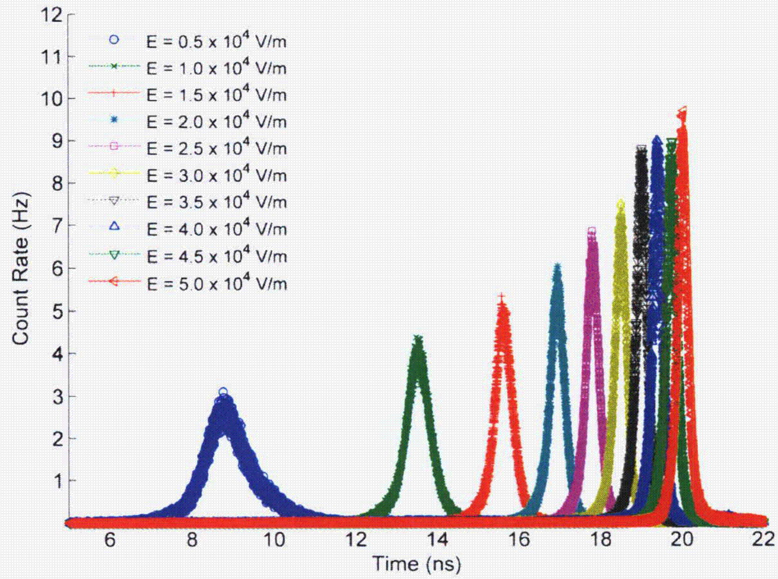

Figure 4. Time spectra of **1.5-*MeV*** alpha beam at various electron acceleration fields

The improvement in peak resolution is conspicuous. The standard deviation of distributions start at approximately 420 ps for $500\ V$ and reduces to $110\ ps$ for $5000\ V$. The variation of the standard deviation is plotted in Figure 5. As can be seen in the figure, the spread drops off faster in the beginning, but it starts to level off as the electric field further increases. The limit it reaches, i.e. $\sim 100\ ps$, indicates other broadening mechanisms.

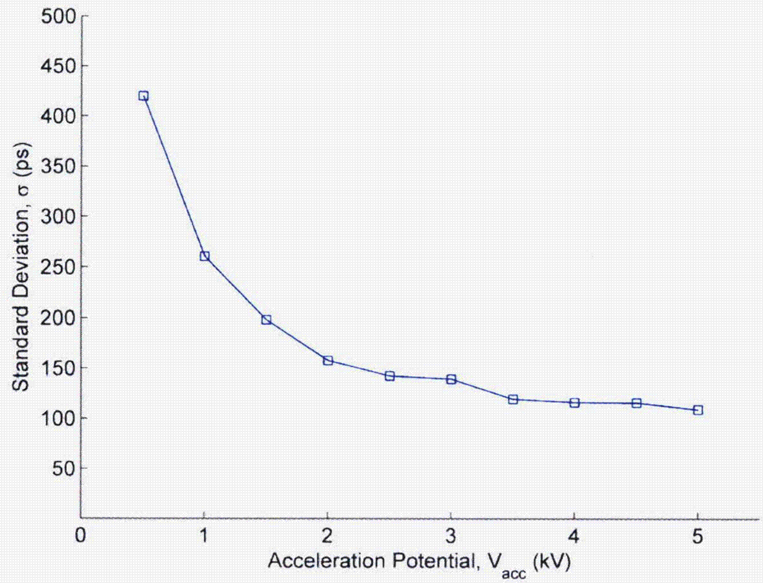

Figure 5. Improvement of the spectrometer resolution with the acceleration potential

Figure 6 shows the energy spectra of 1.5-MeV alpha beams taken at three different acceleration potentials. The spectra were obtained by conversion of the time spectra shown in Figure **4**. The centroids of the peaks are calculated as 1.481 MeV, 1.486 MeV, and 1.485 MeV for 1000-V, 3000-V and 5000-V acceleration potentials. The standard deviations of the peaks are 35.51 keV, 18.97 keV and 14.82 keV, respectively. The improvement in spectral resolution is significant as the acceleration potential is increased.

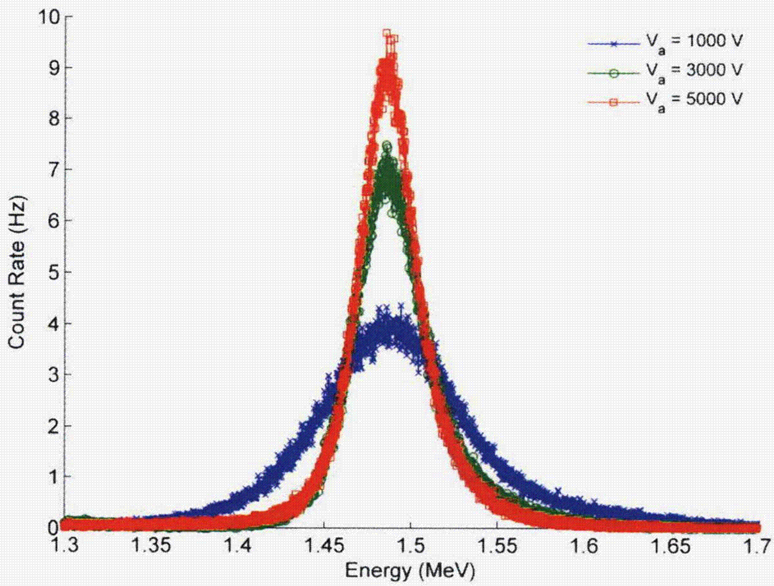

Figure 6. Energy spectra obtained from corrected time spectra at different acceleration potentials

CROSS ELECTRIC MAGNETIC (CEM) FIELD SPECTROMETER

A time-of-flight spectrometer was designed based on an earlier proposed design by Bowman et al [4]. An electric field is established between parallel frames at equal potential differences. The energetic ion goes through a thin carbon foil stretched on an aperture. The passage of the particle through the foil generates the secondary electrons. The ion continues on its straight path, exits the spectrometer and hits the ion detector. The generated electrons are focused on a microchannel plate positioned on the same plane with the carbon foil. A three-dimensional drawing of the electron acceleration unit is shown in Figure 7.

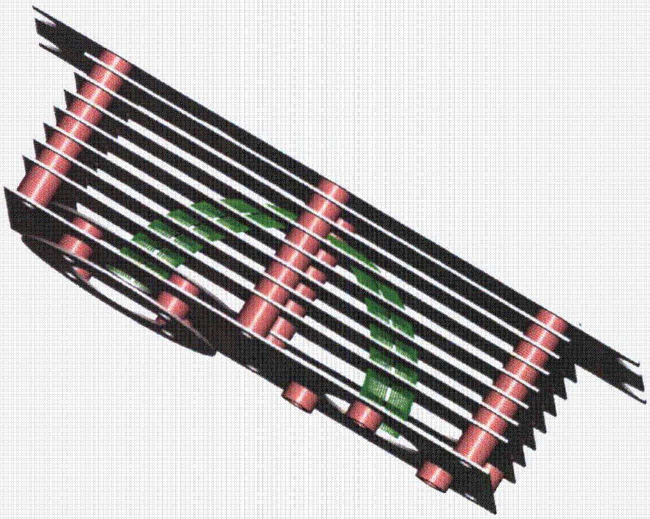

Figure 7. Electron acceleration unit of the CEM field spectrometer

A Helmholtz pair consists of two identical circular magnetic coils that are placed symmetrically one on each side of the experimental area along a common axis, and separated by a distance equal to the radius of the coil. A cylindrical region extending between the centers of the two coils and approximately $1/5^{th}$ of the diameter will have a nearly spatially uniform magnetic field. The coil pair was constructed of AWG #23 copper wire coated with regular enamel. The aluminum cores have an inner diameter of $150\,mm$. Each coil has $N = 725$ number of turns. The magnitude of maximum field at the center of the pair is approximately $70 \times 10^{-4}\,T$ at $1\,A$ electrical current through each coil. A three-dimensional drawing of the Helmholtz coil is shown in Figure 8.

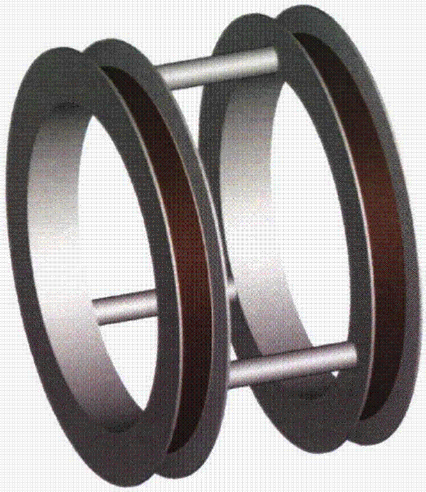

Figure 8. Helmholtz coil pair

Time-of-flight spectra were obtained at $150\ V$ and $600\ V$ acceleration potentials. The magnet current was adjusted to create a magnetic field value that matches the electric field value to transport the ejected electrons onto the electron microchannel plate. In this measurement, the signal from the ion microchannel plate was used as the start trigger, and the electron signal was used as the stop trigger. The stop signal line was delayed by $\tau_{\text{delay}} = 60\ ns$. The data from the measurements is plotted in Figure **9**.

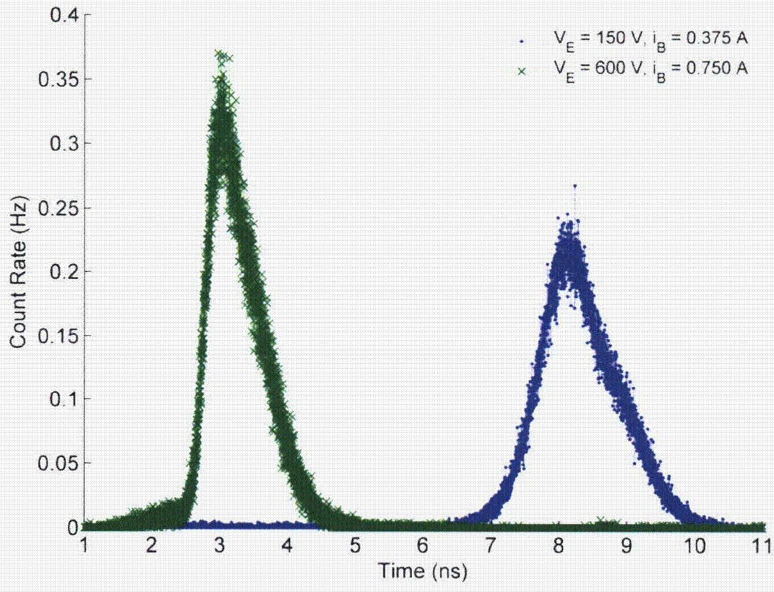

Figure 9. Time spectra obtained at two acceleration potentials

The peak centroids were calculated to be at $13.264\,ns$ for $600\,V$ and $18.314\,ns$ for $150\,V$, from which the spectral shift was found $\Delta\tau_{\mathbf{exp}} = 5.049\,ns$. Using the definition of cycloid period $\tau = {}^{2\pi m_e}/_{e_0 B}$, the expected spectral shift can be calculated as follows:

$$\Delta\tau = \tau_2 - \tau_1 = \frac{2\pi m_e}{e_0}\left(\frac{1}{B_2} - \frac{1}{B_1}\right) = \left(\frac{5}{4}\right)^{\frac{3}{2}} \frac{2\pi m_e r}{e_0 \mu_0 n}\left(\frac{1}{i_2} - \frac{1}{i_1}\right)$$

Using the parameters of the first designed Helmholtz coil, $r = 62.5\,mm$, $n = 600$, the expected shift from $i_1 = 0.375\,A$ to $i_2 = 0.750\,A$ is $\Delta\tau_{\mathbf{theo}} = 4.993\,ns$, which is within 1% of the experimental result.

Figure **10** shows the energy spectra of the alphas ejected by the ^{210}Po source. The peak locations are found to be $4672\,keV$ for the spectrum acquired with 150-V acceleration, and $4631\,keV$ for the spectrum acquired with 600-V acceleration. From the TRIM simulation, the peak location was expected to be located at $4464\,keV$. The deviation between the measured and simulated results is within 5%. The major source of the deviation is the uncertainty in the thickness of the source layer: The manufacturer's specification gives a broad range for the thickness of the layer.

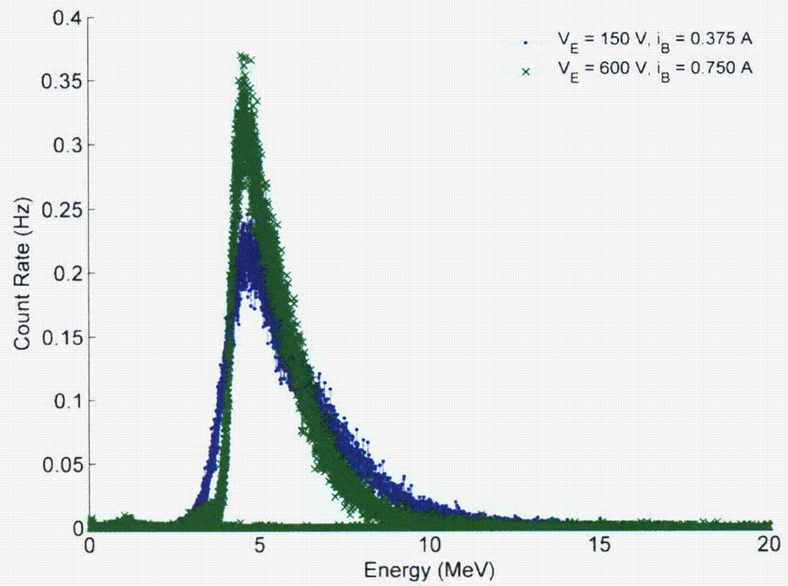

Figure 10. Energy spectra obtained by offset and delay corrected time spectra

ACKNOWLEDGEMENTS

This project is sponsored by the U.S. DOE under Nuclear Engineering Education Research (NEER) grant.

REFERENCES

1. J. F. ZIEGLER, G. W. COLE, J. E. E. BAGLIN, J. Appl. Phys., v. 43 (1972), p. 3809.
2. W. K. CHU, V. L. MORUZZI, J. F. ZIEGLER, J. Appl. Phys., v. 46, No. 7 (1975), pp. 2817-2820.
3. J. P. BIERSACK, D. FINK, R. HENKELMANN, K. MÜLLER, Nuc. Inst. Meth., v. 149 (1978), pp. 93-97.
4. J. D. BOWMAN, R. H. HEFFNER, Nucl. Instrum. Meth. **148**, pp. 503-509 (1978).

PUBLICATIONS

1. S. M. CETINER, K. ÜNLÜ, R. G. DOWNING, *"Development of time-of-flight neutron depth profiling at Penn State University"*, presented in 11th Int. Conf. on Modern Trends in Activation Analysis, University of Surrey, Gilford, UK, 2004; Journal of Radioanalytical and Nuclear Chemistry, Vol. 217, No. 2 (2007) 275-281.
2. S. M. CETINER, K. ÜNLÜ, R. G. DOWNING, *"Development and applications of time-of-flight neutron depth profiling"*, presented in 7th Methods and Applications of Radioanalytical Chemistry (MARC), Kona, HI, 2006; proceeding will be published in Journal of Radioanalytical and Nuclear Chemistry.
3. S. M. CETINER, K. ÜNLÜ, *"Depth profiling of boron in ultra-shallow junction devices using time-of-flight neutron depth profiling (TOF-NDP)"*, presented in Symposium on Radioation Measurements and Applications, Ann Arbor, MI, 2006; Nucl. Instrum. Meth. Phys. Res. A, Vol. 579, No. 1 (2007) 148-152.

THERMAL-HYDRAULIC ANALYSIS OF NEUTRON COOLING SYSTEMS

Participants: S. Yavuzkurt, Prof. of Mechanical and Nuclear Eng. Dept
K. Ünlü, Prof. of Mechanical and Nuclear Eng. Dept.
H. Melaku, Ph.D. student at Mechanical and Nuclear Eng. Dept
C. Celik, Ph. D. student at Mechanical and Nuclear Eng. Dept

Services Provided: Neutron Beam Laboratory

Sponsors: DOE-INIE, RSEC, Penn State Mechanical and Nuclear Eng. Dept.

INTRODUCTION

Cold neutrons can be obtained in several ways. Only two cold neutron beam facilities were developed at the U.S. university research reactors, namely at Cornell University and the University of Texas at Austin. Both facilities used mesitylene moderator. The mesitylene moderator in the Cornell Cold Neutron Beam Facility (CNBF) [1] which is no longer available – was cooled by a helium cryorefrigerator via a copper cold finger to maintain the moderator below 30 K at full power reactor operation. The Texas Cold Neutron Source (TCNS) [2] also uses mesitylene moderator cooled via a thermosyphon containing neon. The operation of the TCNS is based on a helium cryorefrigerator, which liquefies neon gas in a 3 m-long thermosyphon. The thermosyphon cools and maintains mesitylene moderator at about 30 K in a chamber. Neutrons streaming through the mesitylene chamber are moderated and thus reduced in energy to produce a cold neutron distribution.

The basic principle used in both systems is similar. However, the thermal-hydraulic mechanism of removing the heat from the moderator chamber that is near the reactor core to the cold head that is placed outside the biological shield of the reactor is different. The CNBF system uses copper rod to transfer heat by conduction to the cold head. In the TCNS system the basic mode of heat removal involves conduction through the wall, free convection and mainly pool boiling of cold neon inside the thermosyphon. In this study the mechanisms of heat removal is analyzed and evaluated both analytically and using computational fluid dynamics and heat transfer codes mainly by using commercially available FLUENT [5] code. The advantages and disadvantages of each system will be determined. FLUENT [5] through parametric studies is being used to design a new Neutron Cooling System (NCS) for university research reactors and particularly for PSU reactor. In this paper, preliminary results of CFD simulation of TCNS are presented.

CURRENT STUDY

This study focuses on detailed thermal-hydraulic analysis of both the TCNS and the CNBF cooling systems, analytically and using standard commercial thermo-fluid dynamic code such as FLUENT6.1 [5]. At the current stage of this study, the transient cooling down process of the thermosyphon is being studied. By observing the earlier measured data [1] and using equilibrium model to derive neon temperature and mass flow rate, it has been concluded that the basic mechanism of the cooling down process consists of four dominant stages as shown in Figure 1: 1. Transient startup, 2. Cooling down of neon gas 3.Cooling down of the moderator, 4. Condensation and pool boiling.The neon temperature and mass flow rate were derived using ideal gas model from the measured pressure data and assuming thermodynamic equilibrium conditions.

The various models of heat transfer process are being developed in order to incorporate them into the FLUENT solver. The computational domain is prepared using GAMBIT software which is the default grid generation tool for FLUENT. Figure 2a and Figure 2b show the result of the temperature distribution at the inlet to the thermosyphon during the early stages of the cooling down process. Sufficiently fine computational grid sizes ranging from 60,000 to 120,000 cells depending on the flow regime were required to capture the high temperature gradient and for ease of convergence of the solution. However, this comes at the expense of calculation time for the transient system with a relatively large aspect ratio of the domain.

In this case the computational domain is of 3.35 m long and of 19 mm diameter thermosyphon tube connected to a 6.5 l neon reservoir. Efforts are being made to reduce the skewness factor of the grid as low as possible by using hexagonal mesh wherever possible in the flow domain.

The computational result together with the experimental data obtained previously is expected to lead to a better design for the Penn State cold neutron source.

SET UP AND PREPARATION OF THE CFD SIMULATION

The default preprocessor software for Fluent which is GAMBIT was used to prepare the computational domain of the TCNS and generate the finite volume cells. The total number of cells of the flow domain was 6700 cells. The mesh sizes were varied according to the anticipated flow structure such that more cells were used wherever there is large velocity or temperature gradients. To take advantage of the flow symmetry and save computation time the analysis was made by splitting the above flow domain in half along the length of the tube. Symmetry boundary condition will then be applied along the cutting plane. In order to perform an accurate CFD simulation, all the boundary conditions at the various surfaces of the flow domain must be known. Due to the nature of the operational temperature range of the system, the cold head temperature can be affected by even a small exposed (un-insulated) thermocouple wire. The operation manual recommends that these wires should be thermally shielded. The amount of heat removed by the cryorefrigeration system at the cold head during the cooling down stages of the TCNS is not known. However, the temperature at the cold head during cooling down stages was measured previously[1] and this was taken as a temperature boundary condition for the CFD simulation. The temperature data was curve fitted and a "C" code was written to interface it within FLUENT as a UDF after compiling.

The geometry and material properties of the tube that connects the neon tank and the thermosyphon affect the heat transfer. In this revised simulation the length of the tube was increased to 5 m. The internal diameter of the tube is 3 mm. From the initial simulations it appears that the neon tube is a major heat load to the cooling system in the initial cooling period. The boundary condition at the surface of the neon tube was set to be room temperature of 300 K.

The reservoir was located outside the biological shield and hence the surface temperature should be assumed to be room temperature of 300 K. Since it is located inside the biological shield, the boundary condition for the thermosyphon wall was set to be an insulated wall.

The working fluid for the TCNS thermosyphon was neon gas. The initial condition of the gas is a room temperature of 300 K and pressurized to 10 atm. In this simulation neon was considered as an ideal gas and hence the ideal-gas model was selected for the variation of density in the simulation. In order to account for the continuous drop of absolute pressure in the system during cool down, the floating pressure option was activated. Previous simulations have shown that this was a major source of instability in the convergence of the simulation.

TWO-PHASE FLOW ANALYSIS

The condensation and boiling of the neon gas inside the thermosyphon should be modeled using the general two phase modules of FLUENT. This can be accomplished by using a two phase flow UDF to simulate the condensation and boiling inside the thermosyphon. Condensation on the inside wall of the cold head starts when the neon gas inside the thermosyphon reaches at or below the saturation temperature at the prevailing saturation pressure. Since the pressure inside the thermosyphon continuously changes the saturation temperature also changes continuously. The UDF that should be incorporated should account for the continuously changing saturation condition. The saturation temperature vs. pressure of neon was incorporated into FLUENT by using a curve fit.

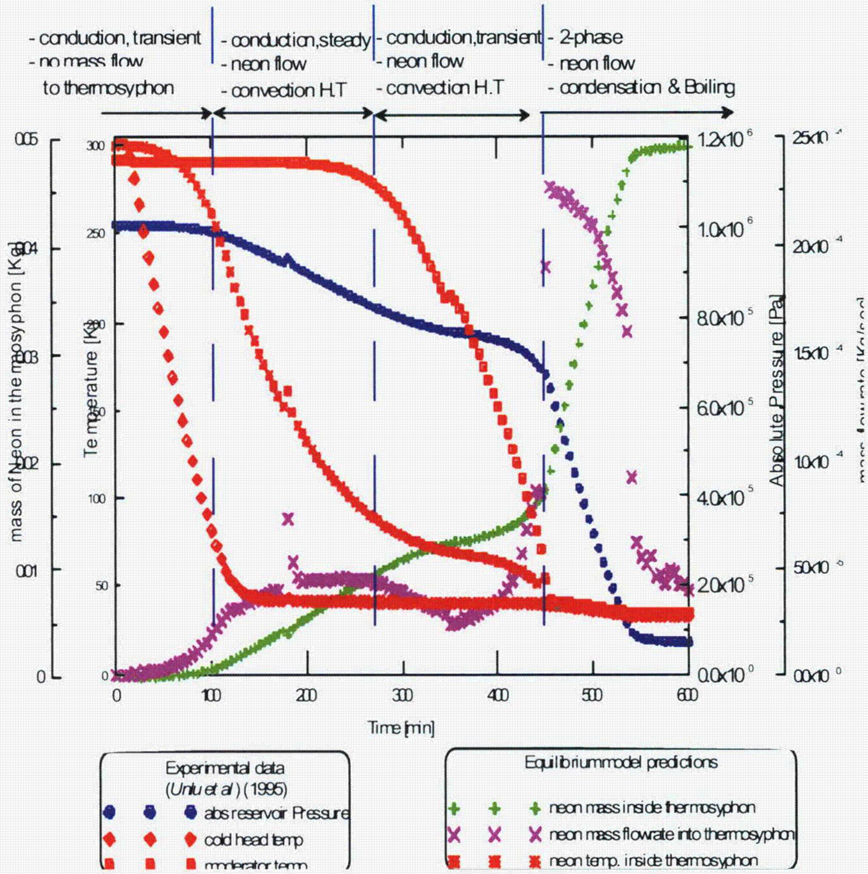

Figure 1. The thermal and flow properties of the TCNS at various stages of the cooling down process. The neon mass flow into the thermosyphon increases substantially at the beginning of the fourth stage when condensation starts

PRELIMINARY RESULTS

The simulation result shown in figure 3 is the latest result of prediction of the absolute pressure in the neon reservoir. This simulation was carried out by taking the variation of physical and thermal properties of both aluminum and neon with temperature. The operating temperature and pressure range of the TCNS was about 28 K and 40 kPa respectively. At such a low temperature the thermal properties were found to be exteremely sensitive to temperature. These effects were included during the simulation. From the result it was possible to see that the absolute pressure in the neon reservoir was accurate up to the beginning of condensation. At this point the simulation beyond the condensation point is being carried out. The simulation result of the moderator temperature, that is not shown here was not in a good agreement with the data which suggests that there needs to be improvement to the condensation modeling. However initial results shown in Figure 4 show how the condensed neon liquid accumulates at the moderator end of the thermosyphon.

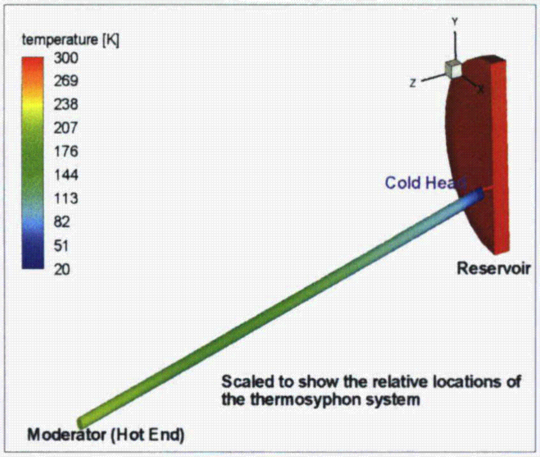

Figure 2a. Temperature distribution in the TCNS cold head, Moderator, Thermosyphon and Reservoir predicted using FLUENT code at the beginning of the cool down process

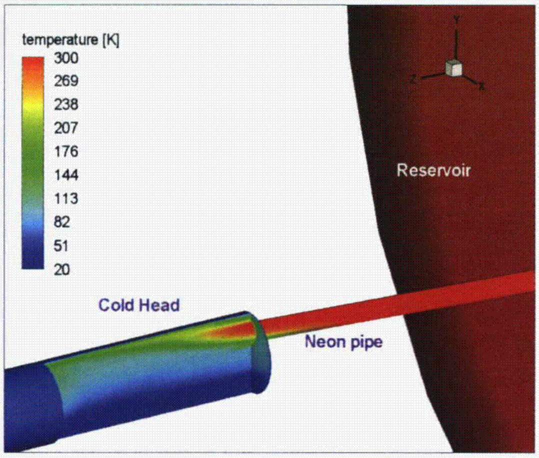

Figure 2b. Temperature distribution in the TCNS cold head predicted using FLUENT code at the beginning of the cool down process. Reservoir temperature remains constant

CONCLUSIONS

Neutronic performance of both the CNBF and TCNS systems are known and published previously. However, thermal and thermal-hydraulic behavior of both systems have never been analyzed in detail. Currently both the TCNS and the CNBF cooling systems are being analyzed in order to design and build a third generation mesitylene based cold neutron source at Penn State. The Penn State cold neutron source will be designed with a superior cooling system and an optimized cold neutron beam output. A parallel research to this proposed study is ongoing for the size and shape optimization of Penn State cold moderator chamber. An equilibrium analysis of the experimental data gave four distinctive thermal regimes when plotted as a function of time. These are being used to make the thermal modeling easier. Results from the initial analysis of the TCNS cooling system using FLUENT are encouraging. Following the characterization of the thermal behavior of both systems and parametric studies, a model will be developed for the best performance of university reactor based cold neutron source.

REFERENCES

K. Ünlü, C. Rios-Martinez, B. W. Wehring, "The University of Texas Cold Neutron Source," Nucl. Instr. and Meth.," A 353, (1994),397

D. D. Clark, C. G, Quellet, and J. S. Berg, "On the Design of Cold Neutron Source," Nucl. Sci. Eng. 110 (1992) 445

C. Rios-Martinez, K. Ünlü, Thomas L. Bauer and B. W. Wehring, "Performance of neon thermosiphon in the Texas cold neutron source," *Trans. Am. Nucl. Soc.*,71 692 (1994)

C. Rios-Martinez, K. Ünlü, and B. W. Wehring, "Thermal-Hydraulic and Neutronic Performance of the Texas Cold Neutron Source," Sociedad Nuclear Mexicana, IV. Congreso Anual Memorias, Vol 1, 148 (1993)

FLUENT-Computer Code, FLUENT Inc. Centerra Park Lebanon, New Hampshire 03766

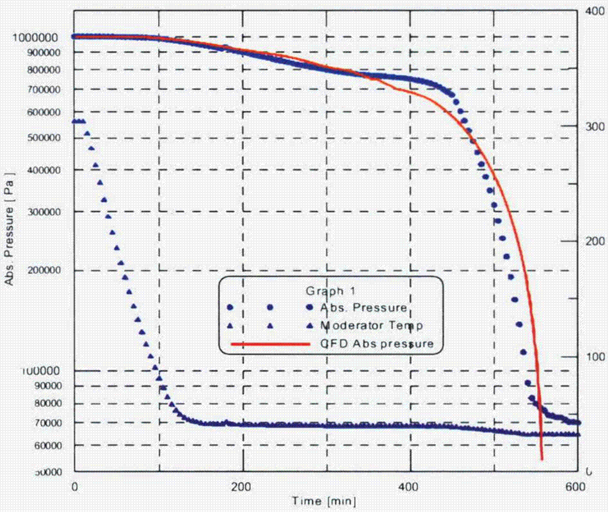

Figure 3 Comparison of simulation and experimental data of absolute pressure in thermosyphon during cool down

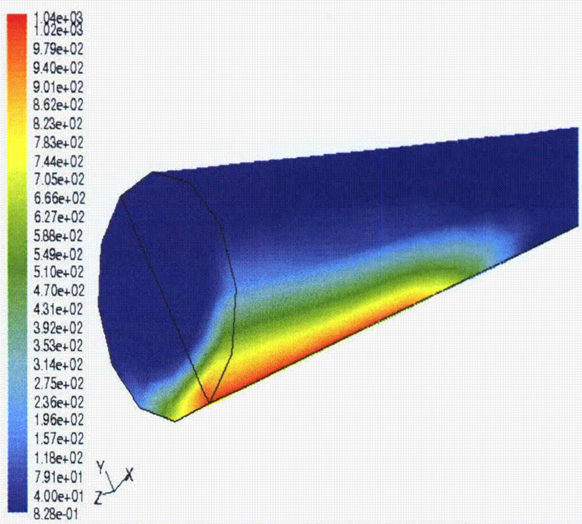

Figure 4 Condensation of neon inside TCNS thermosyphon

MODELLING OF EXISTING BEAM-PORT FACILITY AT PENN STATE UNIVERSITY BREAZEALE REACTOR BY USING MCNP

Participants: K. Ivanov, Prof. Mechanical and Nuclear Engineering Dept.
Y. Azmy, Prof. Mechanical and Nuclear Engineering Dept.
J. Brenizer, Prof. Mechanical and Nuclear Engineering Dept.
K. Ünlü, Prof. Mechanical and Nuclear Engineering Dept.

K. Bekar,PhD Student, Mechanical and Nuclear Engineering Dept.
C. Celik, PhD Student, Mechanical and Nuclear Engineering Dept.
J. Butler, MSc Student, Mechanical and Nuclear Engineering Dept.

Services Provided: Neutron Beam Laboratory

Sponsor: DOE, Innovations in Nuclear Infrastructure and Education (INIE)

INTRODUCTION

The Penn State University (PSU) Code System that has been developed to perform computer simulations of the beam port facility at the Reactor Science and Engineering (RSEC) at PSU consists of two major parts, the core model and the beam port model. The core model is needed to compute the flux at the reactor core – beam port facility boundary so that it can be used to compute the flux at the end of beam port where the experimental data were taken. Core calculations are performed by using the nodal diffusion code ADMARC-H [1]. The few-group cross section library needed to perform the diffusion calculations with ADMARC-H has been generated by the lattice physics code HELIOS [2]. The beam port calculations require very detailed geometrical definition of the system. This complexity of the geometrical model and the number of materials used in modeling the beam port facility prevent the use of deterministic codes in this study. Therefore, because of its geometrical flexibility a general Monte Carlo N-Particle Transport Code, MCNP5 [3], is used in this study to model the beam port facility. The source distribution used in beam port model is taken from the ADMARC-H code. An interface program has been developed at PSU to link the diffusion code to the neutron transport code. This interface reads the ADMARC-H output then computes the source term for MCNP and finally prepares the

VERIFICATION AND APPLICATION OF THE PSU CODE SYSTEM

Verification

The results of the overall PSU Code Package, which contains the core model, the beam port model that consists of the D_2O tank and the beam port tube models, and the interface module to link these two models are verified by comparing these results with the available experimental data [4] as shown in Figure 1.

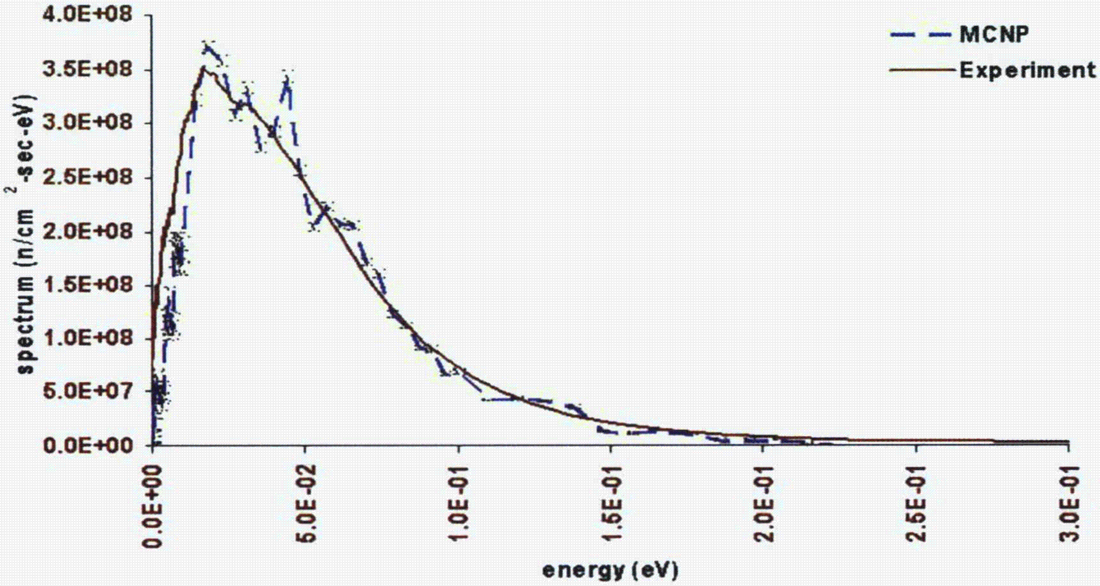

Figure 1: Comparison of the results of the PSU Code Package with the experimental data for the exit of the beam port #4. The solid curve represents the experimental data and the dashed line represents the model predictions with the associated error bars (the dotted vertical lines).

Applications

After establishing the tools for the beam port design study, these tools were used to model beam port #7. Two different MCNP generated plots of the model are given in Figures 2.a and 2.b since beam port #4 and #7 are axially located at different elevations.

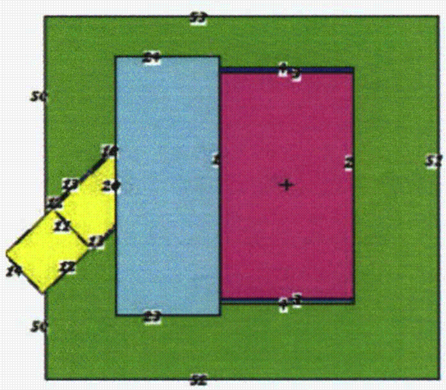

Figure 2.a: BP#7 @ pz=7.0 cm plane

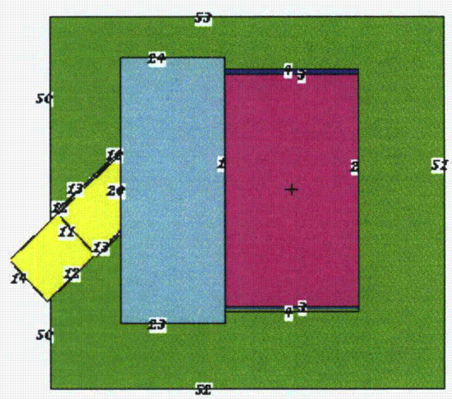

Figure 2.b: BP #7 @ pz=12.7 cm

Both figures show the top view of the system at different axial locations. Since both beam ports and the D_2O tank are cylindrical in shape, in both plots, their sizes differ at different elevations. The same methodology used in the BP #4 calculations was applied for the BP #7 calculations. The results of the D_2O tank model for $9x10^8$ neutron histories with the associated statistical errors are shown in Figure 3.

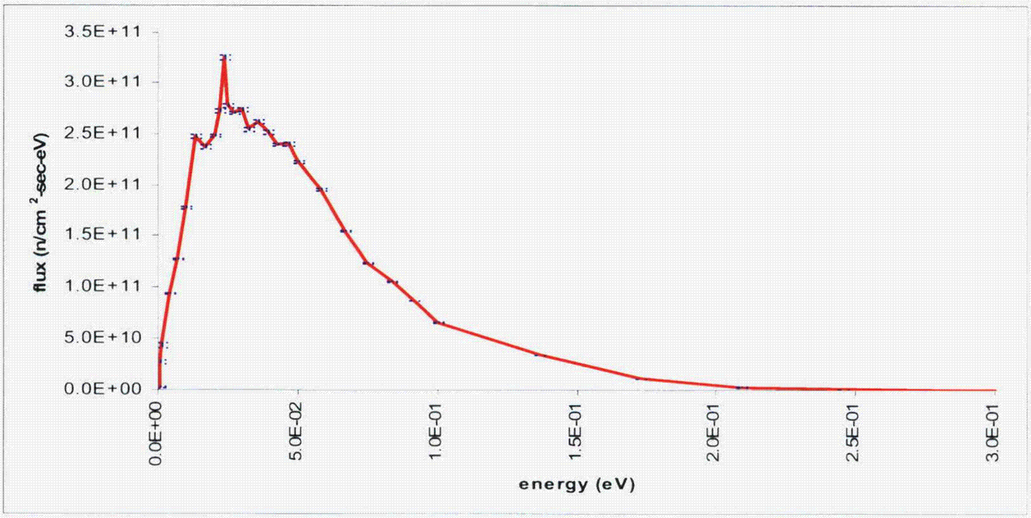

Figure 3: The D_2O tank results for BP #7 (all angles). The solid line represents the model predictions and the dotted lines represent the associated error bars (statistical error in the calculations)

This result represents the spectrum at the tallied surface for all angles. However, in order to prepare the input for the beam guide tube, a highly collimated neutron flux was needed. Therefore, the D_2O tank model was designed to tally for this very highly collimated flux, and this study is still underway and has been running.

Even though the verification of the system was made for the neutron analysis, we turned on the gamma analysis option in the MCNP calculations and performed an analysis for the neutron induced gammas within the system (not core gammas). Figure 4 shows the plot of the gamma spectrum at the beginning of the beam port guide tube (end of D_2O tank model) for all angles.

CONCLUSIONS AND FUTURE WORK

In this study, the existing beam port facilities at PSU Breazeale Reactor were modeled by using a code package developed at PSU, which consists of two major steps, the core calculations and the beam port facility calculations. The core calculations were performed by using the diffusion code ADMARC-H, which utilizes a few-group cross section library developed with HELIOS. MCNP5 was used to perform the beam port facility model calculations. The link between the core calculations and the beam port calculations was established with an interface program specifically prepared for this study.

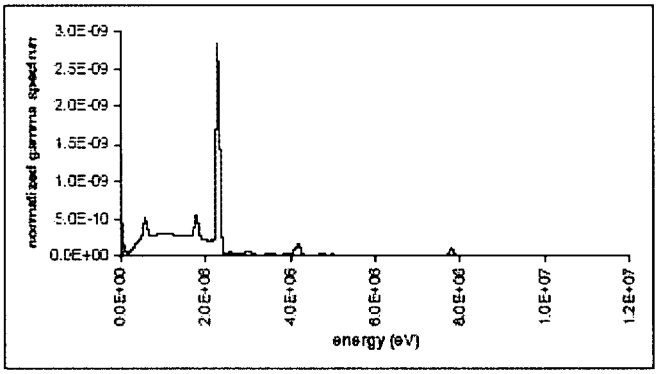

Figure 4: Gamma spectrum at the entrance of the beam port guide tube (BP #4)

The beam port #4 model was used to verify the PSU code package since the experimental data for this beam port and core configuration was available. The results presented for the beam port #4 model showed that the prediction of PSU code system agrees well with the available experimental data [5,6].

The same tools and methodology were used to simulate the beam port #7. Since beam port #7 is located 5" lower than beam port #4, which is exactly located at the axial centerline of the reactor core and since there is more D_2O and an extra graphite block in between the beam port #7 and the reactor core, the number of neutrons that can reach up to the beam port #7 is much less than that of the beam port #4. Therefore, the statistics of the beam port #7 calculations were worse than that of the beam port #4 calculations for the same number of histories. Hence, beam port #7 calculations were performed for much longer histories.

REFERENCES

1. K.N. Ivanov, N. Kriangchaiporn, "*ADMARC-H Manual", the Pennsylvania State University, 2000.*

2. "*HELIOS Methods*", StudsvikScandpower, 2000.

3. X-5 Monte Carlo Team, "*MCNP – A General Monte Carlo N-Particle Transport Code, Version 5, VolumeI: Overview and Theory*", LA-UR-03-1987, April 24, 2003.

4. J.H.J. Niederhaus, "*A Single-Disk-Chopper Time-of-Flight Spectrometer for Thermal Neutron Beams*", M.S. Thesis, the Pennsylvania State University, University Park, PA (2003).

5. B. Sarikaya, "*Modeling of Existing Beam Port Facility at Penn State Breazeale Reactor by Using MCNP5*", M.S. Thesis, the Pennsylvania State University, University Park, PA (2004).

6. B. Sarikaya, F. Alim, K. Ivanov, J.Brenizer, K. Ünlü, and Y. Azmy, "Modeling of the Existing Beam Port Facility at the PSU Breazeale Reactor by Using MCNP", Proceedings of PHYSOR 2004, Chicago, April 2004, USA.

LIQUID WATER STORAGE AND REMOVAL FROM POLYMER ELECTROLYTE FUEL CELLS

Participants: M. M. Mench, Assistant Prof. of Mechanical and Nuclear Engineering Dept.
J. Brenizer, Prof. of Mechanical and Nuclear Engineering Dept.
K. Ünlü, Prof. of Mechanical and Nuclear Engineering Dept.
K. Heller, PhD student at Mechanical and Nuclear Engineering Dept.
A. Turhan, PhD student at Mechanical and Nuclear Engineering Dept.
L. Shi, PhD student at Mechanical and Nuclear Engineering Dept.
J. J. Kowal, M.S. student at Mechanical and Nuclear Engineering Dept.
C.Chacko, M.S. student at Mechanical and Nuclear Engineering Dept.

Services Provided: Neutron Beam Laboratory

Sponsor: Automotive Manufacturer (1 domestic, one foreign), INIE, and US DoE NEER Program

INTRODUCTION

The residual water content stored in fuel cell media under steady or time-varying operation is of great interest, because it can play a critical role in the operating performance, pressure loss, degradation via ionic contaminants or mechanical damage, and time to start and degradation from a frozen condition. Liquid water storage and distribution in the diffusion media of polymer electrolyte fuel cells (PEFCs) is not solely a function of the diffusion media properties, however, and although the diffusion media plays a strong role in water removal, the interface between the land and diffusion media also has an important influence on the water storage and removal rate under steady and transient operation. In these studies, the relationship between the diffusion media, channel geometry, land area, and interfacial forces on the water storage in the fuel cell are being investigated. Non-intrusive water visualization within a full-sized fuel cell is not possible without neutron radiography. It produces excellent resolution and remains non-intrusive. This is helpful in performance tests and model validation efforts.

EXPERIMENTAL SETUP

The tests in this study were done in the Neutron Beam Lab at the Penn State Radiation Science and Engineering Center and the Breazeale Nuclear Reactor provided the thermal neutron beam. The water in the fuel cell attenuates the neutron beam and a CCD camera is used to capture both steady state images and transient videos. Custom software developed by PSU quantifies the liquid water in the cell and produces water mass versus cell location images. The water in the channels and in the DM under the channels is also differentiated from the water under the landings of the flow field using a masking technique.

One of the many fuel cells used is shown in Figure 1. On the left side, a black and white neutron image of an operating, $50cm^2$ active area fuel cell is shown. On the right side, the active area of the fuel cell (area in which electrochemical reaction takes place) is magnified, and the image has been falsely colored to identify liquid water storage locations. Through extensive experimental study, we have found that a complex interaction exists between the fuel cell media, geometry, interfaces, and surface properties which controls the liquid water stored in the diffusion media. The greatly complicates matters compared to traditional theory, which only considered the material properties of the diffusion media to dominate multi-phase flow in these media. This work has therefore opened up a new area of study in fuel cell science, that is trying to define this complex relationship.

Testing for these studies has involved small and full size stack cells, at ambient, heated, and even frozen conditions. Figure 2 shows a 7 channel parallel fuel cell that has been frozen to -12°C after shutdown.

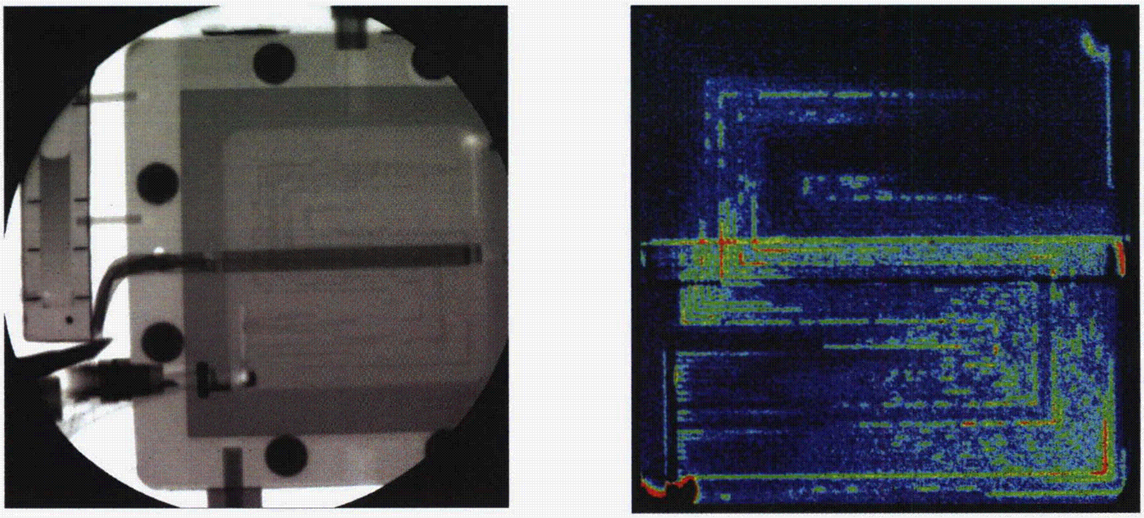

Figure 1: Raw Neutron Image and Processed False Color Image of a 50 cm2 Fuel Cell Used in This Study

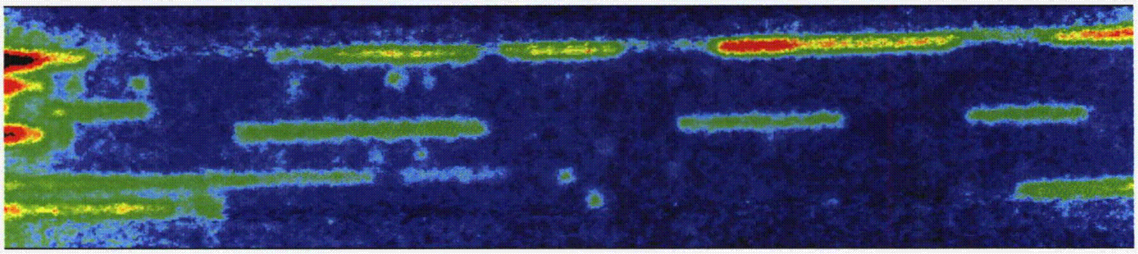

Figure 2. False color neutron image of a fuel cell frozen to -10oC, showing distribution of ice formations in a parallel flow channel fuel cell (Red is high ice thickness, blue is low ice thickness).

RESULTS

Surface Treatment

Space limitations preclude the complete discussion of the results of the channel geometry, frozen cell, neutron tomography, and DM studies. In this brief report, the effect of channel wall surface treatment is discussed. Figure 3 is a preliminary result comparing a gold-coated hydrophilic wall fuel cell at 10A, 80°C, with 100/100 humidity inlets, with the same fuel cell having one half of the wall surfaces coated with a hydrophobic wall treatment. The landing area was not altered for testing, only the channel walls were treated to provide a hydrophobic surface that is very different than the normal hydrophilic surface of the gold plating used. Clearly, there is a significant difference generated by the hydrophobic surface treatment, but this interfacial effect is not included in any published multi-phase models.

Channel/Land Geometry

Other results illustrate the large influence that the channel/land geometry and diffusion media type have on water storage. Figure 4 shows the area water density measured in the fuel cell under the lands and in/under the channels measured for two different channel/land geometries. In these cases tested with a hydrophobic diffusion media, there is more water stored under the lands than in/under the channels. This is a result of the relatively low temperature and flow blockage affect of the land, although the imbalance between the land versus channel water content in the diffusion media appears to also be a function of the in-plane liquid permeability of the diffusion media. For the woven cloth diffusion media tested, there is a reduced difference between channel and land water content, and the channel to land liquid water ratio is nearly 50:50 for a wide range of operating conditions. For paper DM, however, there is a greater difference between channel and land DM saturation in steady state. Also from Figure 4, it can be seen that the fuel cell with the largest channel to land ratio has the lowest water for a given condition. This condition was observed in all comparison cases, and is a result of the noted excessive liquid buildup under the land for the paper diffusion media. In general, to minimize liquid water storage in the diffusion media, a large channel to land ratio should be used with a DM with high in-plane liquid permeability.

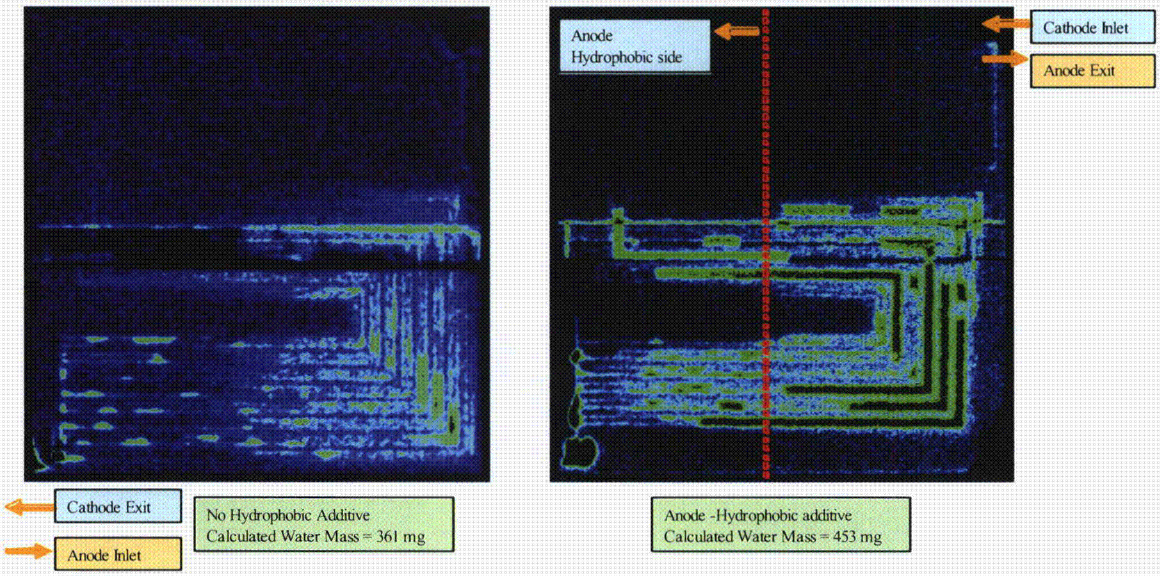

Figure 3. Comparison of fuel cell with a) hydrophilic gold channel walls with b) one half hydrophobic anode side walls. All other walls are still gold coated without hydrophobic additive.

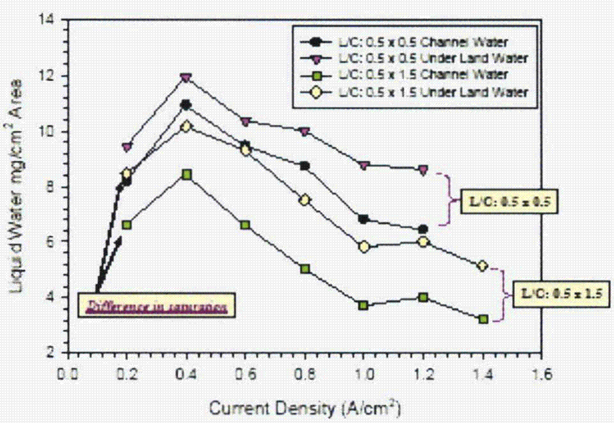

Figure 4. Area water density measured in the fuel cell under the lands and in/under the channels measured for two different channel/land geometries.

CONCLUSIONS

Neutron radiography is an excellent non-intrusive technique to visualize the water distribution in a PEFC. There are several ongoing projects at the RSEC that investigate the liquid water storage and distribution in a PEFC. Several new physical phenomena have been revealed that are not currently considered in state-of-the-art computational models of PEFCs. In particular, the strong role of interfacial contact area and surface energy has been shown, that will continue to lead us toward a cell design with optimized water management.

RELATED REFERENCES AND PRESENTATIONS

[1] Turhan, A., Heller, K., Brenizer, J. S., and Mench, M. M. 2006. Quantification of Liquid Water Accumulation and Distribution in a Polymer Electrolyte Fuel Cell Using Neutron Imaging. *Journal of Power Sources*, 160, pp. 1195-1203.

[2] Kowal, J. J., Turhan, A., Heller, K., Brenizer, J. S., and Mench, M. M. 2006. Liquid Water Storage, Distribution, and Removal from Diffusion Media in PEFCs. *Journal of Electrochemical Society*, 153, pp. A1971-A1978.

[3] Pekula, N., Heller, K., Chuang, P. A., Turhan, A., Mench, M. M., Brenizer, J. S., and Ünlü, K. 2005. Study of Water Distribution and Transport in a Polymer Electrolyte Fuel Cell using Neutron Imaging. *Nuclear Instruments and Methods in Physics Research Section A: Accelerators, Spectrometers, Detectors and Associated Equipment*, 542, Issues 1-3, 21, pp. 134-141.

[4] Turhan, A., Kowal, J. J., Heller, K., Brenizer, J., and Mench, M. M. 2006. Diffusion Media and Interfacial Effects on Fluid Storage and Transport in Fuel Cell Porous Media and Flow Channels. *ECS Transactions, 3, 1, Proton Exchange Membrane Fuel Cells 6, Eds. T. Fuller, C. Bock, S. Cleghorn, H. Gasteiger, T. Jarvi, M. Mathias, M. Murthy, T. Nguyen, V. Ramani, E. Stuve, T. Zawodzinski*, pp. 435-444.

[5] Chuang, P. A., Turhan, A., Heller, A. K., Brenizer, J. S., Trabold, T. A., and Mench, M. M. 2005. The Nature of Flooding and Drying in Polymer Electrolyte Fuel Cells. *Proceedings of the Third ASME International Conference on Fuel Cell Science, Engineering and Technology*, Paper #74051.

[6] Pekula, N., Heller, K., Chuang, P. A., Turhan, A., Mench, M. M., Brenizer, J. S., and Ünlü, K. 2004. Study of Water Distribution and Transport in a Polymer Electrolyte Fuel Cell using Neutron Imaging. *Proceedings of the 5th International Topical Meeting on Neutron Radiography (ITNMR-5)*, Munich, Germany, September 2004.

[7] Turhan, A., Kowal, J. J., Heller, K., Shi, L., Brenizer, J., and Mench, M. M. 2006. Interaction of Design, Materials, and Interfacial Forces on Liquid Water Storage and Distribution in Polymer Electrolyte Fuel Cells. *8th World Conference on Neutron Radiography (WCNR-8)*. NIST, October 16 - 19, 2006.

[8] Heller, K., Shi, L., Brenizer, J., and Mench, M. M. 2006. Error Analysis of Water Quantification Using Neutron Imaging. *8th World Conference on Neutron Radiography (WCNR-8)*. NIST, October 16 - 19, 2006.

[9] Shi, L., Heller, K., Brenizer, J., and Mench, M. M. 2006. The Penn State University Neutron Computed Tomography Facility. *8th World Conference on Neutron Radiography (WCNR-8). NIST*, October 16 - 19, 2006.

[10] Mench, M. M., Turhan, A., Keller, K., Ünlü, K., and Brenizer, J. 2005. INIE Big-10 Consortium Enabled Research: A New Physical Model of Two-Phase Transport in Polymer Electrolyte Fuel Cells Using Neutron Imaging at Penn State. *Trans. American Nuclear Society*, Vol. 93, pp. 74-75.

[11] Pekula, N., Mench, M. M., Heller, K., Ünlü, K., and Brenizer, J. 2004. Neutron Imaging of Two-phase Transport in a Polymer Electrolyte Fuel Cell. *Trans. American Nuclear Society*, Vol. 90, pp. 309-310.

[12] Turhan, A., Kowal, J. J., Heller, K., Brenizer, J., and Mench, M. M. 2006. Diffusion Media and Interfacial Effects on Fluid Storage and Transport in Fuel Cell Porous Media and Flow Channels. *presented at the 210th Electrochemical Society Meeting*, Cancun, Mexico

[13] Turhan, A., Kowal, J. J., Heller, K., Shi, L., Brenizer, J., and Mench, M. M. 2006. Interaction of Design, Materials, and Interfacial Forces on Liquid Water Storage and Distribution in Polymer Electrolyte Fuel Cells, *presented at the 8th World Conference On Neutron Radiography (WCNR-8).* NIST, October 16 - 19, 2006.

[14] Heller, K., Shi, L., Brenizer, J., and Mench, M. M. 2006. Error Analysis of Water Quantification Using Neutron Imaging, *presented at the 8th World Conference On Neutron Radiography (WCNR-8).* NIST, October 16 - 19, 2006.

[15] Shi, L., Heller, K., Brenizer, J., and Mench, M. M. 2006. The Penn State University Neutron Computed Tomography Facility. *presented at the 8th World Conference On Neutron Radiography (WCNR-8).* NIST, October 16 - 19, 2006.

[16] Turhan, A., Chuang, P.A., Heller, K., Brenizer, J. S., Mench, M. M., and Trabold, T. 2005. Liquid Water Distribution and Flooding as a Function of Flowfield Design in a PEFC. *presented at the 208th Electrochemical Society Meeting*, Los Angeles, California.

[17] Turhan, A., Heller, K., Brenizer, J. S., and Mench, M. M. 2005. Influence of Operation Parameters on Liquid Water Distribution and Flooding in a PEFC. *presented at the 208th Electrochemical Society Meeting*, Los Angeles, California.

[18] Mench, M. M., Turhan, A., Keller, K., P. A. Chuang, Ünlü, K., and Brenizer, J. 2005. INIE Big-10 Consortium Enabled Research: A new Physical Model of Two-Phase Transport in Polymer Electrolyte Fuel Cells Using Neutron Imaging at Penn State. *presented at the Fall American Nuclear Society Meeting*, November, 2005.

[19] Brenizer, J. S., Mench, M. M., Heller, A. K., and Ünlü, K., K. 2005. (invited), Neutron Imaging at Penn State: Past, Present and Future. *presented at the Joint Meeting of the National Organization of Test, Research, and Training Reactors and the International Group on Research Reactors, Special session honoring the Pennsylvania State University Breazeale Reactor 50th Anniversary*, September 12-16, 2005.

[20] Chuang, P. A., Turhan, A., Heller, A. K., Brenizer, J. S., Mench, M. M., and Trabold, T. A. 2005. The Nature of Flooding and Drying in Polymer Electrolyte Fuel Cells. *presented at the Third International Conference on Fuel Cell Science, Engineering and Technology*, Ypsilanti, MI.

[21] Turhan, A., Chuang, P. A., Heller, A. K., Brenizer, J. S., Mench, M. M., and Trabold, T. A. 2005. Water Distribution at Onset of Flooding and Dry-out in PEFCs. *presented at the 207th Electrochemical Society Meeting*, Quebec, Canada.

[22] Mench, M. M., "Advanced Diagnostics for PEFCs," *(Invited) Gordon Research Conference on Fuel Cells*, Bristol, RI., July 2004.

[23] Pekula, N., Mench, M. M., Heller, K., Ünlü, K., and Brenizer, J. 2004 (Invited speaker). Neutron Imaging of Two-phase Transport in a Polymer Electrolyte Fuel Cell. *presented at the American Nuclear Society Annual Meeting, Session on University Reactor Research and Applications,* Pittsburgh, PA.

[24] Pekula, N., Heller, K., Chuang, P. A., Turhan, A., Mench, M. M., Brenizer, J. S., and Ünlü, K. 2004. Study of Water Distribution and Transport in a Polymer Electrolyte Fuel Cell using Neutron Imaging. *presented at the 5th International Topical Meeting on Neutron Radiography (ITNMR-5)*, Munich, Germany.

NEUTRON ACTIVATION ANALYSIS OF ABSOLUTELY-DATED TREE RINGS

Participants: K. Ünlü, Prof. of Mechanical and Nuclear Eng. Dept.
Asoc. Director for Research, RSEC
T. H. Daubenspeck, Activation & Irradiation Specialist, RSEC

D. K. H. Schwarz, Ph. D. student at Mechanical and Nuclear Eng. Dept.
N. O. Cetiner, MSc. student at Mechanical and Nuclear Eng. Depth.
D. Sahin, MSc. student at Mechanical and Nuclear Eng. Depth.

Services Provided: Neutron Irradiation, Radionuclear Applications Laboratory

Sponsors: NSF, DOE-NEER, Cornell University, Malcolm and Carolyn Wiener Laboratory for Aegean and Near-Eastern Dendrochronology, RSEC

INTRODUCTION

Neutron Activation Analysis is the preferred analysis method for studying the composition of tree-rings. It was hypothesized when the project began that gold would be well-suited as an environmental marker in tree-rings. Much of the work since then has focused on irradiations suited to identify ^{198}Au which has a 2.7 day half-life. Following this goal, four tree samples each over 300 years in length have been analyzed at the Radiation Science and Engineering Center during recent years. Tree samples were cut into individual rings and were irradiated in batches of 40 tree-rings for 4 MegaWatt hours. This procedure allowed for the identification of ^{24}Na, ^{42}K, ^{56}Mn, ^{69}Zn, ^{82}Br, ^{140}La, and ^{198}Au.

Next, four short-lived tree samples (30-60 years in length) were analyzed for a period corresponding to the availability of dust aerosol index data from the Total Ozone Mapping Spectrometer (TOMS). Tree-rings were irradiated in batches of 20-30 rings and each ring was counted for two hours instead of one hour each. This decreased the Au and La detection limits so that they could be more reliably identified. In addition, the rings in each batch of samples were counted for 15 minutes each prior to beginning the 2-hour counts to allow for the identification of Mn in every sample.

Later, each of the tree-rings from two tree samples were recounted for one day each. This additional procedure resulted in the identification of ^{46}Sc, ^{59}Fe, ^{60}Co, ^{65}Zn, ^{110m}Ag ^{124}Sb and ^{134}Cs. The Ag and Au concentrations in C-TU-CAT32 were correlated with each other and appeared to be correlated with the TOMS aerosol index over the forest in Turkey where the tree grew (Figure 1). Ag and Au are the only elements that had the sharp peaks above the level of their continua. It was hypothesized that the unique noble metal characteristics of these elements made them suitable for documenting events in the life of the tree. In particular, the Ag and Au compositions may have been documenting the severity and frequency of Mediterranean dust storms.

EXPERIMENTAL

Ag has a short lived isotope (^{108}Ag) which might be identified with short irradiations of tree rings. Work during the past year was performed to determine if environmentally significant data, especially the concentration of Ag in tree rings, could be determined in a more efficient manner through short irradiations. The Pneumatic Transfer System (PTS) allows samples to be sent from the NAA laboratory directly into the reactor core through a pneumatic tube and with a transfer time of about 5 seconds. A sample of *Pinus brutia* identified as C-CY-RVA5 from Cyprus was analyzed using one-minute irradiations in the PTS. The empty vials were first labeled with a permanent marker and weighed. Individual tree-rings were then cut from the sample using a stainless steel knife chisel cleaned with alcohol and placed in the vials which were heat-sealed and re-weighed. Shortly before each run, sample vials were loaded into the rabbits for irradiation in groups of 25-35 at a time. With each batch of samples, one blank vial and the same sample of NIST standard Rice Flour were irradiated.

Table 2. A Comparison of Three Different Tree-Ring Irradiation Procedures

	Short Irradiations in the PTS	Long Irradiations (short count time)	Long Irradiations (long count time)
Irradiation time	1 min	4 hours	4 hours
Count time	4 min	2 hours	1 day
Reactor time/sample	6 min	8 min	8 min
Samples / week	90	60	7
Elements Identified	O, Na, Mg, Al, S, Cl, K, Ca, V, Mn, Cu, Ag, I	Na, K, Mn, Br, Zn, La, Au	Sc, Fe, Co, Zn, Ag, Sb, Cs

Figure 1. Silver and Gold Concentrations in C-TU-CAT32

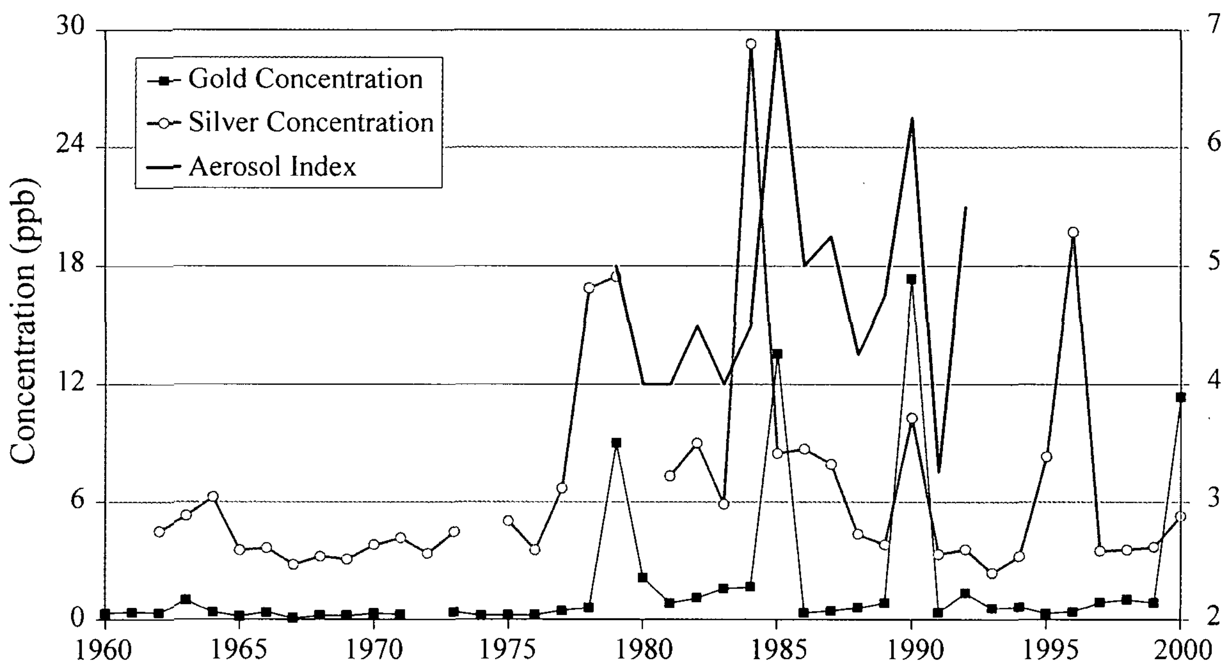

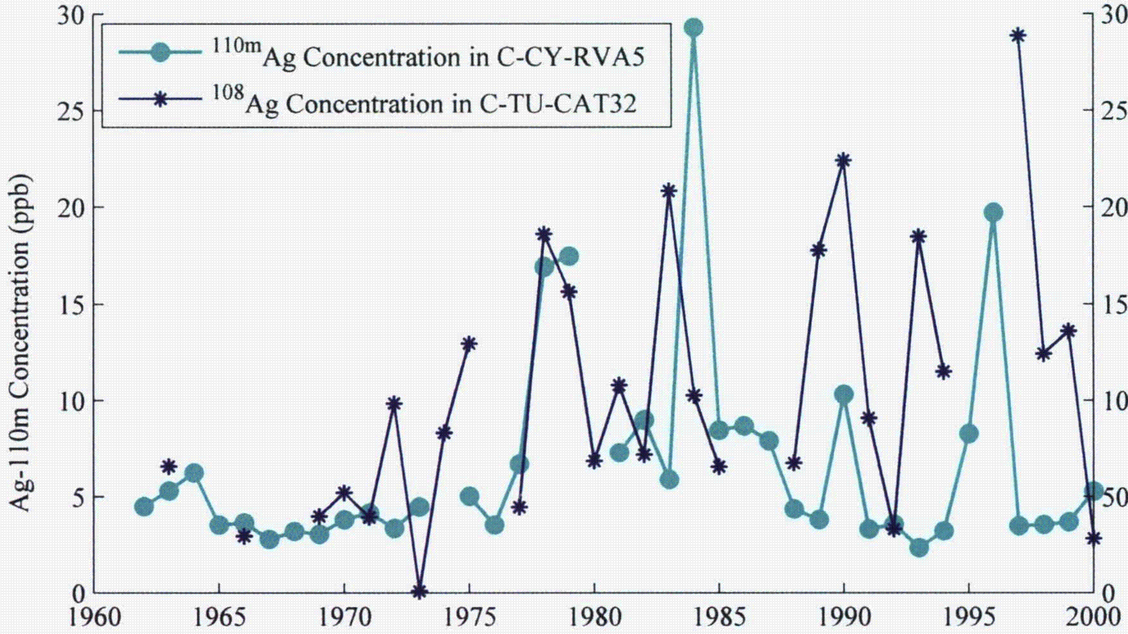

Figure 2. Ag Concentration in Tree Samples C-TU-CAT32 and C-CY-RVA5

PUBLICATIONS:

D. K. H. Schwarz, K. Ünlü, "Dendrochemistry of Pinus Sylvestris Trees from a Turkish Forest," in *Tree Rings, Kings & Old World Archaeology and Environment*, S. W. Manning, Ed., In Press.

D. K. H. Schwarz, K. Ünlü "Typical Elemental Concentrations in Tree-Rings and Appropriate Irradiation Parameters for Determination with NAA" MTAA12

D. K. H. Schwarz, K. Ünlü, "Silver and Gold: Possible evidence of Dust Storms in Tree-rings" ANS conference

DEVELOPING EFFECTIVE ELECTRODEPOSITION METHOD FOR Pu-242

Participants: K. Ünlü, Prof. of Mechanical and Nuclear Eng. Dept.
Assoc. Director for Research, RSEC
S. LaMont, Senior Scientist, Los Alamos National Laboratory

J. Rim, PhD student, Mechanical and Nuclear Eng. Dept.

Services Provided: Los Alamos National Laboratory, RSEC

Sponsors: DOE, Radiochemistry Education Award Program (REAP), Los Alamos National Laboratory, RSEC

INTRODUCTION

The project was aimed to develop a fast and effective electrondeposition method for plutonium-242. Electrodeposition is a process of using electrical current to produce a coating on a metallic surface. The deposition is achieved by putting a negative charge on the object to be coated and immersing it into a solution which contains a salt of the metal to be deposited. The electrical current flows through the solution from a positive end (anode) to a negative end (cathode). As the current flows, metallic particles in a solution also migrate towards a cathode and get deposited on a plate. By utilizing this simple technique, it is possible to deposit a very thin layer of Pu on a stainless steel disk.

EXPERIMENTAL SETUP AND RESULTS

A traceable amount of Pu-242 was used for this experiment. The mixture of sodium bisulfate ($NaHSO_4$), sodium sulfate (Na_2SO_4), and sulfuric acid (H_2SO_4) was used as electrolysis. The volume of each reagent was varied to change pH of the final solution. The pHs of electrolysis solutions used in this experiment were between 1.3 to 2.0. The total volume of the solution was kept constant at 15 mL through out the experiment.

Table 1 – Reagents used in experiment

Reagents	Concentration (M)	Function
Sodium Bisulfate	0.5	Electrolysis
Sodium Sulfate	3.0	Electrolysis
Sulfuric Acid	0.09	Electrolysis
Nitric Acid	8.0	Wet Ashing
Ammonium Hydroxide	1.5	Quenching
DTPA	0.0005	Chelating Agent

As a first step of the experiment, NIST grade traceable amount of Pu-242 and sodium bisulfate solution was mixed and dried at 140 C. Dry sample was then wet-ashed twice with 5 mL nitric acid. Sodium sulfate and sulfuric acid were added into the sample. The final solution was then transferred to Teflon electroplating cell.

In the electrodeposition setup, a platinum wire was used as an anode and a half inch stainless steel disk was used as cathode. The plating was carried out for an hour at constant current of 0.75 A.

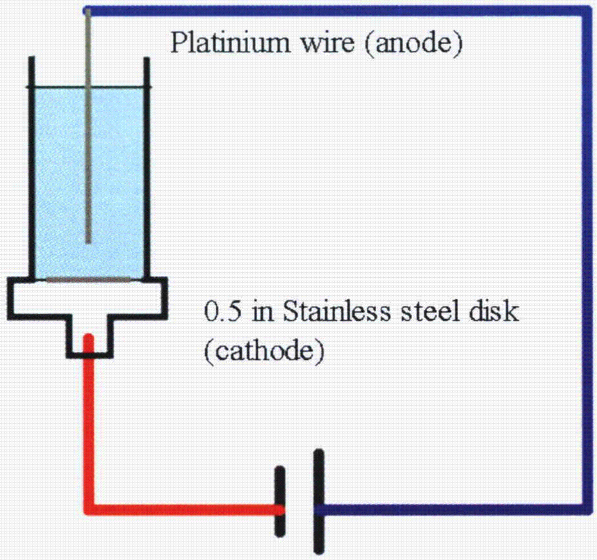

Figure 1 – Electrode position setup diagram

The Pu-242 plated disk was counted with alpha-spec to quantify the recovery rate. Figure-2 shows recovery rate in function of pH. The recovery rate showed dependence on a pH of electrolysis. However, there was no simple trend between pH 1.3 and 2.0. The recovery rates fluctuated between the pH range used. The highest recovery rate was about 74% at pH of 1.37. The lowest was little over 40% at pH 1.64.

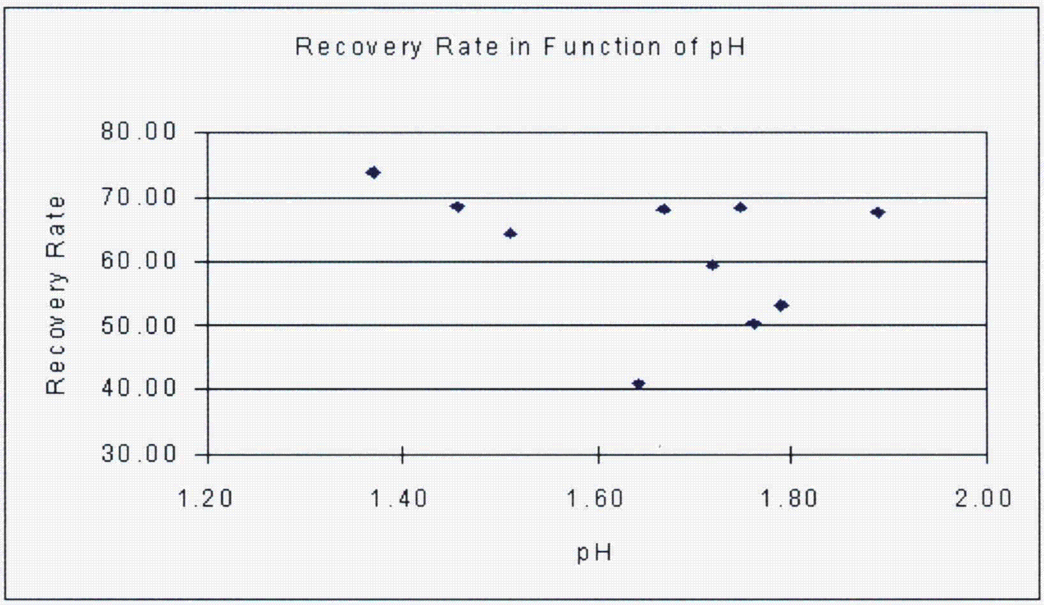

Figure 2 – Recovery rate of Pu-242 between pH 1.3 and 2.0

In selected samples, small concentration of DTPA was injected to study affects of it on a recovery rate and a uniformity of Pu-242 particle distribution. The recovery rate of sample decreased in all samples after injecting DTPA. At pH 1.9, recovery rate decreased by about 32%. The samples with DTPA also showed uneven distribution of Pu particle on a disk. DTPA prevented Pu-242 from depositing on to the center of the disk. Pu-242 was plated in a ring shape on a plating disk. Low pH may have caused this type of behavior. Chelating ability of DTPA would have highly depended on a pH of the electrolysis. At low pH, very small fraction of Pu-242 would have formed a complex with DTPA. The pH of solution needed to be 7 or higher to effectively form a complex between Pu and DTPA.

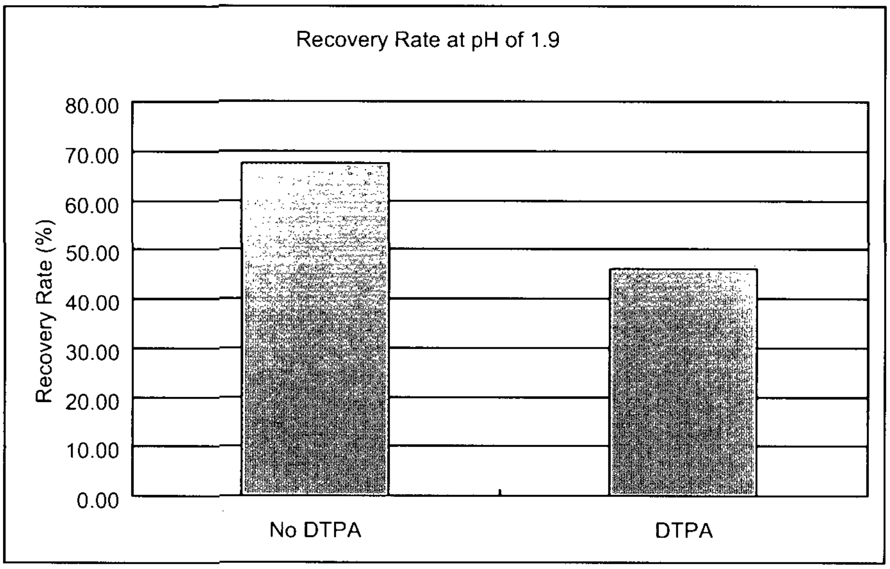

Figure 3 – Affects of DTPA on the recovery rate at pH 1.9

CONCLUSIONS

The pH of electrolysis had effect on the recovery rate of Pu-242. However, no simple recovery rate dependence on pH from 1.3 to 2.0 was observed. The highest recovery rate was about 74% at pH of 1.37. The lowest was around 40% at pH 1.64. DPTA in a solution prevented Pu-242 from plating evenly on a disk. It also lowered the recovery rate. In case of pH 1.9, recovery rate was lowered by 32%.

DEVELOPMENT OF THE NEUTRON COMPUTED TOMOGRAPHY SYSTEM

Participants: J. Brenizer, J. "Lee" Everett Professor of Mechanical and Nuclear Engineering
M. M. Mench, Assoicate Prof. of Mechanical Engineering

K. Heller, PhD Graduate Student
L. Shi, PhD Graduate Student
A. Turhan, PhD Graduate Student

Services Provided: Neutron Beam Laboratory, Machine Shop, Electronics Shop

Sponsors: DOE- INIE, DOE NEER, RSEC and MNE

INTRODUCTION

Dynamic neutron imaging (radioscopy) has proved a valuable research tool. The success of this technique has generated a demand for more comprehensive neutron imaging techniques, especially those that provide 3D volumetric data (computed tomography) for fuel cell research, which would enable easy discernment between anode and cathode flow fields. The development of a neutron computed tomography system has been undertaken by the neutron imaging team at the Radiation Science and Engineering Center (RSEC) in order to meet this demand. The following sections describe the upgrades, additions and installations of the new hardware and software to our imaging and post-collection image processing systems as well as the initial results.

EQUIPMENT UPGRADES

Neutron computed tomography requires capturing images of an object at evenly spaced angular intervals between 0° and 180°, called "projections." In some applications the source and detector are rotated around an object, in others the object itself is rotated while the source and detector remain stationary. The latter method is the one employed by the RSEC neutron imaging team. Since the interval between angles during rotation and image capture must be even, a Newport 855C programmable controller and rotary turntable (with resolution of 0.001°) were interfaced with the existing dynamic image acquisition system computer.

For the past few years our imaging facility has contained a "turn-key," completely digital, dynamic image acquisition system purchased through the company "I-Cubed." The complete system is comprised of a Pentium IV computer system with camera interface card, a Cohu CCD Camera and image capture software. The digital CCD Cohu camera supplied with the system has a 1004x1004 pixel resolution and 10-bit deep grayscale range. When connected to the computer's interface card, frame rates as high as 30fps are possible. The computer system has met all demands for both storage of the large volumes of digital image data being captured during experiments and the running of the in-house developed, post processing and water quantification software for radioscopic (2-D) fuel cell research.

The Newport 855C programmable controller recently interfaced with this system acts as an intermediary between the computer and the rotary turntable; receiving commands from the computer to advance the turntable a fixed increment and sending information to the computer indicating turntable position and status. To properly synchronize communication between the Newport 855C programmable controller and dynamic image acquisition system computer required an in-house developed plug-in to the image capture software.

Norpix's Streampix image capture software was included with the computer. Image capturing and storage is done in the form of proprietary image stacks called "sequence files," which can then be exported to a variety of formats, most notably TIFF and AVI. All post processing is done in the TIFF format since it a lossless image format and can be read on PC, Macintosh or Unix computers. The Streampix software also includes the ability to run user-written plug-ins. This feature allows the synchronization of image capture with external devices through the serial port or external data acquisition cards. Capturing an image at the request of an external device, such as a rotation table signaling proper object alignment, is possible. By sending commands through the dynamic image acquisition system computer to the Newport 855C programmable controller, the in-house developed plug-in ensures the rotary turntable with mounted object is rotated to the proper position before signaling Streampix to capture an image of the rotated object. Figure 1, below, shows the main panel of the plug-in, which allows the user to set a variety of initial conditions before starting data collection. Once the user clicks OK, the entire data collection process of incremental object rotation and image capture is entirely automated.

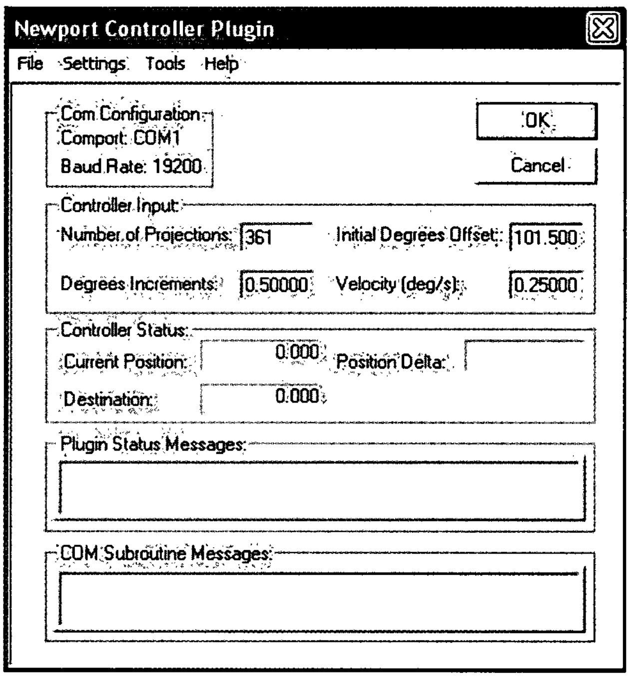

Figure 1. Streampix in-house developed Newport Controller plug-in main window

The decision to use a "turn-key" system was based on the desire to avoid incompatibilities between the various hardware components. An added advantage of the "turn-key" system is the accompanying tech-support, which can troubleshoot problems and provide quick solutions.

NEW POST PROCESSING SOFTWARE AND EQUIPMENT

Once the projections of an object have been acquired, they are used to create 2D tomographic cross section reconstructions. Each pixel row in the images will generate a corresponding cross section image revealing detailed interior information. A variety of algorithms exist to perform the cross section reconstructions and several commercial software packages are available that implement them. One software package, Octopus, written in the Labview programming language has been in use in the X Ray tomography field for years and has been recently used in the neutron imaging field with excellent results. Its combination of parallel beam and fan beam reconstruction algorithms and friendly user interface made it ideal for use with the neutron computed tomography system. Figure 2, below, shows the main panel of the Octopus V8 software.

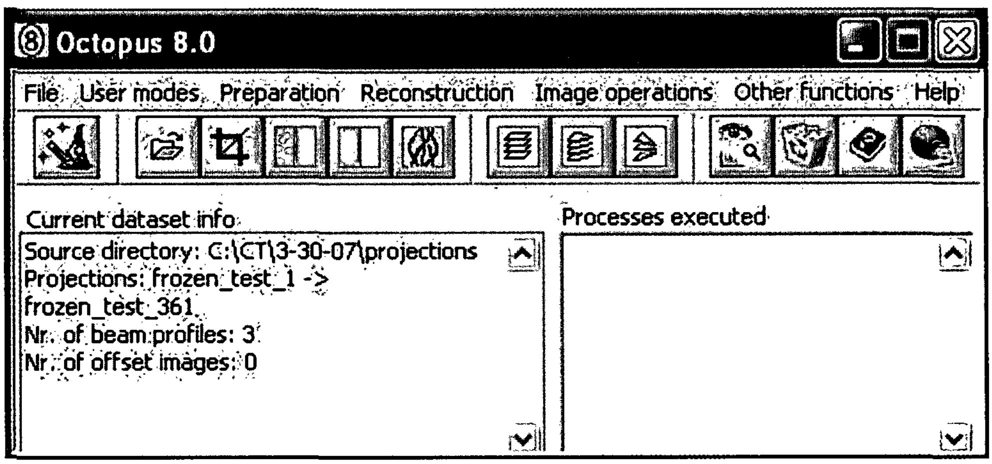

Figure 2. Main panel of Octopus V8

Finally, the 2D cross sections can be stacked on top of one another, like a deck of cards, to produce a 3D reconstruction of the imaged object. Stacking one cross section on another creates a volumetric picture element, or voxel, of which the final reconstruction is comprised. To perform the stacking and manipulate the many voxels, the commercially available and industry standard software, VGStudio Max V1.2 was acquired. VGStudio is short for "Volume Graphics Studio" and, as its name implies, is software dedicated to the processing of volume graphics. A 3D image reconstructed with the software may have many structural components within the image grouped together and manipulated. For example, a 3D reconstruction of an aluminum cylinder with a copper core could have the copper core isolated, removed and then examined independently within the software. This easily lends itself to the differentiation between anode and cathode flow fields in a fuel cell.

Both Octopus V8 and VGStudio Max V1.2 require a great deal of computing power. The existing dynamic image acquisition system, while capable of using the programs, would be slow. In addition, it was desired the imaging system be available for further data collection while reconstructions were being performed. To this end, a dedicated image reconstruction computer was obtained.

Alongside the now dedicated dynamic image acquisition system computer, the image reconstruction computer is the last component in the new neutron computed tomography system, the basic layout of which can be seen in Figure 3.

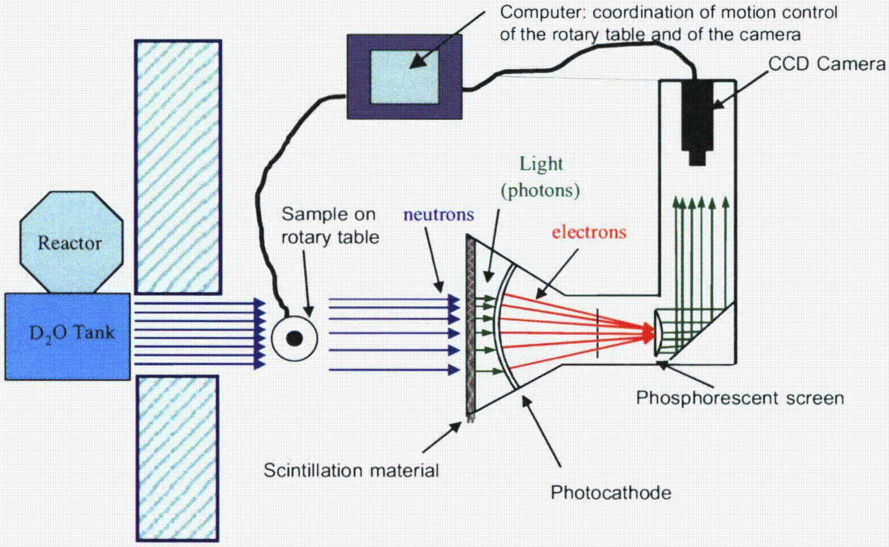

Figure 3. Basic layout of the Neutron Computed Tomography System

With a dual core Pentium processor, 2GB memory and 2x250MB hard disks, the image reconstruction computer can fully utilize both Octopus V8 and VGStudio Max V1.2 and provide a large amount of disk space to store the large data sets generated by these programs.

EXPERIMENTAL MEASUREMENTS AND RESULTS

Before full neutron computed tomography (NCT) fuel cell experiments might be performed, care must be taken to ensure images are taken with the rotation table axis parallel to the vertical pixels lines of the CCD. Currently, a bubble level gauge on the rotary table is used to see if the rotary table axis is correctly aligned, indicated when the water bubble is evenly centered. The calibration work can also be performed by placing a sample test object on the rotary table, taking an image, rotating the test object by 180^0 and taking another image. If the second image is flipped, subtracted from the first image, and the resulting image is totally dark, then the rotary table is adjusted well. Otherwise, the resulting image shows some white areas and the rotary table needs to be adjusted.

Generally, for NCT experiments, two kinds of images are required: 1) At least one blank beam (open beam) image, and 2) A series of 2-D images of the object from different view angles, each image taken at evenly spaced angles. After taking these images, one may start the 3-D image reconstruction. The following are general steps to perform image reconstruction:

1) Acquire images from each projection
2) Reactor power fluctuation correction
3) White spot noise removal
4) Beam shape correction
5) Calculation of the test object's cross section information using "Octopus-8.0"
6) 3-D Visualization of object volume using VG-studio Max V1.2: reconstructed slices from Octopus V8 are loaded into the CT visualization software VG studio Max 1.2 to see detailed internal information of the sample object.

The first reconstructions at the Penn State Radiation Science and Engineering Center are illustrated in the following figures. Figures 4 and 5 show the radioscopic 2-D image experimental measurements of an actual aluminum cylinder with copper tubing wrapped around the outside and detailed calculated cross section information using Octopus V8, respectively.

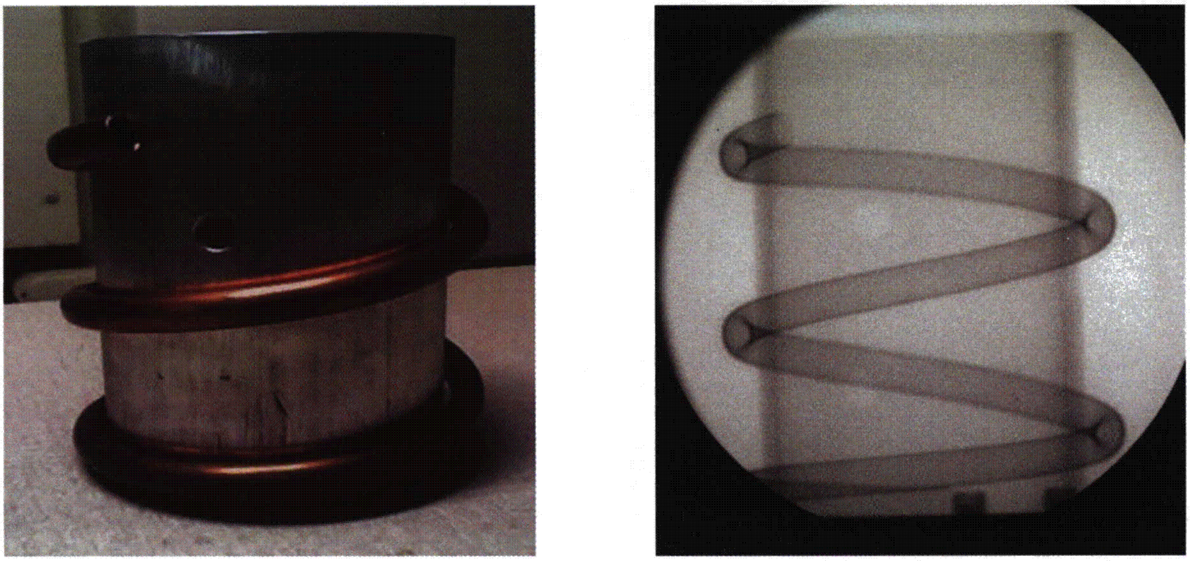

Fig. 4. 2-D radioscopic image acquired with imaging system

Fig 5. Sample aluminum cylinder with copper tubing wrapped around cross section information (361 projections in 180° at 0.2 s/frame)

Fig. 6 Volume reconstruction results of the aluminum cylinder with copper tubing wrapped around detailed internal information using VG-Studio Max. 1.2 On the left, aluminum cylinder and copper tubing. On the right, copper tubing isolated and manipulated independently of aluminum cylinder.

After successfully calculating the detailed cross section information using Octopus V8, the cross section slices were input into VG-Studio Max 1.2 software to visualize the object internal information. Figure 6 shows the volume reconstruction results using VG-Studio Max V1.2.

The volume reconstruction of the aluminum cylinder with copper tubing wrapped around was successful. Although there are still some artifacts in the 3-D images, they are likely due to an insufficient number of projections. Since this test was only to verify the system and software, a lower projection count was used. The imaging setup and software is now ready to directly image frozen fuel cells and reconstruct in 3-D using this approach and software.

MODELING OF A TEST OBJECT AND WATER QUANTIFICATION FOR NCT

Another important ongoing work is the technique for water quantification. To gain a better understanding of the fidelity of the NCT reconstruction software, several ideal CT data sets were generated. The simple neutron attenuation equation was used to model a simple object like an aluminum cylinder with copper core in the center of the object. The purpose of this modeling work is to create ideal data sets which have no artifacts to investigate the neutron scattering effects on tomographic reconstructions and also to verify water/ ice quantification techniques and expected error. Figure 7 shows modeling results of a calculated, aluminum cylinder with copper core, "radioscopic" image using the simplified exponential attenuation equation and the corresponding cross section reconstruction results using the Octopus V8 software.

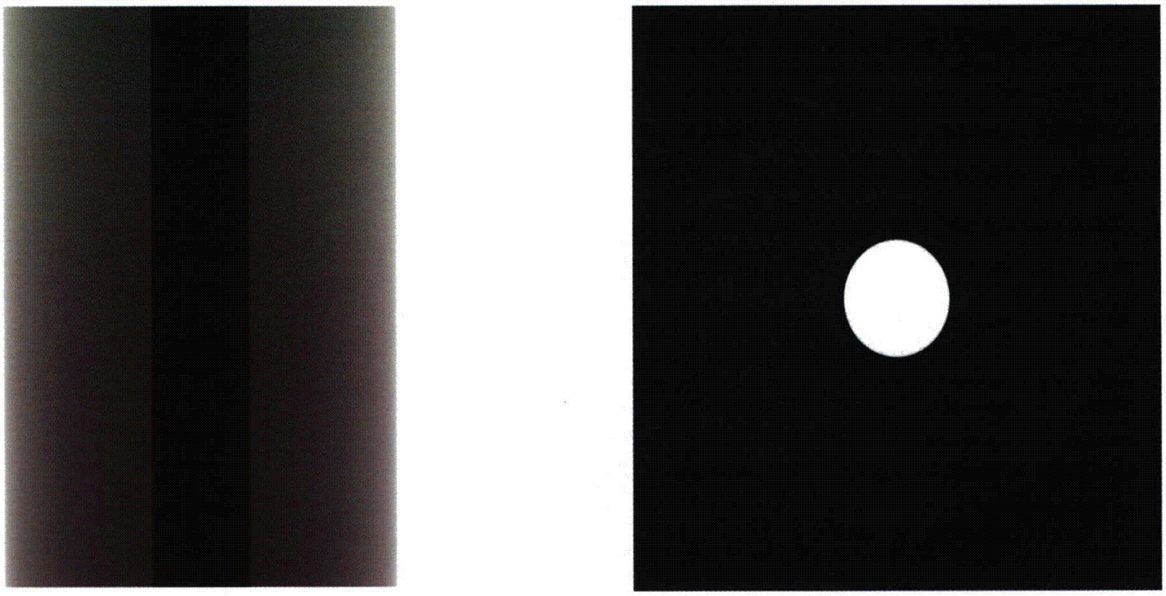

Fig. 7. Aluminum cylinder with copper core "radioscopic" image with calculated data using simplified exponential attenuation equation and the corresponding cross section reconstruction result using Octopus software

After finishing the reconstruction, the cross-sectional slice information was put into VG-Studio Max V1.2 to get the detailed internal information. Figure 8 shows the 3-D visualization results of the modeled object. Other cylindrical objects are presently being similarly modeled in order to investigate the neutron scattering effects on the tomography experiment and to further develop the future water quantification technique in NCT. These cylindrical objects contain columns of water in addition to cores of copper, lead and other materials. This information will provide insight into properly isolating gray level values of water voxels for quantification.

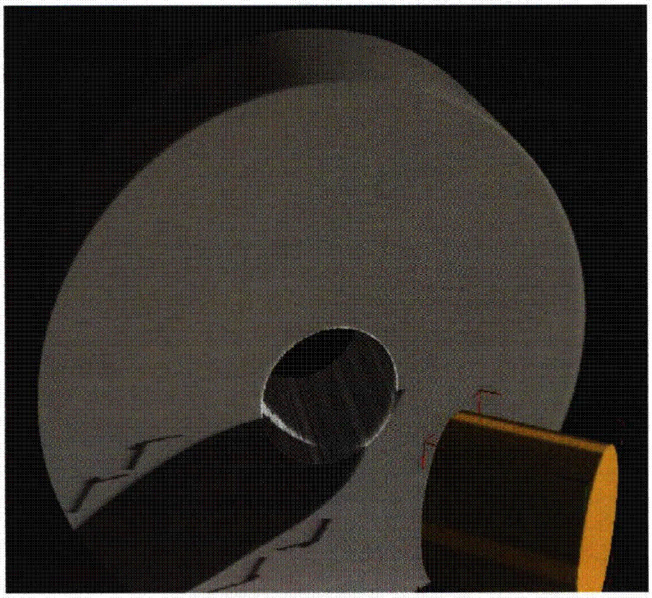

Fig. 8. Visualizing aluminum cylinder with copper core 3-D information using VG-Studio Max V1.2

Figure 9 shows an image of a specially designed seven channel parallel straight 14.5 cm^2 fuel cell after operation and then frozen without purge to -10°C. The distribution of differently sized ice formations (red is high ice thickness, blue is low ice thickness) are clearly seen. This special cell was designed and built because it has no 180° switchbacks that can confuse the interpretation of the fuel cell-related performance results. The long, skinny design of the fuel cell also is designed to minimize the geometric unsharpness, since the cell will be rotated around its length-wise axis. In the future work, 3-D NCT image spaces will be reconstructed of the fuel cell cooled to -40°C from an initial operating state of 80°C, with no purge. The results will show the locations and sizes of the ice formations in the anode or cathode, under lands or channels and above or below. These results have great impact on fuel cell design for durability in frozen environments.

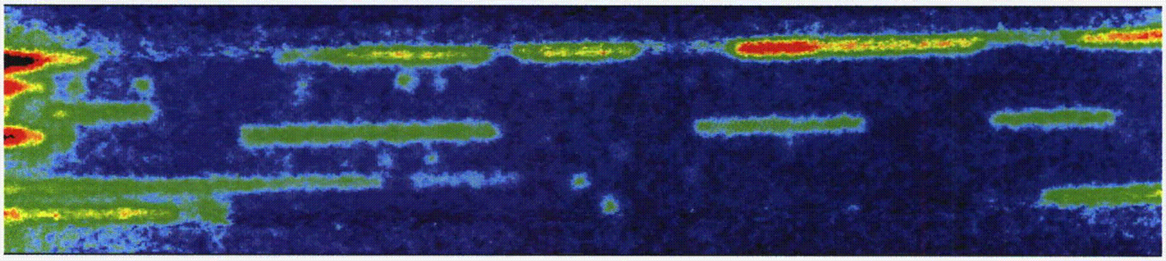

Fig. 9. False color neutron image of a fuel cell frozen to -10°C, showing distribution of differently sized ice formations in a parallel flow channel fuel cell (Red is high ice thickness, blue is low ice thickness)

FUTURE WORK

In the future, work will continue on the improvement of the neutron compute tomography system, specifically:

- Improving NCT system spatial resolution to 50 μm voxel
- Increasing effective L/D ratio to 500 to reduce geometrical unsharpness
- Improving imaging system detector efficiency for low neutron flux
- Reducing artifacts in reconstructed slices

Reducing radiation effects in projection images

-CCD hardening
-Radiation shielding
-Better alignment of objects
-Account for neutron scattering effects

- Further development of the water quantification technique
- Using NCT to investigate frozen water distribution in a fuel cell

SOFT ERROR ANALYSIS TOOLSET (SEAT) DEVELOPMENT

Participants: V. Narayanan, Prof. of Computer Science and Engineering Dept.
M. J. Irwin, Prof. of Computer Science and Engineering Dept.
K. Ünlü, Prof. of Mechanical and Nuclear Engineering Dept.
Y. Xie, Prof. of Computer Science and Engineering Dept.

V. Degalahal, Ph.D, Intel Corp., Mobile Platforms Architecture and Development
S. M. Çetiner, Ph.D. candidate, Mechanical and Nuclear Engineering Dept.

Services Provided: Neutron Beam Laboratory

Sponsor NSF, Penn State Dept. of CSE, RSEC

INTRODUCTION

Soft errors, or single event effects (SEE), are transient circuit errors caused due to excess charge carriers induced primarily by external radiation. Radiation, directly or indirectly, may induce localized ionization that can flip the internal values of the memory cells.

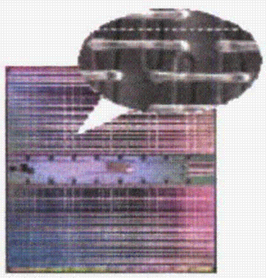

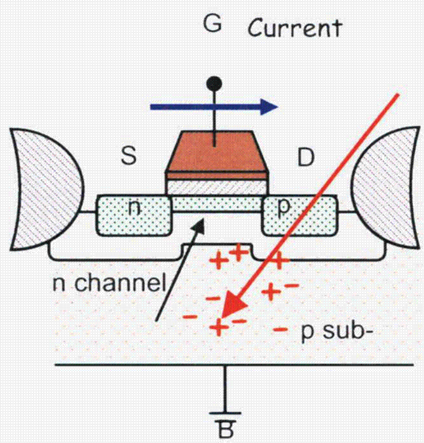

Figure 1. A 65-nm DRAM (left) and a schematic that conceptualizes the soft error phenomenon (right): Electron-hole pairs created through ionization by radiation might get drawn to node terminals before they recombine in the substrate causing a transient glitch in the device node. This temporary pulse might flip the internal state of the memory bit.

Cosmic ray particles have the ability to either toggle the state of memory elements or create unwanted glitches in combinational logic that may be latched by memory elements. As supply voltages reduce and feature sizes become smaller in future technologies, soft error tolerance is considered a significant challenge for designing future electronic systems. For example, a 1 GB memory system based on 64Mbit DRAMs has a combined error rate of 3435 FIT (failure in 10^9 hours of operation) when using single error correction and double error detection. An even higher soft error rate of 4000 FIT was reported for a typical processor with approximately half of the errors affecting the processor core and the rest affecting the cache. Such errors also affect the fast growing FPGA (Field Programmable Gate Array) segment.

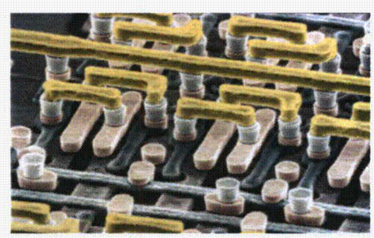

Figure 2. Integrated curcuits (IC) are becoming a major component of modern societies.

As earth's atmosphere shields most cosmic ray particles from reaching the ground and charge per circuit node used to be large, SEE on terrestrial devices has not been important until recently. The galactic flux of primary cosmic rays (mainly consisting of protons) is very large, about 100,000 particles/m^2s as compared to the much lower final flux (mainly consisting of neutrons) at sea level of about 360 particles/m^2s [1]. Only few of the galactic particles have adequate energy to penetrate the earth's atmosphere. However, with continued scaling of feature sizes and the use of more complex systems, soft errors in terrestrial applications are becoming an increasing concern and have drawn attention since late 1990s.

The issue of SEE was first studied in the context of scaling trends of microelectronics in 1962 [2]. Interestingly, the forecast from this study that the lower limit on supply voltage reduction will be imposed by SEE is shared by a recent work from researchers at Intel [3]. However, most works on radiation effects, since the work in 1962, focused on space applications rather than terrestrial applications.

There have been various documented failures due to soft errors ranging from memories used in large servers and aircrafts to implantable medical devices like cardiac defibrillators [4]. A widely cited soft error episode involves L2 caches with no error correction or protection that caused Sun Microsystems' flagship servers to crash suddenly and mysteriously [5]. This problem resulted in loss of various customers for Sun Microsystems. More ominous than this failure can be errors in embedded devices such as cardiac defibrillators that are becoming an integral part of our society. As computing systems develop into indispensable part of various critical applications ranging from medical implants to fly-by-wire aircrafts, immunity against soft errors becomes more critical for the society as a whole.

The importance of dealing with the soft error problem can be evidenced by the large number of papers and articles that flooded the scientific community over the last decades. However, most researchers are impeded by access to realistic fault models and real soft error data. This limitation results from confidentiality of soft error data of chips tested by semiconductor companies and the limited access to accelerated soft error testing facilities for academics. Most commercial soft error testing in U.S.A. is performed at the Los Alamos test facility, access to which is expensive and cumbersome due to security clearances required.

THE IMPETUS BEHIND THE SEAT

Radiation-induced SEE may seem to be easily solved through techniques such as radiation-hardened processing. These kinds of countermeasures have been traditionally and successfully adopted to remedy radiation effects in space applications. However, they are not suitable for commercial manufacturers of terrestrial devices as many of the solutions consume more power, reduce manufacturability and severely influence IC performance [6]. Even space applications are moving away from the use of radiation hardened process technology. They are using commercial off-the-shelf components that employ soft error protection techniques at software and architecture level for cost and performance reasons. As a result, many researchers have been focusing on employing new soft error countermeasures ranging from process to software levels.

Advances in process technology such as adoption of silicon-on-insulator (SOI), elimination of boron-10 impurities are expected to mitigate the soft error problem to a certain extent. However, solutions at higher levels are still essential for reliable operation of the computing system. The lack of fault models that abstract the physical phenomena of soft errors accurately in a fashion that is accessible to computer engineers and the absence of tools that analyze the effectiveness of soft error countermeasures are affecting researchers in their quest for taming the soft error problem.

There is an obvious need for a community resource for researchers and industrial practitioners studying radiation-induced SEE on computing systems. Existing tools either do not address the problem in full extent or they are kept confidential by the sole proprietorship of commercial entities, and therefore are not available to the research community. The SEAT will serve a critical purpose in providing researchers of electrical, computer, information sciences or nuclear origin with an open, modular, flexible yet a comprehensive tool.

The SEAT has emerged as a complementary tool to furnish theoretical foundation to experimental radiation-induced soft error research at Penn State Breazeale Nuclear Reactor by Mechanical and Nuclear Engineering, and Computer Science and Engineering Departments. More details can be found in [7] in this annual report. The experiments performed are compiled into an "accelerated soft error testing dataset". The researchers are then able to seek to duplicate these observations by the SEAT or vice versa.

The strength of the SEAT is the fact that it is built upon the combined expertise of computer and nuclear engineers. The SEAT hierarchy starts with modeling the ionization effects of particle strikes on semiconductor devices, and then creates higher-level abstractions of these effects for analysis at the circuit and architecture level. This infrastructure will enable researchers working on circuit, architectural and software countermeasures for soft errors to obtain a better perspective of the physical phenomena, and help them tune their techniques accordingly. If the fault model used at architecture or circuit-level fails to model the SEE accurately, the underlying value of solutions proposed at higher abstractions become meaningless. In this report, we will present details of SEAT-DA, the device level abstraction of the toolset.

SEATDA TOOL

Soft error induced transient pulse generation is dependent on exact charge deposited by the neutron-Si interaction and its subsequent collection. SEAT-DA is a tool flow built on top of three different tools as shown in Figure 3. It models both charge deposition and charge collection as described in the following subsections.

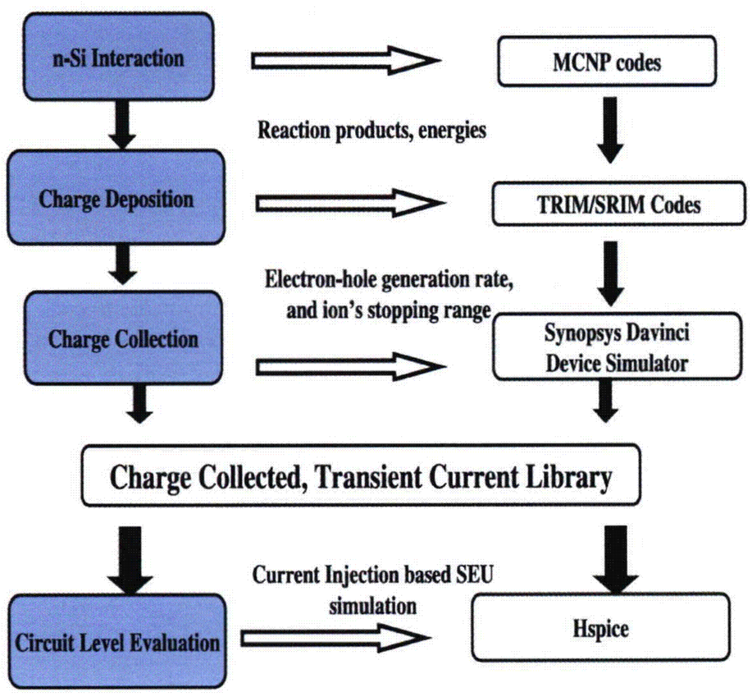

Figure 3. SEAT-DA Simulation Tool Flow

Charge deposition by neutron induced soft errors

To study n-Si interactions, we use the Monte Carlo N Particle (MCNP) toolset. Input to MCNP includes a model of silicon substrate and the description of the neutron flux. MCNP can be made to run with the right reaction codes and neutron data files to model various reactions. This feature is particularly useful as the neutron flux is dependent on the location and altitude, we may setup MCNP with the exact distribution of neutron flux at a given place to calculate the exact n-Si interaction. We have also created customized scripts that parse the MCNP output to identify the different reactions and their outputs. MCNP is used for studying neutron, photon, electron, or coupled neutron/photon/electron transport. This tool has been traditionally used in nuclear engineering for applications such as, reactor designs, radionuclide based imaging, and others. Neutron-Si reactions can be classified into two main groups: elastic and inelastic. MCNP can model both elastic and inelastic scattering. Elastic scattering, due to the low mass of the neutrons, does not produce significant ionizations. In contrast, inelastic reactions occur when the neutron enters the nucleus and the unstable nucleus disintegrates to smaller particles. Many reactions are possible and various particles may be emitted (Please see Equation 1; we will refer to these reaction by the numbers given below).

$n + {}^{28}Si$	$\rightarrow p + {}^{28}Al$	$\rightarrow 1$	
	à $n + \alpha + {}^{24}Mg$	$\rightarrow 2$	
	à $n + p + {}^{27}Al$	$\rightarrow 3$	
	à $\alpha + {}^{25}Mg$	$\rightarrow 4$	(1)
	à ${}^{3}He + {}^{26}Mg$	$\rightarrow 5$	
	à $2\alpha + {}^{21}Ne$	$\rightarrow 6$	
	à $\gamma + {}^{29}Si$	$\rightarrow 7$	
	à $n + {}^{29}Si$	à 8	
	à etc.		

Once the different reactions products are obtained, we use Transport of Ions in Matter (TRIM) simulator to calculate the charge deposited by these ions. Interfacing MCNP and TRIM together enables an accurate analysis of the charge creation. TRIM is used to calculate the stopping power of ions. TRIM identifies the range of these ions and the charge these ions are capable of depositing. Once the ion distribution resulting from a particle strike is known, its range and charge generation rate is calculated using TRIM. This generation rate is fed to a 3D device simulator to calculate the charge collected in a given region of the device. Among the above set of possible reactions, inelastic scattering produce byproducts that are heavier than the original neutrons, hence they deposit more charge as they travel in silicon. In terms of the susceptibility, transient pulse caused by the inelastic scattering is of higher magnitude than elastic scattering errors. For this reason, it can cause errors on even nodes with large capacitance, or alternatively will not be easily attenuated by the electrical and latching window masking effects. However, it should be noted that these occur fewer in numbers in comparison to the elastic scattering. However, in this work we just present the results from for inelastic reactions, as we believe these are the upper bound worst case scenarios that require to be addressed to ensure a reliable circuit operation. A circuit designed for these conditions will be immune to errors due the elastic scattering.

Charge collection

After the reaction products of n-Si interactions deposit charge, this charge may either recombine or get collected on the device terminal to generate current. For modeling charge collection we use Synopsys TCAD Davinci 3D device simulator. Davinci uses the physical model and equation interface (PMEI) to perform simulations that incorporate user-defined physical models and equations. The input to the 3D simulator includes the device structure, device parameters and device level equations. The charge may be collected in the device terminals by either drift or diffusion processes.

In the case where the ion track is sufficiently far from the space charge zone of the drain junction, the carriers generated in the track mainly move by diffusion. However, for charge collection, the most sensitive regions are reverse biased p/n junctions of the transistor. The high field present in a reverse-biased junction depletion region can collect the charge generated by the ion tracks through drift processes, leading to a transient current at the junction. An important phenomenon associated with the charge collection is called field funnel. Charge generated along the ion track can locally collapse the junction electric field due to the highly conductive nature of the charge track and separation of charge by the depletion region. Figure 8 shows the field in a device after the field has collapsed. The funneling effect can increase charge collection at the struck node by extending the junction electric field away from the junction and deep into the substrate such that charge deposited some distance from the junction can be collected through the efficient drift process.

In deep-sub-micron technology, another phenomenon termed as alpha-particle source-drain penetration effect (ALPEN) also contributes to the phenomenon of charge collection. Due to ALPEN, if a particle strike passes through both the source and the drain at near-grazing incidence, a significant but short-lived source-drain conduction current that mimics the "on" state of the transistor, is generated. However, in sub-100nm devices, when electron-hole pairs are generated there is a high probability that such a generation spans a region greater than the gate length. Hence, we will expand the definition of ALPEN to include these effects. In addition, we will refer to the processes of funneling and ALPEN as drift processes.

The simulator was setup to use the physical models that include standard drift-diffusion laws and classical physical models. These models include: Carrier-carrier scattering mobility model (CCSMOB), to account for the large carrier concentrations present in the charge column. CCSMOB also includes effects of doping and temperature on mobility. Field-dependent mobility model (FLDMOB), to account for reverse biased junction, and high electric fields in the depletion region. Shockley-Read-Hall and Auger recombination models to account for recombination of the carriers. Band-gap-narrowing (BGN) model is used to model the pn junction as a bipolar device. The device was loaded with lumped resistance and capacitance models to ensure realistic conditions.

The electron-hole pairs are introduced in the simulation as a charge column. The charge column is assumed to have a Gaussian profile. The charge is generated over a period of about 6 picoseconds using a Gaussian waveform. The structure was setup to solve time-dependent solution lasting up to 5ns. This is sufficient to resolve the drift and diffusion component of the charge collection process. However, the diffusion charge collection may continue for a longer period, but its contribution to total charge collection is negligible. The output from the 3D simulation analysis is used to generate current profiles for the different particle strikes. The current is integrated over the time to calculate the charge collected by the soft error.

Hence, a typical transient current generated by a soft error has a high drift component, which lasts for a few picoseconds and after the collapsed field is re-established, the charge collections is predominantly due to diffusion. For glitch based circuit level analysis, it is important to model both drift and diffusion component accurately as the drift process is responsible for the peak, and the diffusion process is responsible long tail of the fast-rising slow decaying current pulse.

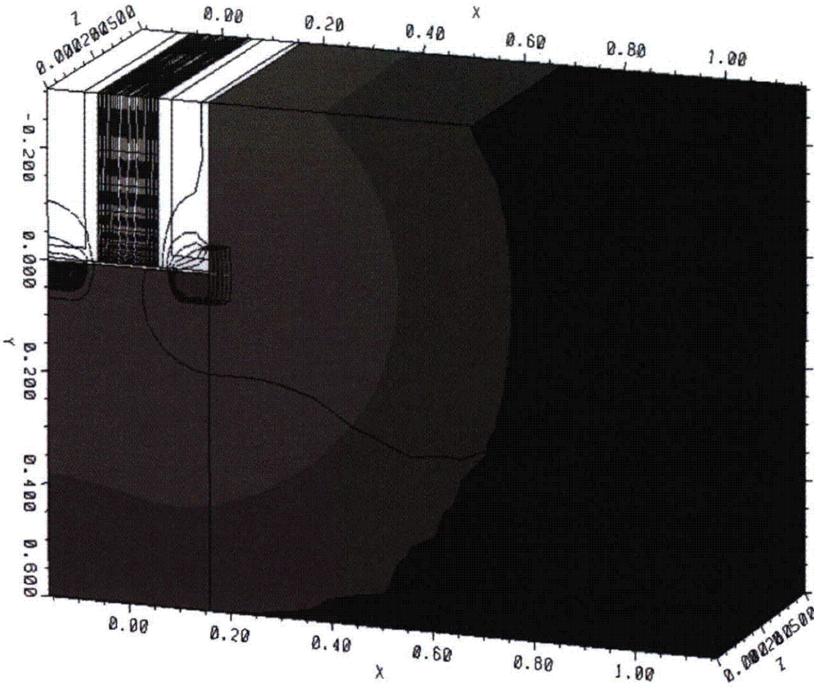

Figure 4. Funneling

CONCLUSIONS AND FUTURE WORK

The SEAT seems to fill a critical need, particularly in research community. With its current stage, it received a great deal of interest from both the academia and industry. We received many positive critiques in a conference that we presented the SEAT the first time [9]. Many industry affiliates stated their interest in the tool.

Even though neutrons account for the majority of the cosmic particles at sea level, the contribution of other particles, particularly protons, become dominant to the soft error problem at higher altitudes. For a more through analysis and more extensive applicability, other particle interactions should also be incorporated into the simulation. At this stage of the tool, we managed to include proton flux in the cosmic rays into the analysis. This, however, does not include nuclear-level interactions of protons with the medium, but it does take into account their direct ionization effect. For better modeling of physics, nuclear interactions of protons with the host nuclei must be accounted for since this dominates proton-related single-event effects.

REFERENCES

1. J. F. ZIEGLER, *Terrestrial Cosmic Ray Intensities*, IBM Journal of Research and Development, v. 40, No: 1, pp. 19-39, 1996.

2. J. WALLMARK, S. MARCUS, *Minimum Size and Maximum Packaging Density of Non-redundant Semiconductor Devices*, Proceedings of IRE, 50, 1962.

3. S. BORKAR, T. KARNIK, V. DE, *Design and Reliability Challenges in Nanometer Technologies*, Proceedings of 41st Design Automation Conference, San Diego, 1994.

4. P. D. BRADLEY, E. NORMAND, *Single Event Upsets in Implantable Cardioverter Defibrillators*, IEEE Trans. Nucl. Sci., v. 45, pp. 2929-2940, Dec. 1998.

5. Sun Microsystems, *Soft Memory Errors and Their Effect on Sun Fire Systems*, 2002.

6. P. E. DODD, L. W. MASSENGILL, *Basic Mechanisms and Modeling of Single-event Upset in Digital Microelectronics*, IEEE Trans. Nucl. Sci., v. 50, pp. 583-602, June 2003.

7. N. VIJAYKRISHNAN, M. J. IRWIN, K. ÜNLÜ, V. DEGALAHAL, S. M. ÇETINER, *Testing Neutron-induced Soft Errors in Semiconductor Memories*, Breazeale Nuclear Annual Report, December 2004.

8. J. F. ZIEGLER, http://www.srim.org/

9. V. DEGALAHAL, S. M. CETINER, F. ALIM, N. VIJAYKRISHNAN, M. J. IRWIN, K. ÜNLÜ, *SESEE: A Soft Error Simulation and Estimation Engine*, 7th Int. Conf. on Military and Aerospace Programmable Logic Devices (MAPLD), September 8-10, 2004.

TESTING FAST NEUTRON-INDUCED SOFT ERRORS IN SEMICONDUCTOR MEMORIES

Participants: K. Ünlü, Prof. of Mechanical and Nuclear Eng. Dept., Assoc. Director for Research, RSEC
N. Vijaykrishnan, Prof. of Computer Science and Eng. Dept.
M. J. Irwin, Prof. of Computer Science and Eng. Dept.
B. Heidrich, Sr. Research Assistant, RSEC

C. Çelik, Ph.D. student at Mechanical and Nuclear Eng. Dept.
K. Ramakrishnan, Ph.D. student at Computer Science and Eng. Dept.

Services Provided: Neutron Beam Laboratory

Sponsors: NSF, INIE Mini Grant, RSEC, Penn State Dept. of CSE

INTRODUCTION

Soft errors are transient circuit errors caused due to excess charge carriers induced primarily by external radiations. Radiation directly or indirectly induces localized ionization that can flip the internal values of the memory cells. Our current work tries to characterize the soft error susceptibility for different memory chips working at different technology node and operating voltage.

BACKGROUND AND RELATED WORK

Advances in VLSI technology have ensured the availability of high performance electronics for a variety of applications. The applications include consumer electronics like cellular phones and HDTVs; automotive electronics like those used in drive-by-wire vehicles, and million dollar servers used for storing and processing sensitive and critical data. These varied applications require not only higher throughput but also dependability. Even if a microprocessor is shipped without any design errors or manufacturing defects, unstable environmental conditions can generate temporary hardware failures. These failures, called *transient faults*, cause the processor to malfunction during operation time. The major sources of transient faults are electromagnetic interference, power jitter, alpha particles, and cosmic rays. Studies in [1, 2] have shown that a vast majority of detected errors originate from transient faults. Even a single-bit error may eventually lead to a computation failure. Therefore, managing the soft errors is a critical problem to solve in fully realizing dependable computing.

Soft error rate (SER) testing of devices has been performed for both neutron and alpha particles. Beam 30L of Weapon Neutron Research at the Los Alamos National Laboratory is a JEDEC prescribed test beam for soft errors, and is the only one of its kind. This beam is highly stable and it closely replicates the energy spectrum of terrestrial neutrons in the 2-800 MeV range while providing a very high neutron flux. The SER testing reported in literature recently were performed at this facility [4, 5]. However, the beam availability is limited. Alternatively in the past, experiments were carried out with alpha particles originating from ^{238}Th foil on 0.25 μm-generation SRAMs [7]. Elimination of borophosphosilicate glass (BPSG) and ^{10}B from the process flow in the 180-nm generation has made the low-energy (<1 eV) neutron SER negligible [3]. High-energy (1-1000 MeV) neutrons often dominate SER in advanced CMOS logic and memories. The reaction cross sections for important isotopes for thermal and fast neutrons are given in Table 1. As seen from the Table 1, for high-energy neutrons all selected reactions have the same order of magnitude cross sections. Hence, the need for accessible neutron testing facilities is critical for design of the next generation semiconductor devices.

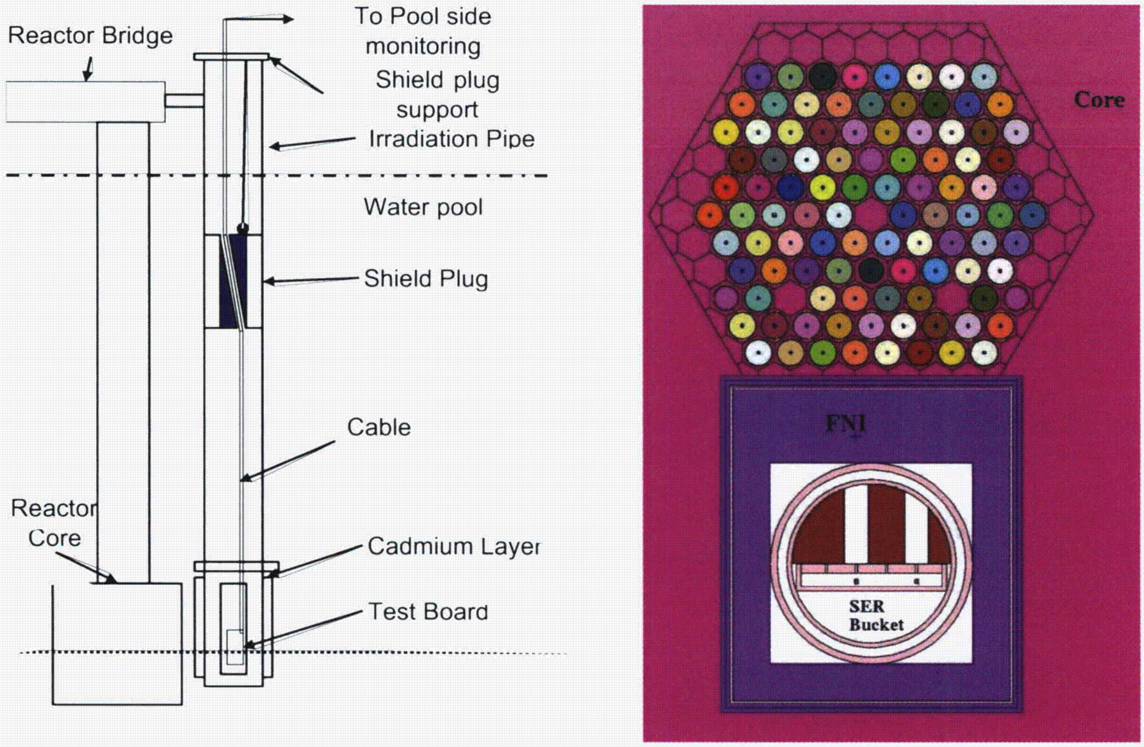

Figure 1. (Left) Fast neutron test setup near the reactor core, (Right) MCNP Model of the core and

This study intends to observe the effect of ^{10}B and high-energy neutrons on soft error rate. In order to investigate the effect of boron-10 on SER, a fast neutron irradiator (FNI) is used as shown in Figure 1. The fast neutrons available near the reactor core by inserting a test circuit into a stand-up pipe adjacent to the reactor core face.

Table 1. Reaction cross sections

Reaction	Products	Q-Value (MeV)	Cross Section (at 0.0017 eV)	Cross Section (at 0.0253 eV)	Cross Section (at 14 MeV)
10B+n	7Lia	2.79	~ 17000 b	~ 3837 b	~ 49 mb
11B+n	8Lia 7Lia	-6.63 -8.66	~ 20 mb	~ 50 mb	~ 32 mb
28Si+n	25Mga	-2.65	~ 0	~ 2 mb	~ 222 mb
30Si+n	27Mga	-4.20	~ 0	~ 60 mb	~ 68 mb

EXPERIMENTAL SETUP AND RESULTS

Penn State Breazeale Nuclear Reactor was used as the neutron source in the experiments. The maximum rated power of the reactor is 1 MW in the continuous mode, and 2000 MW in the pulse mode. The high neutron flux allows for accelerated testing of the phenomenon.

The experimental setup consists of a custom board interfaced with a computer through a GPIB card (from National Instruments). The board itself has off-the-shelf SRAM memory chips. The board is controlled through a LabVIEW interface. The controlling application consists of simple routines to read and write a user specified value across the whole memory. During the readout, it compares the written value to the value in each address. The circuit board is secured in the beam cave, and connected to a PC outside using a 25-ft cable. This configuration allowed for continuous read-write, and for changing the operating conditions without interrupting the experiment.

As mentioned earlier, the neutron flux around the reactor core is much higher than that at the neutron beam ports. Therefore, the circuit board will also be placed by the periphery of the reactor core via a vertical standpipe in order to observe the effect of fast neutrons on soft error rate. The fast neutron flux at the core boundary is 5×10^{12} neutrons/cm^{2}sec, and thermal flux is 1.3×10^{13} neutrons/cm^{2}sec at 1MW steady state reactor operation. The reactor can be pulsed for a very short duration of time, around 10 milli-sec at its Full-Width Half-Maximum, at which it generates a fast flux of about 1×10^{16} neutrons/cm^{2}sec at the core periphery. This amounts to about four orders of magnitude increase in the fast flux. The time duration is very limited, yet the amount of fast flux is immense. The test circuits will be let inside the standpipe and the reading will be taken. In addition, the walls of the pipe will be covered with boron. Boron will absorb the thermal component of the flux so that the board is affected only by fast neutrons.

RESULTS AND DISCUSSION

The setup described in this report allows for accelerated testing of semiconductor memory devices fast neutrons. The experiments and analyses have been performed only on soft errors due to fast neutrons. Neutron flux at the sample box of the SER bucket in the FNI has been measured. Currently, Monte Carlo simulations by using MCNP-5 [8] for the neutron flux measurements and possible improvement methods for fast neutron flux are in progress. Neutron flux measurements carried out by aluminum, sulfur, and gold samples for three neutron energy group fast, epi-thermal, and thermal respectively. The energy groups are defined as given in the Table 2 for MCNP model. Front view of the SER bucket is shown in Figure 2 with two big irradiation holes in the polyethylene in row C.

Table 2. Neutron energy groups in MCNP-5

Group	Energy Range (MeV)
Thermal	1.000×10^{-11} to 0.625×10^{-6}
Epi-Thermal	0.625×10^{-6} to 1.000×10^{-3}
Fast	1.000×10^{-3} to 2.000×10^{1}

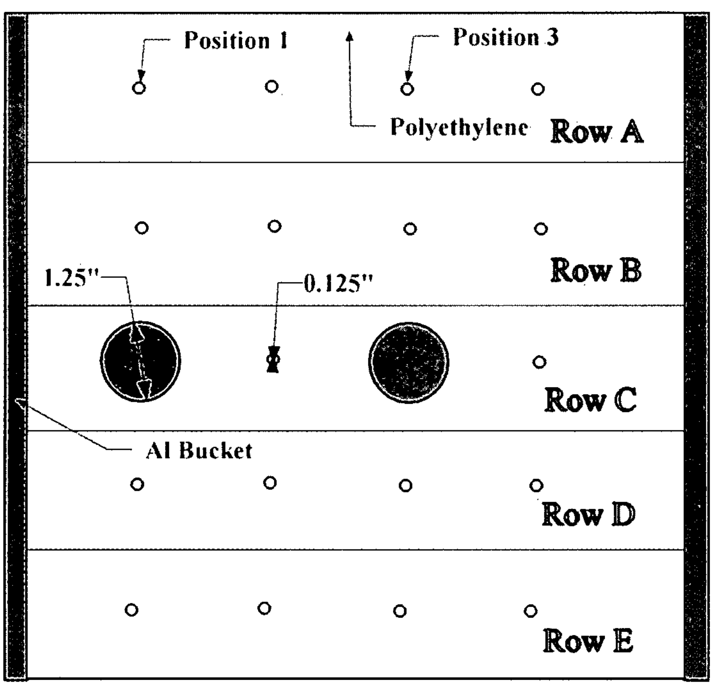

Experimental results have relative errors of 25 % for the neutron flux measurements. MCNP-5 simulation results with an assumption on the total number of fission neutrons in the core of 8.4×10^{16}n/sec and experimental results for neutron flux at the irradiation point in the sample box are given in Table 3. A detailed neutron flux spectrum for the MCNP-5 calculation is also shown in the Figure 3 for better understanding of pre-defined energy group neutron fluxes.

Both, measurement and simulation results showed higher thermal neutron flux values than the expected value. Therefore, new materials, dimensions, or designs for SER bucket are in progress.

Table 3. Neutron flux measurement and simulation results

Position	$f_{thermal}$	$f_{epi\text{-}thermal}$	f_{fast}
A1	7.939E+11	2.114E+11	3.170E+11
A3	6.310E+11	3.485E+11	4.703E+11
B1	9.282E+11	1.100E+11	2.109E+11
B3	5.448E+11	2.122E+11	1.598E+11
C1	**1.061E+12**	**2.226E+10**	**3.506E+11**
$C1^{exp}$	**7.990E+10**	**7.890E+10**	**2.700E+10**
C3	**6.503E+11**	**5.550E+10**	**2.526E+11**
$C3^{exp}$	**7.000E+10**	**7.460E+10**	**2.400E+10**
D1	7.450E+11	2.262E+11	7.166E+10
D3	7.543E+11	1.814E+11	1.749E+11
E1	9.912E+11	1.117E+11	1.338E+11
E3	6.412E+11	2.079E+11	1.851E+11

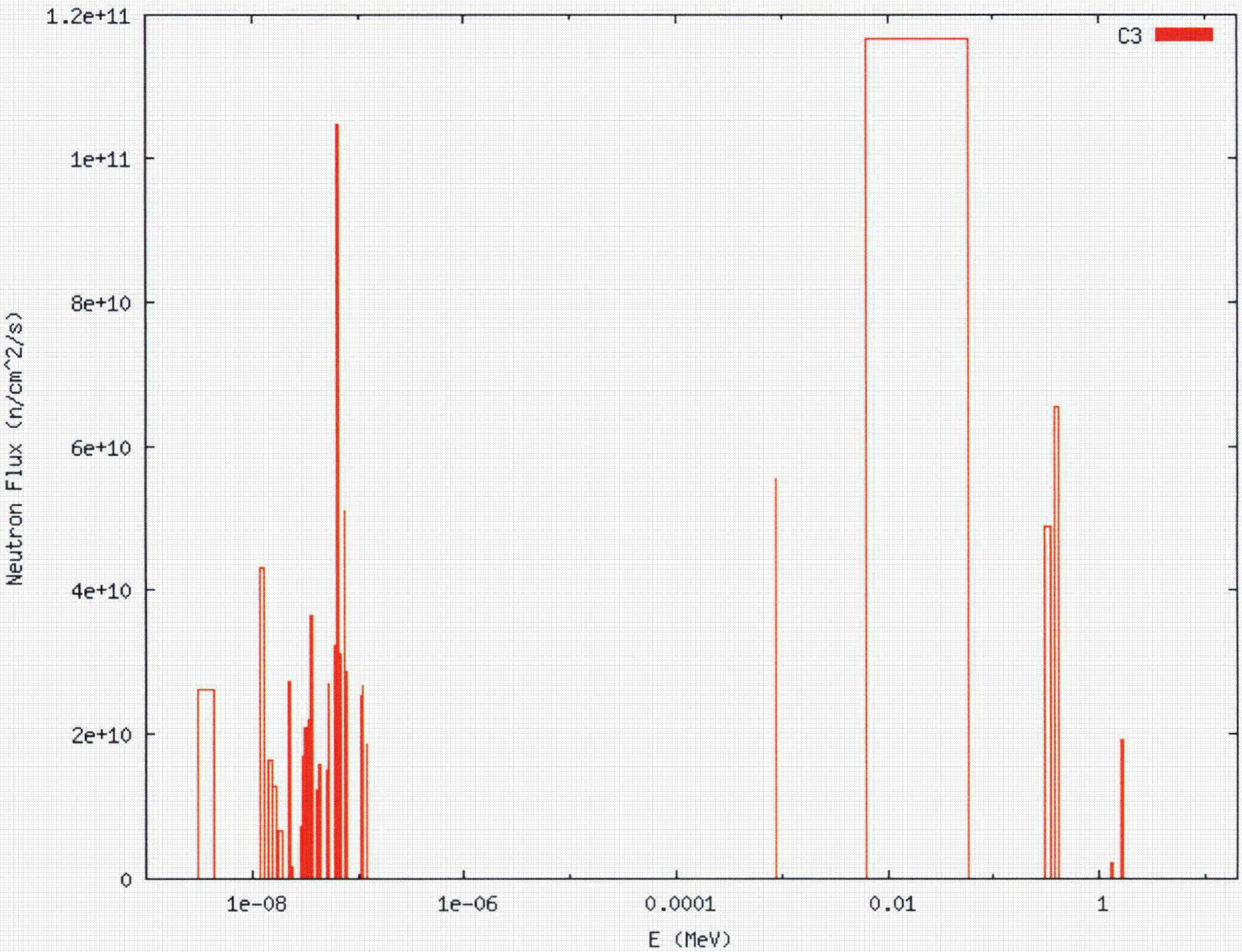

Figure 3. Neutron spectrum for position C3 in the SER bucket

FUTURE WORK

This report briefly summarizes the study focused on fast neutron absorption on soft error rate. The fast neutron flux at the core boundary is 5×10^{12} neutrons/cm^{2}sec, and thermal flux 1.3×10^{13} neutrons/cm^{2}sec at 1-MW steady state reactor operation. Also, apart from memory chips, other processing circuits will also be put to test in similar fashion and the results observed.

The reactor can be pulsed for a very short duration of time, around 10 msec at FWHM, at which it generates a fast flux of about 1×10^{16} neutrons/cm^{2}sec at the core periphery. This amounts to about four orders of magnitude increase in the fast flux. The time duration is very limited, yet the amount of fast flux is immense. That might also reduce the experiment times significantly and help perform more tests with various technologies and designs.

The thermal neutron flux in the SER bucket will be decreased in order to study the fast neutron absorption on soft errors in the future by investigating the MSNP-5 simulations and experiments on materials and design of the SER bucket.

REFERENCES

J. SOSNOWSKI, *Transient fault tolerance in digital systems*, IEEE Micro, v. 14 No. 1, pp. 24-35, February 1994.

D. P. SIEWIOREK, R. S. SWARTZ, *Reliable Computer Systems: Design and Evaluation,* 2nd edition, Digital Press, Burlington, MA.

R. BAUMANN, *The impact of technology scaling on soft error rate performance and limits to the efficacy of error correction,* IEDM '02 Technical Digest, IEEE International, pp. 329-332, 8-11 Dec. 2002.

P. HAZUCHA, T. KARNIK, J. MAIZ, S. WALSTRA, B. BLOECHEL, J. TSCHANZ, G. DERMER, S. HARELAND, P. ARMSTRONG, S. BORKAR, *Neutron soft error rate measurements in a 90-nm CMOS process and scaling trends in SRAM from 0.25-/spl mu/m to 90-nm generation,* IEDM '03 Technical Digest, IEEE International, pp. 21.5.1-21.5.4, 8-10 Dec. 2003.

J. MAIZ, S. HARELAND, K. ZHANG, P. ARMSTRONG, *Characterization of multi-bit soft error events in advanced SRAMs,* IEDM '03 Technical Digest, IEEE International, pp. 21.4.1-21.4.4, 8-10 Dec. 2003.

N. SEIFERT, D. MOYER, N. LELAND, R. HOKINSON, *Historical Trend in Alpha-Particle induced Soft Error Rates of the Alpha Microprocessor,* IEEE 39th Annual International Reliability Physics Symposium, pp. 259-265, 2001.

TESTING THERMAL NEUTRON-INDUCED SOFT ERRORS IN SEMICONDUCTOR MEMORIES

Participants: N. Vijaykrishnan, Prof. of Computer Science and Eng. Dept.
M. J. Irwin, Prof. of Computer Science and Eng. Dept.
K. Ünlü, Prof. of Mechanical and Nuclear Eng. Dept., Assoc. Director for Research, RSEC
K. Ramakrishnan, Ph.D. student at Computer Science and Eng. Dept.
S. M. Çetiner, Ph.D. student at Mechanical and Nuclear Eng. Dept.
C. Çelik, Ph.D. student at Mechanical and Nuclear Eng. Dept.

Services Provided: Neutron Beam Laboratory

Sponsors: Department of Energy, INIE Mini Grant, RSEC, Penn State Dept. of CSE

INTRODUCTION

Soft errors are transient circuit errors caused due to excess charge carriers induced primarily by external radiations. Radiation directly or indirectly induces localized ionization that can flip the internal values of the memory cells. Our current work tries to characterize the soft error susceptibility for different memory chips working at different technology node and operating voltage.

BACKGROUND AND RELATED WORK

Advances in VLSI technology have ensured the availability of high performance electronics for a variety of applications. The applications include consumer electronics like cellular phones and HDTVs; automotive electronics like those used in drive-by-wire vehicles, and million dollar servers used for storing and processing sensitive and critical data. These varied applications require not only higher throughput but also dependability. Even if a microprocessor is shipped without any design errors or manufacturing defects, unstable environmental conditions can generate temporary hardware failures. These failures, called *transient faults*, cause the processor to malfunction during operation time. The major sources of transient faults are electromagnetic interference, power jitter, alpha particles, and cosmic rays. Studies in [1, 2] have shown that a vast majority of detected errors originate from transient faults. Even a single-bit error may eventually lead to a computation failure. Therefore, managing the soft errors is a critical problem to solve in fully realizing dependable computing.

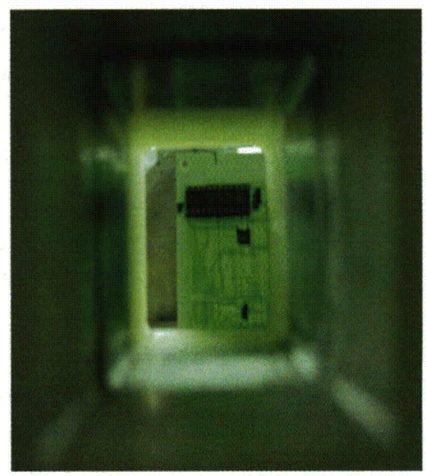

Figure 1. Test chip as seen through the narrow opening in the polyethylene/lead

Soft error rate (SER) testing of devices has been performed for both neutron and alpha particles. Beam 30L of Weapon Neutron Research at the Los Alamos National Laboratory is a JEDEC prescribed test beam for soft errors, and is the only one of its kind. This beam is highly stable and it closely replicates the energy spectrum of terrestrial neutrons in the 2-800 MeV range while providing a very high neutron flux. The SER testing reported in literature recently were performed at this facility [4, 5]. However, the beam availability is limited. Alternatively in the past, experiments were carried out with alpha particles originating from ^{238}Th foil on 0.25 µm-generation SRAMs [7]. Elimination of borophosphosilicate glass (BPSG) and ^{10}B from the process flow in the 180-nm generation has made the low-energy (<1 eV) neutron SER negligible [33].

High-energy (1-1000 MeV) neutrons often dominate SER in advanced CMOS logic and memories. Hence, the need for accessible neutron testing facilities is critical for design of the next generation semiconductor devices.

This study intends to observe the effect of ^{10}B and high-energy neutrons on soft error rate. In order to investigate the effect of boron-10 on SER, a thermal neutron beam is used as shown in Figure 2.

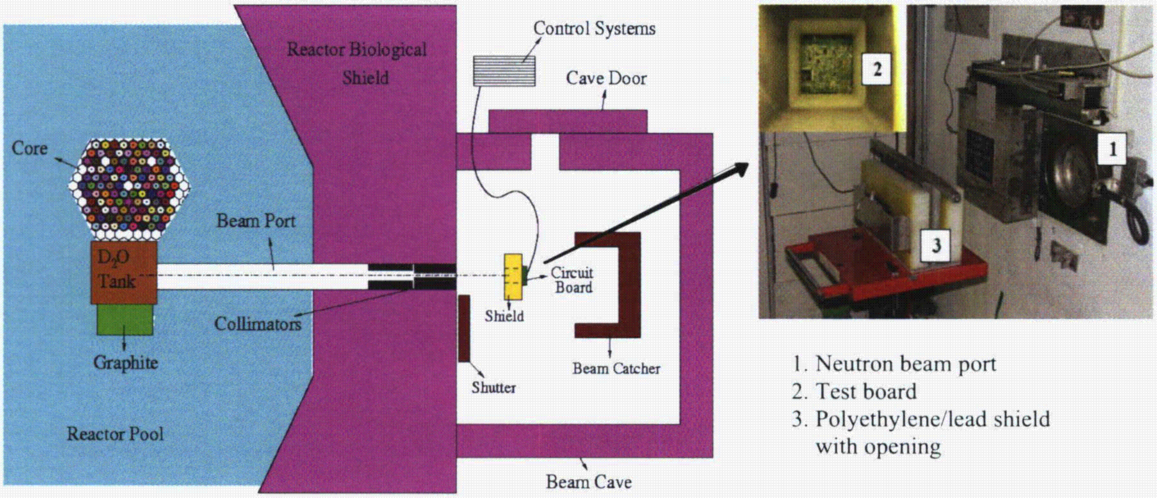

Figure 2. (Left) Simplified layout of the test board, (Right) test chip placed in front of the beam tube with the polyethylene/ lead shield for thermal neutron testing

EXPERIMENTAL SETUP AND RESULTS

Penn State Breazeale Nuclear Reactor was used as the neutron source in the experiments. The maximum rated power of the reactor is 1 MW in the continuous mode, and 2000 MW in the pulse mode. The reactor power is adjusted from 10 W to 1MW observe the soft error rate dependence on neutron flux. No pulse-mode operation has been performed. Figures 1 and 2 show the test chip and the experimental setup.

For the beam port that was used in the experiments, the beam tube looks at the D_2O tank to get a well-thermalized beam. The average thermal flux at the exit of the beam port is about 3×10^7 neutrons/cm^{2}sec. The high neutron flux allows for accelerated testing of the phenomenon.

The experimental setup consists of a custom board interfaced with a computer through a GPIB card (from National Instruments). The board itself has off-the-shelf SRAM memory chips. The board is controlled through a LabVIEW interface. The controlling application consists of simple routines to read and write a user specified value across the whole memory. During the readout, it compares the written value to the value in each address. The circuit board is secured in the beam cave, and connected to a PC outside using a 25-ft cable. This configuration allowed for continuous read-write, and for changing the operating conditions without interrupting the experiment.

The selected section of the board is tested on-line multiple times in the actual setup before the reactor is started. The board is exposed to neutron flux after the reactor reaches the stable power level.

RESULTS AND DISCUSSION

The setup described in this report allows for accelerated testing of semiconductor memory devices with thermal neutrons. The experiments and analyses have been performed only on soft errors due to thermal neutrons. Currently, a 16-kbit for Vendor A and a 4-Mbit memory from Vendor B were tested at various supply voltages and reactor power levels. The chip from Vendor A is rated to operate at 5V, but was found to operate as low as 3V. Figures 3 (a) shows the effect of changing the supply voltage on registered soft errors in one hour. A more salient behavior can be observed with the chip from Vendor B. Vendor B chip was known to be denser (4-Mbits compared to 16-kbits) and was expected to have higher soft error vulnerability. Figure 3 (b) shows the effect of supply voltage change on measured soft errors in one hour.

As presented in Equation 1 below, the soft error rate is expected to depend on the $Q_{critical}$ and hence on the operating voltage.

$$SER = Nflux * CS * \exp(-Q_{critical}/Q_s) \quad (1)$$

where Nflux is the intensity of neutron flux, CS is the area of cross section of the node, Q_s is the charge collection efficiency, $Q_{critical}$ is the charge that is stored at the node and hence is equal to VDD * C_{node}, where VDD is the supply voltage and C_{node} is the nodal capacitance. Figures 3 (a) and (b) confirm the exponential dependence of soft error rate on device operating voltage as well as other specifications of the device as pointed out by several authors before [7].

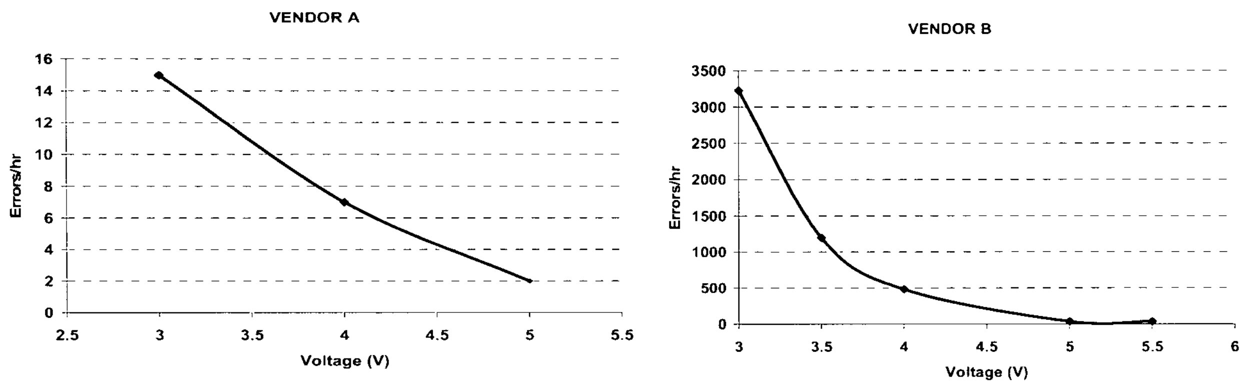

(a) (b)

Figure 3. Effect of supply voltage on soft errors

While employing voltage scaling for power reduction, there is a reduction in the $Q_{critical}$ of the cell. Now, if all the other factors remained the same there should be a super-linear increase in the SER. However, based on the Figures 3, we see a linear increase in the SER for a corresponding decrease in the voltage. This is because for a change in supply voltage, the resultant current transient also changes. As the supply voltage reduces, the magnitude of the current changes. This affects the regenerative feedback of the SRAM cell. Thus, the soft error rate is inversely proportional to the supply voltage.

For examining the statistical accuracy of the accelerated tests, the tests were performed at various reactor power levels. Since the reactor power and the flux at the exit of the beam port are directly correlated, changing the reactor power effectively changes the neutron flux impinging on the test sample, hence is expected to increase the soft error rate. The results are presented in Figures 5 (a) and (b).

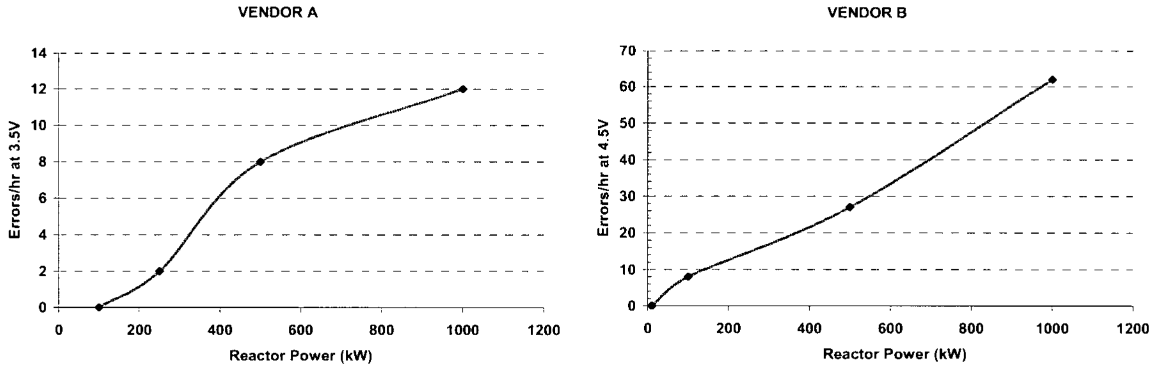

(a) (b)

Figure 4. Effect of neutron flux on soft errors

Both figures prove that the soft error rate increases as the reactor power increases. That the soft error rate for the chip from Vendor A is not as linear as the chip from Vendor B is attributed to the relatively small size of the first one. Hence, for statistical accuracy of accelerated soft error rate measurements, it is suggested that the measurements be performed using high capacity chips.

FUTURE WORK

This report briefly summarizes the first phase of the study that focused only on the effect of ^{10}B fission caused by thermal neutron absorption on soft error rate. The elimination of BPSG layer in new device technologies and considerable reduction of ^{10}B content in the p-dopant significantly dropped the contribution of boron fission as a source of soft error. Therefore, for younger-generation technologies, one needs to take into account the high-energy neutron impact on device operation for proper soft error rate analysis.

The experiments will be carried out with different chips and required coupling with Soft Error Analysis Toolset (SEAT) will be studied in the later phase.

REFERENCES

J. SOSNOWSKI, *Transient fault tolerance in digital systems*, IEEE Micro, v. 14 No. 1, pp. 24-35, February 1994.

D. P. SIEWIOREK, R. S. SWARTZ, *Reliable Computer Systems: Design and Evaluation,* 2nd edition, Digital Press, Burlington, MA.

R. BAUMANN, *The impact of technology scaling on soft error rate performance and limits to the efficacy of error correction,* IEDM '02 Technical Digest, IEEE International, pp. 329-332, 8-11 Dec. 2002.

P. HAZUCHA, T. KARNIK, J. MAIZ, S. WALSTRA, B. BLOECHEL, J. TSCHANZ, G. DERMER, S. HARELAND, P. ARMSTRONG, S. BORKAR, *Neutron soft error rate measurements in a 90-nm CMOS process and scaling trends in SRAM from 0.25-/spl mu/m to 90-nm generation,* IEDM '03 Technical Digest, IEEE International, pp. 21.5.1-21.5.4, 8-10 Dec. 2003.

J. MAIZ, S. HARELAND, K. ZHANG, P. ARMSTRONG, *Characterization of multi-bit soft error events in advanced SRAMs,* IEDM '03 Technical Digest, IEEE International, pp. 21.4.1-21.4.4, 8-10 Dec. 2003.

N. SEIFERT, D. MOYER, N. LELAND, R. HOKINSON, *Historical Trend in Alpha-Particle induced Soft Error Rates of the Alpha Microprocessor,* IEEE 39th Annual International Reliability Physics Symposium, pp. 259-265, 2001.

P. HAZUCHA and C. SVENSSON, *Impact of CMOS Technology Scaling on the Atmospheric Neutron Soft Error Rate,* IEEE Transactions on Nuclear Science, v. 47, No. 6, pp 2586-2594, Dec. 2000.

College of Agriculture

ESTIMATION OF CARBON POOLS AND FLUXES IN HIGH ALTITUDE ANDISOLS CHARACTERISTIC OF THE UPPER CHIMBO WATERSHED

Participants: Jonathan Lynch, Prof, Horticulture Dept.

Raul Jaramillo, Graduate Student, Horticulture Dept.
Amelia Henry, Graduate Student, Plant Biology

Services Provided: Gamma Spectrometry

To characterize the soil carbon storage level among different land use classes in the chimbo watershed of Ecuador. The gamma spectrometry at the RSEC is being performed to compare relative soil degradation levels of several land use categories, ranging from annual cropping to natural forest.

Publications:

SANREM Quarterly Report: Year 1
Watershed-based Natural Resource Management in Small-scale Agriculture:
Sloped Areas of the Andean Region
PI: Jeffrey Alwang
December, 2006

Sponsor: $70,000 (with overhead) from the SANREM CRSP of US AID

CHEMISTRY DEPARTMENT

DEVELOPMENT OF PROTON CONDUCTING MEMBRANES FOR METHANOL FUEL CELL APPLICATIONS

Participants: Harry R. Allcock, Evan Pugh Professor

Rich Wood, Graduate Student
Shih-To Fei, Graduate Student

Services Provided: Gamma Irradiation

The goal of the project is to develop a polymer electrolyte for direct methanol fuel cell applications. The principal aspects of this work include polymer design, synthesis, and membrane properties optimization, plus membrane fabrication and characterization. We utilize the radiation facility to cross-link our polymeric materials. The process of cross-linking produces mechanically strong membranes, and reduces membranes water uptake as well as methanol crossover.

PhD Thesis:

Wood, R. and Allcock, H. R., Novel Ion-Conductive Polymeric Materials for Fuel Cell Applications, 2006

CIVIL AND ENVIRONMENTAL ENGINEERING

BIOLOGICAL MANGANESE OXIDATION IN MINE WATER TREATMENT

Participants: Bill Burgos, Associate Professor

Hui Tan, Graduate Student

Services Provided: Gamma Irradiation

Manganese is a common contaminant in mine water discharges. The presence of manganese in water can cause odor, color and taste problems. Active manganese removal often involves addition of chemicals to raise pH or to promote the oxidative precipitation, therefore very costly. Passive limestone treatment system may be very effective in removing manganese from mine water discharge. At our field site at Fairview, PA, the treatment bed successfully removed manganese from influent water of over 100ppm to below 0.02ppm. However, the mechanisms of manganese removal are not clear. Seasonal data showed huge difference in manganese removal between summer and winter time. Lab experiments also showed greater manganese removal rate with non-sterile mine water compared to autoclaved ones. These evidences suggest biological activities are playing important role in manganese removal. We try to understand what variables affect the oxidation kinetics of manganese, including dissolved oxygen, pH, temperature and microbial community. Molecular characterization of the microbial community will be important to our work.

COLLEGE OF SCIENCE

BIOLOGY

FUNCTIONAL ANALYSIS OF RAD51 LIKE GENESE IN MEIOSIS AND MITOSIS IN ARABIDOPSIS

Participants: Hong Ma, Professor

Rong Xiao, Graduate Student (M.S.)
Wuxing Li, Graduate Student (Ph.D.)

Services Provided: Gamma Irradiation

Sponsor: NIH, $1,000,000

We are interested in understanding the function of the AtRAD51B, AtRAD51B, and AtXRCC2 genes in DNA damage repair in mitotic cells. The hypothesis is that one or more of these genes might play a critical role in DNA repair caused by gamma radiation. To test this, we obtained knockouts of these genes, and generated mutant plants with 2 or 3 of these genes knocked out. Seeds of these knockouts, as well as wild type seeds as control, were treated with gamma radiation. Growth of the seedlings was assessed to detect whether any lines show hypersensitivity to ionizing radiation.

COLLEGE OF ENGINEERING

TISSUE-ELECTRODE INTERFACE MONITORING FOR INTRACORTICAL PROBES

Participants: Dr. Ryan Clement, Assistant Professor, Bioengineering
Kunal Paralikar , Student, Bioengineering
Joy Matsui, Student, Bioengineering

Services Provided: Gamma Irradiation

Intra-cortical electrode arrays have the potential to provide a chronic connection between brain and the external environment. Their spatial and temporal resolution far exceeds those enabled by current brain-machine interface technologies. However their high degree of invasiveness exposes them to variable degree of immune response that limits the long-term functionality of these probes. In its initial phase, this response is characterized by activation of microglia, macrophages while in the latter phase activated astrocytes tend to form a physical barrier between the implant electrodes and healthy neural tissue. This knowledge is the result of end-point histology studies carried in the past decade. The goal of our research is to develop techniques that can allow for real-time monitoring of interface degradation. It is hypothesized that a built of microglia and astrocytes is accompanied by a change is tissue impedance. Hence research in our lab is carrying out impedance spectroscopy with the goal of correlating it with histology results. At the same time we are undertaking magnetic resonance imaging (MRI) to observe any gross changes at the interface that can help explain the degradation in neural tissue. Both impedance spectroscopy and magnetic resonance imaging techniques are currently being pursued with the ultimate goal of developing a model that can predict the interface quality based only on these parameters without the need for end-point histology.

Master's Thesis Completed:
Matsui, J. T. (R. S. Clement, adviser). Characterizing the Interface Between Functioning Implantable Neural Probes and Their Surrounding Cortical Tissue. August 2007.

Ph.D. Thesis:
Paralikar, K.J. (R.S. Clement, adviser). Characterization of the Tissue-electrode Interface Based on Electrophysiology, Histology and Magnetic Resonance Imaging. December 2008

Publications:

Paralikar, K. J., J. K. Lawrence and R.S Clement. **Collagenase-aided Insertion of Intracortical Microelectrode Arrays: Evaluation of Insertion Force and Chronic Recording Performance**. Engineering in Medicine and Biology Society, 2006. EMBS '06. 28th Annual International Conference of the IEEE
Aug. 2006 Page(s):2958 - 2961

Matsui, J.T., K.J. Paralikar, S. Pekney, M. Polons, A. Barber, and R. Clement. **Exploring Links in Recording Performance, Impedance, and Histology in Chronic Intracortical Implants.** Annual Meeting of the Biomedical Engineering Society, September 2007, p. 106.

THE USE OF HIGH-ENERGY GAMMA-IRRADIATION TO EFFECT CRYOREDUCTION OF METALLOENZYMES FOR SPECTROSCOPIC CHARACTERIZATION.

Participants:			
	Bollinger, J. Martin, Jr.	Associate Professor	Biochemistry
	Krebs, Carsten	Associate Professor	Biochemistry
	Tamanaha, Esta Y.	Graduate Student	Biochemistry
	Diao, Yinghui	Graduate Student	Biochemistry
	Jiang, Wei	Graduate Student	Biochemistry

Service Provided: Gamma Irradiation

Sponsors: Project (1) is funded by a grant from the American Chemical Society, Petroleum Research Fund to CK and JMB.

Project (2) is supported by a grant from NIH to CK and JMB.

Project (3) is supported by a grant from NIH to JMB.

Enzymes containing metal ions are wide-spread in Nature and play a pivotal role in almost every aspect of life; they catalyze numerous biochemical transformations, such as key steps in the biosynthesis of DNA and antibiotics. The main purpose of our research program is to define the mechanisms on a molecular level, by which metallo-enzymes catalyze these reactions. To accomplish this goal, we employ time-resolved spectroscopic methods with the aim to identify and characterize reaction intermediates and thereby deconvoluting the catalytic mechanism.
Significant information about such species can be gained from studies of samples that have been exposed to gamma-irradiation (total dose 2 to 5 Mrad) at low-temperatures (77 K), a.k.a. 'cryoreduction'. It has been demonstrated (Davydov et al. JACS 1994, 116, 11120-11128 and references therein) that this procedure allows reduction of the metal clusters while retaining the geometry of the oxidized cluster, because the molecular motion of the radiolytically reduced metal center is impeded due to the low temperature.
This method is extremely valuable for the study of diamagnetic species, because they can be converted to paramagnetic species, which can then be interrogated in detail by paramagnetic methods, such as EPR, ENDOR, ESEEM, and Mössbauer spectroscopies.

We employ this methodology to study the following projects:

- We have recently used this method to support the Fe(IV) intermediate in a mononuclear non-heme Fe-enzyme, Isopenicillin N Synthase (IPNS). In particular, formally a high-spin Fe(IV) intermediate that is EPR silent but characterized by Mössbauer was confirmed by converting to Fe(III) by cryoreduction . Status: in progress

- In collaboration with Brian Hoffman, Northwestern University, we will study *myo*-inositol oxygenase, which use unusual mix-valence dinuclear cluster as an active species. Again, we will attempt to convert the diamagnetic cluster to a paramagnetic cluster by cryoreduction and gain information about this species by the above methods. Status: in progress

- We use this method to study the structure of a novel heterodinuclear Mn/Fe clusters in Chlamydia trachomatis ribonucleotide reductase R2 protein. This enzyme plays a key role in the production of the deoxyribonucleotides utilized in DNA biosynthesis. Status: in progress

Ph.D. Thesis:

Jiang, Wei, Bollinger, J. Martin, Jr. (advisor) and Krebs, Carsten (co-advisor) "Mechanism of Ribonucleotide Reductase R2 Protein in Chlamydia Trachomatis." Diao, Yinghui, Bollinger, J. Martin, Jr. (advisor) and Krebs, Carsten (co-advisor)

"Mechanism of Activation of a Novel Dinuclear Oxygenase, *myo*-inositol Oxygenase" Tamanaha, Esta Y., Bollinger, J. Martin, Jr. (advisor) and Krebs, Carsten (co-advisor) "Mechanism of Isopenicillin N Synthase"

Publications:

Eser BE, Barr EW, Frantom PA, Saleh L, Bollinger JM Jr, Krebs C, Fitzpatrick PF Direct Spectroscopic Evidence for a High-spin Fe(IV) Intermediate in Tyrosine Hydroxylase. J Am Chem Soc. 2007 Sep 19; 129(37): 11334-5

NORTHEAST TECHNOLOGY CORPORATION

TESTING AND INSPECTION OF NEUTRON ABSORBER MATERIAL THAT ARE USED FOR THE SAFE STORAGE OF NUCLEAR FUEL

Participants: K. Lindquist, Ph.D.
A. Portanova

Services Provided: Neutron Irradiation, Neutron Radiography, Laboratory Space

Sponsors: Various Utility Clients

Neutron absorber materials are used to maintain nuclear fuel in storage in a safe and subcritical condition. Testing including physical characterization of these materials is conducted to assure these neutron absorber materials are serving their intended functions. Testing includes high resolution digital photographed measurement of dimensions, weights, density, hardness and boron-10 aerial density. Mater tested included Boraflex, Boral, borated stainless steel and various aluminum/boron carbide metal matrix composite.

SECTION B. OTHER UNIVERSITIES, ORGANIZATIONS, AND COMPANIES UTILIZING THE FACILITIES OF THE RSEC

University or Industry	Type of Use
AMD-Cerium Laboratories	Semi-Conductor Irradiation
Bloomsburg University	Gamma Irradiation
Central Virginia Governor's School	Gamma Irradiation
Cogema (AREVA)	Neutron Transmission
Cornell	Gamma Irradiation
Eagle-Picher	Neutron Transmission Neutron Radioscopy
Elizabeth Forward High School	Gamma Irradiation
Florida Power and Light	Neutron Transmission
Fairchild Corporation, South Korea	Semi-Conductor Irradiation
Hyundai (South Korea)	Neutron Radioscopy
Idaho State University	Gamma Irradiation
Lockheed Martin	Semi-Conductor Irradiation
Metamic LLC	Neutron Transmission
NETCO (Northeast Technology Corporation)	Neutron Transmission Neutron Radiography
Northrup-Grumman	Semi-Conductor Irradiation
Physical Acoustics	Gamma Irradiation
Point Beach Energy Center	Gamma Irradiation
Powdermet	Neutron Transmission
Purdue University	Gamma Irradiation
Pure Fishing	Gamma Irradiation
Raytheon Systems Company, El Segundo, CA	Semi-Conductor Irradiation
State College Area High School	Gamma Irradiation
Spectrum Technologies	Gamma Irradiation
TRACERCO	Isotope Production
Tru-Tec	Isotope Production
University of Iowa	Neutron Activation Analysis
University of Maryland	Gamma Irradiation
University of Pittsburgh, Greensburg	Neutron Activation Analysis
Vectron International	Gamma Irradiation

PUBLICATIONS

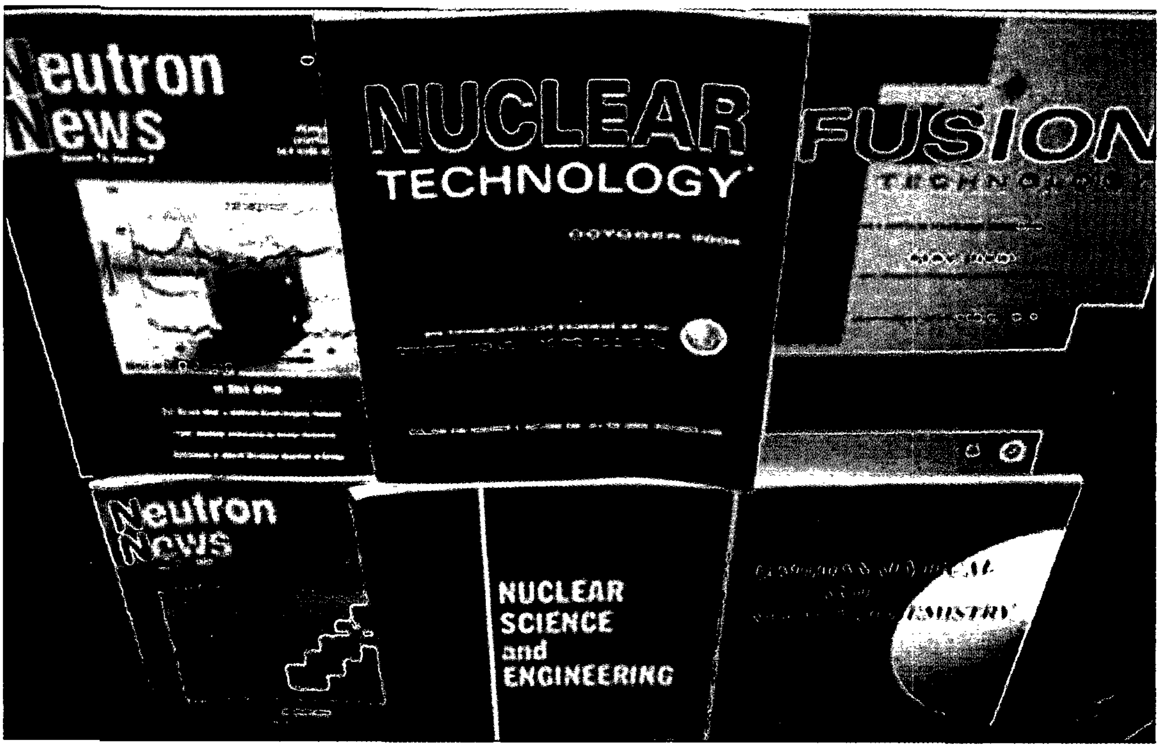

PUBLICATIONS

S. M. Cetiner, K. Ünlü, , G. Downing, "*Development and Applications of Time-of-Flight Neutron Depth Profiling,*" Journal of Radioanalytical and Nuclear Chemistry, Vol, 276, No 3 (2008) http://dx.doi.org/10.1007/s10967-008-0609-7

N. Ö. Çetiner, K. Ünlü, J.S. Brenizer, "*Compton Suppression System at Penn State Radiation Science and Engineering Center,*" Journal of Radioanalytical and Nuclear Chemistry, Vol, 276, No 3 (2008)

R. Ramaranayaran, V. Degalahal, R. Krishnan, J. S. Kim, V. Narayanan, Y. Xie, M. J. Irwin, K. Ünlü, *Modeling Soft Errors at Device and Logic Level for Combinational Circuits*, accepted for publication in IEEE Transactions in Nuclear Science, (2007)

S. M. Cetiner, K. Ünlü, *Depth profiling of boron in ultra-shallow junction devices using time-of-flight neutron depth profiling (TOF-NDP),* Nucl. Instr. and Meth. A (2007)
http://dx.doi.org/10.1016/j.nima.2007.04.027

K. Ünlü, V. Narayanan, S. M. Cetiner, V. Degalahal, M. J. Irwin, *Neutron-induced soft error rate measurements in semiconductor memories*, Nucl. Instr. and Meth. A (2007)
http://dx.doi.org/10.1016/j.nima.2007.04.049

C. Celik, K. Ünlü, S. Cetiner, V. Narayanan, M. J. Irwin, Y. Xie, V. Degalahal, *Soft Error Rate Measurements in Semiconductor Memories at Pennsylvania State University*, Transactions of American Nuclear Society (ANS), Vol. 97, p 292, November 2007, Washington, D.C.

D. K. H. Schwarz, K. Ünlü, *Silver and Gold: Possible Evidence of Dust Storms in Tree-Rings*, Transactions of American Nuclear Society (ANS), Vol. 97, p 257, November 2007, Washington, D.C.

K. Burns, N. Hertel, K. Ünlü, J. Brenizer, C. Celik, , D. K. H. Schwarz, Transactions of American Nuclear Society (ANS), Vol. 97, p 290, November 2007, Washington, D.C.

D. K. H. Schwarz, K. Ünlü "*Typical Elemental Concentrations in Tree-Rings and Appropriate Irradiation Parameters for Determination with NAA*" presented in International Conference of Modern Trends in Activation Analysis 12 (MTAA12), Tokyo, Japan, September 2007, Accepted publication in Journal of Radioanalytical and Nuclear Chemistry.

F. Alim, K. Bekar, K. Ivanov, K. Ünlü, J. Brenizer, Y. Azmy, *Modeling and Optimization of Existing Beam Port Facility at PSBR*, Annals of Nuclear Energy, Vol. 33, Issues 17-18, p1391-1395, (2006)

K. B. Bekar, Y. Azmy, K. Ünlü, J. Brenizer, "*A Case Study to Bound the Search Space of the Optimization Problem for the PSBR Beam Tube*", PHYSOR 2006 Advances in Nuclear Analysis and Simulation, September 10-14, 2006, Vancouver, BC, Canada

R. G. Downing, S. M. Cetiner, *Enhanced Reaction Rates in NDP Analysis by Neutron Scattering*, Transactions of American Nuclear Society (ANS), Vol. 95, pp. 459-460, November 12-16, 2006, Albuquerque, NM

D.K. H. Schwarz, K. Ünlü, " *Dendrochemistry of Pinus Sylvestris trees from a Turkish forest: Identifying the effects of Pinatuba*," (abstract, full paper will be published in a book or special issue of a relevant journal), Tree-rings, Kings, and Old World Archaeology and Environment: Cornell Dendrochronology-Archaeology Conference in Honour of Peter Ian Kuniholm, 3-5 November 2006

K. Ünlü, P. I. Kuniholm, D. K. H. Schwarz, N. Ö. Cetiner, and J. J. Chiment, "*Neutron Activation Analysis of Dendrochronologically-dated Trees*," (abstract, full paper will be published in a book or special issue of a relevant journal), Tree-rings, Kings, and Old World Archaeology and Environment: Cornell Dendrochronology-Archaeology Conference in Honour of Peter Ian Kuniholm, 3-5 November 2006

K. Ünlü, G. Catchen, J. Brenizer, "*Starting Radiochemistry Education and Research Program at Penn State,*" (abstract, invited) International Conference on Methods and Applications of Radioanalytical Chemistry, Kailua-Kona, Hawaii, April 3-7, 2006

K. Ünlü, "*Radiochemistry Education and Research Program at Penn State: A New Start,*" (abstract, invited), Accepted, 232nd American Chemical Society National Meeting, Division of Nuclear Chemistry and Technology, San Francisco, CA, September 10-14, 2006

A. Turhan, K. Heller, J. S Brenizer, and M. M. Mench, *Quantification of Liquid Water Accumulation and Distribution in a Polymer Electrolyte Fuel Cell Using Neutron Imaging*. Journal of Power Sources, 160, pp. 1195-1203.

Kowal, J. J., Turhan, A., Heller, K., Brenizer, J. S., and Mench, M. M. 2006. *Liquid Water Storage, Distribution, and Removal from Diffusion Media in PEFCs*. Journal of Electrochemical Society, 153, pp. A1971-A1978.

Turhan, A., Kowal, J. J., Heller, K., Brenizer, J., and Mench, M. M. 2006. *Diffusion Media and Interfacial Effects on Fluid Storage and Transport in Fuel Cell Porous Media and Flow Channels*. ECS Transactions, 3, 1, Proton Exchange Membrane Fuel Cells 6, Eds. T. Fuller, C. Bock, S. Cleghorn, H. Gasteiger, T. Jarvi, M. Mathias, M. Murthy, T. Nguyen, V. Ramani, E. Stuve, T. Zawodzinski, pp. 435-444.

Turhan, A., Kowal, J. J., Heller, K., Shi, L., Brenizer, J., and Mench, M. M. 2006. *Interaction of Design, Materials, and Interfacial Forces on Liquid Water Storage and Distribution in Polymer Electrolyte Fuel Cells*. 8th World Conference On Neutron Radiography (WCNR-8). NIST, October 16 - 19, 2006.

Heller, K., Shi, L., Brenizer, J., and Mench, M. M. 2006. *Error Analysis of Water Quantification Using Neutron Imaging. 8th World Conference on Neutron Radiography (WCNR-8).* NIST, October 16 - 19, 2006.

Shi, L., Heller, K., Brenizer, J., and Mench, M. M. 2006. *The Penn State University Neutron Computed Tomography Facility. 8th World Conference on Neutron Radiography (WCNR-8).* NIST, October 16 - 19, 2006

Mench, M. M. (in press). *Fuel Cell Engines*, John Wiley and Sons, Inc. To be available December, 2007.

Turhan, A., Kowal, J. J., Heller, K., Brenizer, J., and Mench, M. M. *Diffusion Media and Interfacial Effects on Fluid Storage and Transport in Fuel Cell Porous Media and Flow Channels*. Presented at the 210th Electrochemical Society Meeting, Cancun, Mexico 2006.

Khandelwal, M., Kumber, E.C., and Mench, M. M. 2006. *Interfacial and Bulk Thermal and Mass Transport Parameters in Fuel Cell Media.* Presented at the 210th Electrochemical Society Meeting, Cancun, Mexico

Turhan, A., Kowal, J. J., Heller, K., Shi, L., Brenizer, J., and Mench, M. M. 2006. *Interaction of Design, Materials, and Interfacial Forces on Liquid Water Storage and Distribution in Polymer Electrolyte Fuel Cells*. Presented at the 8th World Conference On Neutron Radiography (WCNR-8). NIST, October 16 - 19, 2006.

Brenizer, J. S., Mench, M. M., Heller, A. K., and Ünlü, K., K. 2005. (invited), Neutron Imaging at Penn State: Past, Present and Future. *presented at the Joint Meeting of the National Organization of Test, Research, and Training Reactors and the International Group on Research Reactors, Special session honoring the Pennsylvania State University Breazeale Reactor 50th Anniversary*, September 12-16, 2005.

Mench, M. M., Turhan, A., Keller, K., Ünlü, K., and Brenizer, J. 2005. INIE Big-10 Consortium Enabled Research: A New Physical Model of Two-Phase Transport in Polymer Electrolyte Fuel Cells Using Neutron Imaging at Penn State. *Trans. American Nuclear Society*, Vol. 93, pp. 74-75.

Turhan, A., Kowal, J. J., Heller, K., Brenizer, J., and Mench, M. M. 2006. Diffusion Media and Interfacial Effects on Fluid Storage and Transport in Fuel Cell Porous Media and Flow Channels. *presented at the 210th Electrochemical Society Meeting*, Cancun, Mexico

APPENDICES

APPENDIX A: Personnel Utilizing RSEC Facilities

Faculty (F), Staff (S), Graduate Student (G), Undergraduate (U), Visiting Professor (VP), Visiting Scholar (VS), Faculty Emeritus (FE), Post-Doctoral (PD)

COLLEGE OF AGRICULTURE	
Crop & Soil Science	
Fricks, Barbara	F
Lewis, David	F
Food Science	
Belman, Robert	F
Horticulture	
Lopez, Juan	S
Plant Pathology	
Juba, Jean	S
Veterinary and Biomedical Sciences	
Bruce, Danny	G
Weaver, Veronica	S

COLLEGE OF EARTH & MINNERAL SCI-	
Geology	
Kump, Lee	F
Narayan, Beepa	G

COLLEGE OF ENGINEERING	
Bioengineering	
Clement, Ryan	G
Civil & Environmental Engineering	
McElhoe, Jen	G
Schoenebeck, Greg	G
Tan, Hui	G
Computer Science & Engineering	
Irwin, Mary Jane	F
Narayanan, Vijay Krishan	F
Electrical Engineering	
Krishnan, Ramakrishnan	G
Ramanarayanan, Rajaraman	G
Engineering Science & Mechanics	
Bittle, Brad	G
Campbell, Jason	G
Material Science & Engineering	
Krishnan, Venkatesh	G
Ravi, Dhurati	G
Unal, Burcu	G
Mechanical & Nuclear Engineering	
Azmy, Yousry	F
Brenizer, Jack	F
Bryan, Mac	S
Catchen, Gary	F
Cetiner, Nesrin	S
Cetiner, Sacit	G
Cihangir, Celic	G
Daubenspeck,Thiery	S
Davison, Candace	S
Dorn, Mark	U
Edwards, Bob	F
Flinchbaugh, Terry	S
Ferrer, Rudolfo	G
Heidrich, Brenden	F
Heller, Kevin	G
Hochreiter, Larry	F
Ivanov, Kostadin	F
Kowal, Jj	G
Kriangchaiporn, Nateekool	G
May, Seth	G
Mench, Matt	F
Miller-Krishart, Amy	U
Morlang, Michael	G
Motta, Arthur	F
Portanova, Alison	S
Rim, Jung	G
Schwarz, Danielle	G
Schwarz, Eric	U
Sears, C. Frederick	F
Shields, Dan	G
Skilone, Dan	U
Spielman, Dennis	U
Tippayakul, Chanatip	G
Trivelpiece, Cory	G
Turhan, Ahmet	G
Unlu, Kenan	F
Yetzer, Korrie	U

COLLEGE OF SCIENCE	
Biochemistry / Molecular Biology	
Jiang, Wei	G
Diao, Yinghui	G
Chemistry	
Allcock, Harry	F
Behan, Rachel	G
Fei, Shih-To	G
Latham, Andrew	G
Stone, Kari	G
Vaish, Amot	G
Wood, Rich	G
Welkel, Arlin	G

MATERIALS RESEARCH INSTITUTE (MRI)	
Dewan, Hardial	F
Rao, Manau	PD

OFFICE OF ENVIRONMENTAL HEALTH & SAFETY	
Bertocchi, Dave	S
Boeldt, Eric	S
Hermann, Greg	S
Linsley, Mark	S
Morlang, Suzanne	S
Wiggins, Jim	S

INDUSTRIES, COLLEGES, HIGH SCHOOLS, ETC.	
AMD - Cerium Lab	Hossain, Tim
Bloomsburg University	Simpson, David
Central VA Governors School	Lindeman, Cheryl Bae, Young Conrad, Collin Dewberry, Will Gorman, Philip Laverty, B. Krotks, Jenna Mahanry, J. Malocc, JP Morcom, Randall Rahman, Andaleeb Sarvoo, Rodrigo
Cogema (AREVA)	Bonnet, Gilles
Cornell	Podaras, Peter
Eagle-Picher	Rushin, Sandi
Elizabeth Forward HS	Vitori, Bill
Fairchild	Cho, Bongsin
FPL Energy - Seabrook (NETCO)	Merrill, Alan
GE Inspection Technologies	Aziz, Mark Kochakian, Rich
Georgia Tech	Burns, Kim Hertel, Nolan
HYUNDAI (South Korea)	Ahn, Byung Ki Cho, Kyutaek (PSU) He, Suhao (PSU) Jong-Jin, Yoon Kim, Sawhan (PSU) Ohseungchan
Lockheed-Martin	Bruccoliere, Larry
Metamic LLC	Haines, Thomas Turner, S. E.
Northeast Tech (NETCO)	Lindquist, Ken
Northrup-Grumman	Randall, Don
NWT Corporation	Palino, Jerry
Physical Acoustics	Bascara, Caesar
Point Beach Energy Center	Olsen, Lavretta

INDUSTRIES, COLLEGES, HIGH SCHOOLS, ETC. (con't)	
Powdermet	Sherman, Andrew Singh, Raj K
Purdue University	Fischbach, Ephraim Jenkins, Jerre
Pure Fishing	Azari, Arsalan
Raytheon Systems Company	Craig, Ed
Spectrum Technoloogy	Kaylor, Richard
State College Area HS	Gilmour, Tami
Tracerco	Boone, Mike
Transnuclear, NY	Stoltz, Marlin
Tru-Tec	Bocage, Chris Flenniken, Mike Growney, Eric
TRW Incorporated	Cornell, Frank Randall, Don
University of Iowa - INIE	Dennis, Leslie
University of Maryland	Wienke, Jimmy
University of Pitt	Brown, Katrina
Vectron International	Wilson, Harry Salko, Robert

APPENDIX B: Formal Tour Groups

Group Name	Date	#Visitors
Prospective Student	7/6/2006	3
Prospective Student	7/7/2006	3
PGSAS	7/10/2007	33
Nuc E Professor	7/11/2006	1
PGSAS	7/11/2006	34
GE	7/12/2006	1
Guests	7/13/2006	3
MRL/PSU	7/13/2006	2
US Dept of Energy	7/14/2006	2
Guest	7/14/2006	1
RSEC Staff Family	7/21/2006	16
Spend a Summer Day	7/27/2006	12
Chem E Rell	7/27/2006	18
Upward Bound	7/27/2006	12
Spend a Summer Day	7/28/2006	5
Huntington County EMA	7/28/2006	2
Spend a Summer Day	7/31/2006	5
Spend a Summer Day	8/2/2006	9
Telecommunications	8/3/2006	2
Chemistry Group	8/3/2006	2
B and B	8/3/2006	1
Friends	8/3/2006	2
Spend a Summer Day	8/4/2006	6
Soft Error Group	8/7/2006	3
Spectrum Technologies	8/10/2006	1
Property Inventory	8/14/2006	1
Guest	8/14/2006	1
GREATT	8/16/2006	25
Engineering Professor	8/30/2006	1
Forklift Inc	8/31/2006	1
Salvage and Surplus	9/5/2006	2
Forklift	9/7/2006	1

Group Name	Date	#Visitors
Prospective Student Tour	9/11/2006	3
RSEC Intern Interview	9/12/2006	1
FBI	9/12/2006	1
Property Inventory	9/13/2006	1
FBI	9/14/2006	1
Family and Friends	9/15/2006	14
EPRI	9/15/2006	2
ARL	9/15/2006	3
GE Inspection Technologies	9/20/2006	2
Background Investigation	9/20/2006	1
RSEC Intern Interview	9/21/2006	1
Central Virginia (CVGS)	9/21/2006	17
Student	9/21/2006	1
Spectrum Technologies	9/22/2006	1
Prospective Student	9/22/2006	3
University of Pittsburgh	9/23/2006	31
RSEC Staff Family	9/24/2006	2
Radiation Round Table	9/25/2006	11
Radiation Round Table	9/27/2006	5
Engineering Science Faculty	9/29/2006	1
Prospective Student	10/3/2006	1
RSEC Intern	10/3/2006	1
Student	10/4/2006	1
BMB Graduate Students	10/5/2006	2
Seminar Speaker	10/6/2006	1
Parents and Family Weekend	10/7/2006	158
EHS	10/9/2006	1
Food Science	10/10/2006	22
Nuclear Engineering Class	10/11/2006	39
AMD-Cerium Lab	10/11/2006	1
AMD-Cerium Lab	10/12/2006	1
Student	10/12/2006	1

Group Name	Date	#Visitors
PCI Hitman	10/18/2006	1
Nuc E Alumni	10/18/2006	1
BMB	10/18/2006	1
Seminar Speaker	10/18/2006	1
Engineering Professor	10/18/2006	1
IBM	10/18/2006	3
Lynch Lab Tour	10/19/2006	2
STS Class Tour	10/23/2006	4
Pi Tau Sigma (ME honors)	10/23/2006	12
ENGR House	10/23/2006	5
Higher Education Class	10/25/2006	2
USNRC	10/26/2006	2
STS	10/26/2006	34
Tau Beta Pi	10/28/2006	12
Westinghouse Scholars	10/28/2006	77
Vet Science	10/30/2006	1
DOE Visit	10/30/2006	1
Nuclear Engineering Class	11/2/2006	13
Boalsburg Elementary	11/2/2006	21
Telecommunications	11/3/2006	2
RSEC Staff Friend	11/4/2006	1
Westinghouse Scholars	11/4/2006	84
Houserville Elementary	11/6/2006	29
ASME	11/6/2006	14
Prospective Student	11/7/2006	2
EASI House	11/7/2006	31
Houserville Elementary	11/7/2006	61
Lockhaven University	11/7/2006	12
Boalsburg Elementary	11/9/2006	21
Seminar Speaker	11/9/2006	1
Family and Friends	11/10/2006	2
ADO Candidate	11/16/2006	1

Group Name	Date	#Visitors
Boalsburg Elementary	11/16/2006	19
ADO Candidate	11/17/2006	1
Family and Friends	11/20/2006	3
Prospective Student	11/27/2006	2
Provost/VP for Research	11/29/2006	1
Seminar Speaker	11/30/2006	1
ADO Candidate	11/30/2006	1
Prospective Student	12/1/2006	4
Westinghouse Scholars	12/2/2006	70
AD-14	12/5/2006	6
MRI	12/5/2006	1
Sci Tech HS	12/6/2006	93
Prospective Student	12/6/2006	2
Yough HS	12/7/2006	12
Reading	12/7/2006	2
Areva	12/7/2006	1
Guest	12/8/2006	1
Boy Scouts	12/9/2006	83
Nuclear Engineering Student	12/11/2006	1
Hyundai	12/11/2006	4
Guest	12/12/2006	1
Univ. Police Officer Training	12/13/2006	2
Seminar Speaker	12/14/2006	3
Parking Office	12/19/2006	1
Clarion HS	12/20/2006	5
Holiday Guests	12/21/2006	1
PA State Dept	1/8/2007	2
Berwick HS	1/18/2007	14
Center County Christian Academy	1/27/2007	14
MEP	1/31/2007	3
Dept Speaker	2/1/2007	1
I-Cube	2/2/2007	1

Group Name	Date	#Visitors
Junior Naval ROTC	2/8/2007	19
Junior Naval ROTC	2/8/2007	18
Family and Friends	2/8/2007	4
Property Inventory	2/9/2007	2
Goziortep University Unit	2/12/2007	3
Prospective Student	2/19/2007	2
ITS	2/22/2007	1
Engineering Open House	2/24/2007	140
Nuclear Regulatory Commission	2/26/2007	1
Hollidaysburg HS	2/28/2007	12
Best Line Equipment	3/1/2007	1
Hochreiter	3/1/2007	2
EMS Interest	3/1/2007	25
Personal	3/2/2007	1
Prospective Faculty	3/2/2007	1
Telecommunications	3/2/2007	1
Steelton Science	3/2/2007	50
Boy Scouts	3/3/2007	83
Blue Chip (Potential Grads)	3/3/2007	8
PJSHS	3/5/2007	6
Sci Ed Grad Tour	3/8/2007	3
Northern Potter	3/8/2007	25
Faculty Candidate	3/8/2007	1
Areva Recruiter	3/9/2007	1
RSEC Staff Family and Friends	3/12/2007	4
450 Class help	3/19/2007	1
Nuc E Faculty Candidate	3/19/2007	1
450 Class help	3/20/2007	2
First Energy	3/23/2007	1
Lycoming College	3/22/2007	14
HSLC	3/24/2007	20
TNS-Phone Repair	3/27/2007	1

Group Name	Date	#Visitors
Dept Speaker	3/27/2007	1
Prospective Student	3/30/2007	2
Family	3/30/2007	1
Greensburg Salem	3/30/2007	25
Laser Force	4/2/2007	1
Visitor Alumni	4/3/2007	2
Laser Force	4/3/2007	1
Property Inventory	4/3/2007	1
Bio Sci 415	4/3/2007	30
PSU-Altoona	4/3/2007	13
Prospective Student	4/3/2007	1
EMS	4/4/2007	22
Dept Speaker	4/5/2007	1
Tau Beta Pi	4/5/2007	17
RSEC Staff Family and Friends	4/6/2007	5
Collin's Family	4/6/2007	3
ARL-Experiment Work	4/6/2007	1
Boy Scouts	4/7/2007	86
CLC	4/9/2007	24
Prospective Student	4/9/2007	4
Kane Middle School	4/10/2007	9
Williamson High School	4/11/2007	13
Prospective Student	4/12/2007	2
Hospital Tour	4/12/2007	1
Corner Stone Refrigeration and Heat	4/13/2007	1
Prospective Grad Student	4/13/2007	1
Bald Eagle Area MS	4/16/2007	36
Prospective Student	4/16/2007	3
ASABE	4/18/2007	10
Tyrone MS	4/19/2007	35
Tyrone MS	4/19/2007	34
Student-450 Help	4/19/2007	1

Group Name	Date	#Visitors
Prospective Student	4/20/2007	1
Engineering Mechanics 440	4/20/2007	12
USNRC	4/24/2007	1
Bangor HS	4/24/2007	30
Health Physics	4/25/2007	1
Dept computer Help	4/25/2007	1
Take Our sons and Daughters to work	4/26/2007	24
Take Our sons and Daughters to work	4/26/2007	11
Take Our sons and Daughters to work	4/26/2007	12
IEEE	5/1/2007	17
Royal Navy	5/2/2007	4
Dept Speaker	5/3/2007	1
Radiological Response Training	5/6/2007	20
UMD Student Researchers	5/6/2007	1
Elizabeth Forward HS	5/9/2007	33
LeMay Science Major	5/9/2007	2
Peters Township Elementary	5/16/2007	6
Ligonier HS	5/16/2007	22
Infinity Charter School	5/16/2007	32
Red Lion Christian Academy	5/17/2007	7
Our Lady Victory HS	5/18/2007	48
Our Lady Victory HS	5/18/2007	37
RSEC Staff Family and Friends	5/18/2007	2
McConnellsburg HS	5/21/2007	12
Jefferson MS	5/21/2007	3
Hanover Area HS	5/21/2007	3
Danville HS	5/21/2007	9

Group Name	Date	#Visitors
Portage HS	5/21/2007	3
St. Mary's HS	5/22/2007	7
Guest	5/22/2007	1
Brockway HS	5/23/2007	15
Marion Center HS	5/23/2007	8
Coughlin HS	5/24/2007	27
University Police	5/24/2007	13
Family and Friends	5/29/2007	2
Punxsutawney HS	5/29/2007	15
NRC	5/29/2007	1
NRC	5/30/2007	1
University Police	5/31/2007	19
State College Police	6/1/2007	1
Personal	6/5/2007	1
University Police	6/7/2007	2
Rochester Area SD	6/7/2007	28
ARL and DTRA	6/7/2007	7
NRC Exit Interview	6/7/2007	1
Reading Crane	6/9/2007	2
Food Science Grad Student	6/14/2007	2
Schott and Industrial Research	6/15/2007	2
Nuclear Engineering Class	6/15/2007	4
Georgia Tech University	6/18/2007	2
Guest	6/19/2007	1
Nuclear Engineering Student	6/21/2007	1
Guest	6/28/2007	1
	Total	**2713**